HSRI Report No. PF-100

VEHICLE HANDLING TEST PROCEDURES

Howard Dugoff
R.D. Ervin
Leonard Segel

*Highway Safety Research Institute
University of Michigan
Huron Parkway and Baxter Road
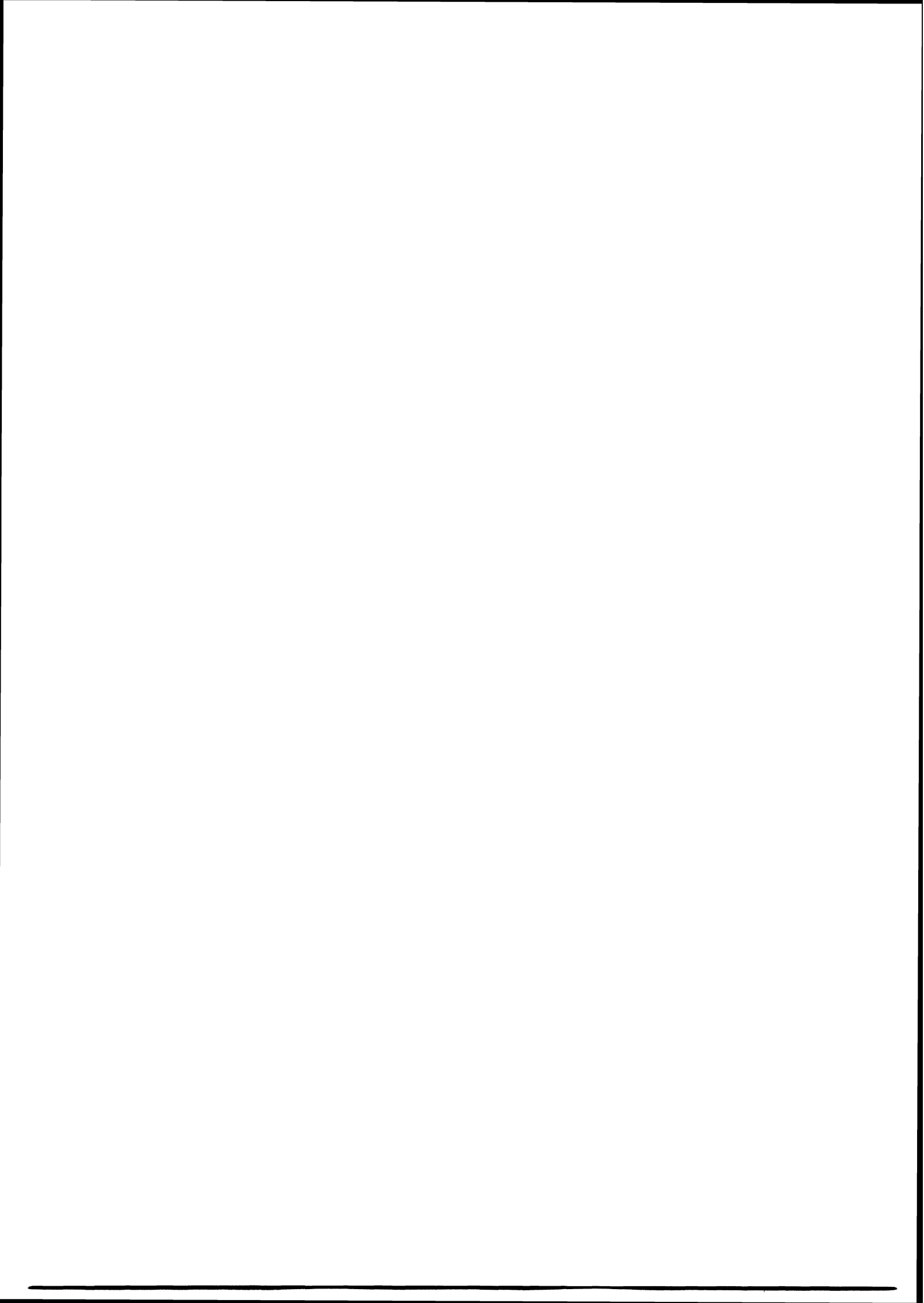Ann Arbor, Michigan 48105*

November 1970

Final Report

1. Report No.	2. Government Accession No.	3. Recipient's Catalog No.

4. Title and Subtitle	5. Report Date
VEHICLE HANDLING TEST PROCEDURES	November 1970
	6. Performing Organization Code

7. Author(s)	8. Performing Organization Report No.
H. Dugoff, R. D. Ervin, and L. Segel	PF-100

9. Performing Organization Name and Address	10. Work Unit No.
Highway Safety Research Institute University of Michigan Huron Parkway & Baxter Rd. Ann Arbor, Michigan 48105	
	11. Contract or Grant No.
	FH-11-7297

12. Sponsoring Agency Name and Address	13. Type of Report and Period Covered
National Highway Safety Bureau U.S. Department of Transportation Washington, D.C. 20591	Final Report-7/69-11/70
	14. Sponsoring Agency Code

15 Supplementary Notes

16. Abstract

A set of safety-relevant performance qualities were defined for the passenger car as a first step in the development of objective measures of precrash safety performance. Measures were sought that stress the performance produced by a passenger vehicle when it is operated under emergency, crash-avoidance conditions. This goal led to the identification of six limit maneuvers, and associated limit responses, to serve as a first-order means of assessing the safety quality of a motor vehicle. Two of the maneuvers involved control inputs so complex that a driver could not perform them with acceptable fidelity. These maneuvers accordingly were performed using an automatic control system to manipulate the steering, braking, and accelerator controls. The viability and discriminatory power of the proposed test procedures were demonstrated by applying these procedures to four separate vehicles reflecting widely different design philosophies and transport objectives.

17. Key Words	18. Distribution Statement
vehicle dynamics, vehicle performance, vehicle handling, crash avoidance, emergency maneuvers, test procedures	Availability is unlimited. Document may be released to the Clearinghouse for Federal Scientific and Technical Information, Springfield, Virginia 22151, for sale to the public.

19. Security Classif (of this report)	20. Security Classif.(of this page)	21. No. of Pages	22. Price
Unclassified	Unclassified	123	

TABLE OF CONTENTS

ACKNOWLEDGMENTS

1.0 INTRODUCTION

This report presents findings, conclusions, and recommendations derived by the Highway Safety Research Institute (HSRI) in a research study for the National Highway Safety Bureau (NHSB) entitled, "Vehicle Handling Test Procedures." The major purpose of the study was the development of objective procedures for measuring safety related aspects of the dynamic performance of passenger cars.

In this report, the terms "vehicle performance" and "vehicle handling properties" refer to equivalent concepts and should be interpreted to mean both the static and dynamic response characteristics of the motor car to the actions of the driver in steering, braking, and accelerating. Vehicle response to disturbing forces originating from the highway environment are included as part of the performance or handling properties description.

At the present point in time, the complex relationship between vehicle performance and highway safety is neither theoretically understood nor experimentally documented. There is nonetheless ample intuitive basis to hypothesize that such a relationship exists and, further, that there are certain specific performance characteristics of motor vehicles which, during either the normal driving process or during emergency situations, cause the potential for loss of control to rise above a threshold beyond which driver skill and experience are of little avail. The problem remains to (1) identify such safety-relevant performance qualities, and (2) develop reliable, objective procedures for their measurement.

Since, as noted above, connections between vehicle performance and safety must presently be based on intuition, the approach adopted herein may be categorized as pragmatic. Such an approach is a proper response to the sponsor's immediate objective (namely establishment of interim standards for vehicle handling), but

certainly no substitute for basic studies of the driver/vehicle system required to gain real understanding of the performance/safety relationship.

In the following section, we discuss the approach in greater detail, attempting to articulate a rational pragmatic viewpoint and to develop from it a consistent and meaningful framework for the definition of handling test procedures. Within this framework, a broad spectrum of considerations ranging from theoretical vehicle mechanics to practical automotive engineering enable us to identify those particular performance qualities viewed as having first-order safety relevance.

Section 3.0 describes the design and conduct of a pilot test program consisting of experiments to measure each of the designated performance qualities for a sample of vehicle configurations of widely different dynamic characteristics. The experiments are explicitly designed to measure vehicle response characteristics independent of the confounding actions of a test driver or drivers (see discussion in Section 2.0). To this end, and to facilitate the precise application of control inputs of prescribed form, certain of the more extreme and complicated experiments involve the use of an automatic control system to manipulate the vehicle's steering, braking, and accelerating controls. The design and operation of this system, considered to represent a uniquely valuable tool for the safety-related evaluation of the motor vehicle, are described in substantial detail.

In Section 4.0, the pilot test results are presented and analyzed to illustrate and rationalize the derivation of safety-related performance measures from the data. The results of supplementary vehicle tests performed especially for the purpose, and the output of a hybrid computer study involving over 1400 simulation runs, are employed to help interpret and generalize

the basic data in this context. The principal conclusions reached are summarized in Section 5.0., mainly in the form of a recommended set of test procedures which effectively define the scope and format of a vehicle handling standard. Specific recommendations for additional research associated with the development and implementation of such a standard are also presented.

The report has two Appendices. The first describes and illustrates the analysis of vehicle-usage survey data to derive realistic ranges of service factors -- tire inflation pressure and vehicle loading -- to be considered in an evaluation of vehicle performance. The second describes the hybrid simulation model employed in the study, and presents comparative experimental and theoretical results to illustrate the degree of validity of the model.

2.0 SAFETY-RELEVANT PERFORMANCE QUALITIES OF MOTOR VEHICLES

2.1 THE RELATIONSHIP OF THE MAN-VEHICLE COMBINATION TO HIGHWAY SAFETY

Although the broad spectrum of highway vehicles categorized as passenger cars can and do differ markedly in their dynamic performance characteristics, it is clear that these qualities do not influence the highway safety record in a directly recognizable manner. Rather these qualities interact with the attitudes and skills of the driving population to produce a variable driver-vehicle element which, in turn, interacts with the remaining elements of the highway system. When the system breaks down (that is, an accident occurs), the driver component is generally heavily involved. It is clear that any attempt to develop the concept of pre-crash safety quality (as possessed by a motor vehicle) must take careful cognizance of the driver role, in terms of both his attitudes and his skills as a tactician and a controller.

Research has shown that the motor vehicle constitutes a mechanical system amenable to control and operation by a population of widely ranging skills [1]. Further, it has been demonstrated that the human operator possesses levels of flexibility and adaptability making it possible for him to adjust easily to a broad range of vehicle characteristics [2].

Given that the above statements are true, the question arises as to whether it is possible to define the pre-crash safety quality of a motor vehicle as a separate entity. Reflection on this problem indicates that such a definition may be possible if facets of vehicle performance can be identified that stress (1) a large demand upon driver skills during emergency conditions, or (2) behavioral characteristics which make the vehicle inherently more or less "roadworthy." The average driver has very little experience in contending with real emergencies. Consequently, a vehicle

4

that behaves very differently in emergencies than it does during routine operations can produce increased demands on driver skill for reasons of unfamiliarity, i.e., a departure from what may be anticipated on the basis of past experience. This quality of a vehicle, namely, presenting an unexpected response, can be identified (with a high level of confidence) as having safety relevance since the phenomenon of driver adaptability is not involved. By "roadworthy" we mean those attributes of a vehicle which give it inherently higher maneuver capabilities irrespective of the skill level of the driver involved. In this instance we are referring to a measure of pre-crash safety quality which is meaningful as long as drivers do not opt to operate a more roadworthy vehicle such as to reduce the margin for error to the same (or a lower) level as prevails with less roadworthy vehicles.

In summary, it appears that if we adopt the premise that vehicles can, and do, differ in their pre-crash safety qualities, these qualities are more logically derived from the limiting maneuver characteristics of a vehicle (as may be called upon in an emergency situation) as opposed to being a function of the dynamic interaction between man and his vehicle. This is not to say that properties of the man-vehicle combination do not possess implications with respect to "safety performance" - they certainly do. However, the subteties of this interaction, and our knowledge of man's adaptability, suggest that _first_ attempts to assess the safety performance of vehicles be restricted to defining and measuring qualities that reside "within" the vehicle. Such attempts should recognize the limited role of the vehicle in accident causation and should thereby stress those qualities that give drivers increased opportunity for avoiding catastrophic consequences of an improper decision or act. Vehicle attributes that result in less demands being placed on drivers as a result of operations in an unfavorable environment should also be considered as having safety relevance.

2.2 THE RELATIONSHIP OF THE MOTOR VEHICLE <u>PER SE</u> TO SAFETY

Given a concept of safety performance as defined above, it is clear that there are no absolute measures. A motor vehicle is never absolutely "safe" or "unsafe". Motor vehicles can presumably be judged to be "more safe" or "less safe" for a given user application. In general, however, such judgments are risky and it appears to be more logical and prudent to assess motor vehicles as being more or less roadworthy or more or less forgiving of driver inadequacies. It follows that vehicles that are deemed to be more roadworthy and/or more forgiving can be viewed as being more desirable vehicles in the context of upgrading the safety performance of the highway transportation system.

Notwithstanding the fact that pneumatic-tire vehicles have been designed and produced for many years, there are, as yet, no commonly accepted qualities or attributes associated with the concepts of "roadworthiness" or "forgiveness." In attempting to formulate a complete catalog of such qualities, we have concluded that they generally are subsumed within the following four major categories:

(1) Controllability sufficient for evasive action

(2) Limit maneuver capabilities, i.e., the upper bounds of maneuvering performance achievable under braking, traction, and cornering conditions

(3) Dynamic response characteristics bearing on the ability of a driver to close the control loop in a stable manner during an emergency maneuver

(4) Insensitivity of limit-maneuver capabilities and dynamic response characteristics to external disturbances, environmental conditions, and service factors.

In our view, particular emphasis should be given to "service factors" in any assessment of roadworthiness. These variables describe the degree to which an operational vehicle departs from a reference design condition. Vehicle loadings ranging from empty to full represent a common-place example of service factor variations. So too do deviations from the nominal (manufacturer's recommended) distribution of tire inflation pressures. It is clear that service factors exert significant influence on performance as achieved in the field and that there are combinations of service factors which mitigate against achieving the levels of performance exhibited by the baseline or reference vehicle.

It is important to recognize that the basic physical scale of a vehicle (size and weight) has a direct influence on many of the dynamic response properties relevant to pre-crash safety. For example, smaller vehicles generally possess greater evasive capabilities than can be achieved with larger vehicles but are more sensitive to wind gusts. Similarly, smaller vehicles because of their large center of gravity height to wheel track ratio are easier to roll over than their bigger cousins. It is rather generally agreed that it is not reasonable to produce a single roadworthiness standard applicable, for example, to passenger vehicles and motor trucks. It should also be acknowledged that variations in the size and transport objective of passenger cars alone will influence individual components of an overall roadworthiness evaluation.

2.3 LIMIT PERFORMANCE MANEUVERS

In light of the premises and conclusions discussed above, we have attempted to define a family of safety-relevant handling test procedures on the basis of a concept of "limit performance maneuvers," i.e., extreme, yet realistic, maneuvers in which vehicle performance qualities deemed to have safety relevance play a

7

significant and clearly defined role. Six limit performance
maneuvers were selected to produce a first-order performance
assessment compatible with technical considerations and with the
practical limitations of time and funds provided by the supporting
contract. The six maneuvers are discussed below.

2.3.1 LIMIT BRAKING (NO STEERING). Braking effectiveness
is a roadworthiness component with an intimate and well recognized
connection to safety -- all other things being equal, the shorter
the distance a car can stop in, the safer it is.* However, stopping
distance (or deceleration) per se is but a partial descriptor of a
motor-car's braking performance. It is also important to take
account of the vehicle's controllability characteristics as it
approaches and attains the braking limit. This can be done very
concisely be making use of the concept of braking efficiency, i.e.,
the ratio of maximum deceleration achievable without wheel locking
to the prevailing pavement friction coefficient. Since wheel
locking is a condition which either makes it impossible to apply
effective steering control (front wheel locking) or dramatically
degrades directional stability (rear wheel locking), braking
efficiency is regarded as a measure of vehicle handling performance
having direct safety implications.

---

*It is, of course, possible to cite anecdotal "evidence" to
the contrary, i.e., recount a tale of an accident in which poor
braking performance resulted in somebody's life being saved. This
is the usual case in highway safety matters, where most "facts"
are actually generalizations based on the weight of statistical
evidence. (Although some people actually do escape death by being
"thrown clear of the car" in an accident, most unrestrained occu-
pants of a collision-involved vehicle are less lucky. It is
therefore generally a good idea to fasten your seatbelt.)

Braking efficiency is a sensitive function of both environmental variables (particularly pavement friction) and service factors (particularly loading distribution) [3]. It follows that a test procedure designed to assess safety performance relative to a straight-line braking maneuver (or for that matter, any aspect of limit maneuver performance) should take due cognizance of these factors.

2.3.2 RESPONSE TO RAPID, EXTREME STEERING (NO BRAKING). This maneuver is performed by applying a quasi-step steering input to a vehicle initially coasting on a straight line path. The spiral trajectory characteristically produced is hardly representative of a realistic highway maneuver. Its initial "J-turn" phase, however, is similar to the real-world emergency produced by entering a turn too fast or, more generally, to the initial phase of a typical obstacle-avoidance maneuver.

If the maneuver is repeated with progressively increasing steering inputs (at a fixed value of initial speed), the results may be interpreted in terms that are analogous to the braking efficiency measure discussed above. The limit response condition can correspond to lateral force saturation either of the vehicle's front tires (drift-out), or of its rear tires (spin-out) [4]. The point at which the limit occurs, its basic character, and how it is affected by realistic variations in service factors are performance characteristics of potential safety-relevance.

2.3.3 BRAKING IN A TURN. In general, the driver's reaction to an emergency traffic situation is the application of a brake input, a steering input, or some combination of the two. Experiments conducted at the General Motors Proving Ground [5] indicate that the typical response to a particular simulated emergency -- a lifelike dummy hurled into the vehicle's path -- is a braking action only. The limit braking (no steering) maneuver described

in Section 2.3.1 provides a vehicle response measure germane to this situation when the nominal trajectory is a straight line path. The maneuver discussed in this section is intended to provide a comparable measure when the nominal trajectory is a path of constant, finite radius.

Measurements of the directional response produced by the application of brake torque to an automobile with fixed (non-zero) steer angle have been performed previously. Bergman [6] conducted several series of such tests, with a fixed value of initial speed (30 mph), and initial values of lateral acceleration equal to 0.2, 0.3, 0.4, and 0.5 g. For each lateral acceleration, braking torque was increased in successive test runs until a breakaway condition was approached. Directional response was expressed in terms of the maximum value of yaw acceleration measured during the maneuver. Yaw responses increasing with brake torque were observed for all initial conditions. Nakatsuka and Takanami [7] compared the limit response characteristics associated with front and rear wheel locking (drift and spinout, respectively), through tests where brakes were applied at one axle only. As would be expected, the rear-lock, or spinout, condition was characterized by extremely severe yawing motions.

Theoretical studies of the fixed-steer braking maneuver have also been performed [7, 8]. Various phenomenological mechanisms influencing the path-curvature response have been discussed [8]:

> "For the (typical) understeer vehicle, there is a
> tendency for the path curvature to increase as the
> forward speed is reduced. There is an opposite ten-
> dency, however, due to the yaw moment produced by
> the braking forces at the steered front wheels.
> Superposed upon these two effects is the influence
> of the nonlinear mechanics of the tires (and suspen-
> sion). If the tires are caused to operate in the
> vicinity of the friction limit, braking in a turn
> may be expected to produce (limit) trajectories highly
> sensitive to (these) nonlinear characteristics."

10

The braking effectiveness achievable at the point of wheel lockup (normalized with respect to the prevailing level of pavement friction) appears to be a significant roadworthiness component relative to any fixed-steer braking maneuver. Important also is the order of tire shear force saturation, which dramatically influences the nature of the limit trajectory response. It follows that the performance qualities manifested in this maneuver can profitably be assessed in terms of a generalized interpretation of braking efficiency, namely, one that takes account not only of the limit longitudinal deceleration, but also of the deviation from the nominal circular trajectory produced as the level of deceleration is increased towards its limit value.

2.3.4 TURNING ON A ROUGH SURFACE. Each of the maneuvers discussed previously (and those to be discussed subsequently) is defined with respect to the ideal "perfectly smooth pavement" which traditionally provides the roadway for discussions and analyses of vehicle handling performance. Vehicle maneuvers in the real-world are in fact performed on surfaces characterized by degrees of irregularity varying over a wide range. That road roughness has a dramatic effect on vehicle handling -- particularly limit performance -- is well known. Proving ground and road test procedures have long been employed within the automobile industry to evaluate vehicle roadholding on a subjective basis.

A maneuver serving to provide an objective roadholding evaluation can be performed by driving a coasting vehicle in a curved path (with the steering wheel held fixed) over a series of pavement irregularities. Qualitatively, the maneuver is very similar to real-world situations quite commonly experienced in driving over washboard roads. By repeating the maneuver over an appropriate range of approach speeds, it is possible to assure that the frequency of encounter with the disturbance inputs will

span the range of wheel hop fundamental frequencies to be found in the motor car population assuming realistic service factor variation. The maximum degree to which the path-curvature response of the fixed-steer vehicle is influenced by the road disturbance would appear to represent a significant component of an overall roadworthiness assessment.

2.3.5 RAPID LANE CHANGING. Traffic conflicts can and do require that very fast lane changes be made to avoid collisions. For purposes of this discussion, a lane change will be defined as a maneuver in which steering input causes a vehicle to be displaced laterally with zero net change in its heading angle. As the speed of travel approaches zero, this maneuver can be executed perfectly be applying a steering input of sinusoidal form. As the speed increases, however, the steering input required to produce a successful lane change becomes considerably more complex. By the same token, the response to a perfectly symmetrical steer input, such as a sinusoid, becomes progressively more asymmetrical. For an input of given size, the magnitude of this asymmetry appears to represent a vehicle response characteristic directly related to the difficulty a driver would encounter in closing the loop to produce a successful lane change. In particular, it is hypothesized that the greater the departure from a trajectory whose final and initial paths are parallel, and the greater the evidence of oscillatory or unstable behavior, the harder it will be for typical drivers to modulate their steering in emergency situations. Again the influence of service factor variations is an important factor in evaluating dynamic response behavior in this open-loop maneuver.

2.3.6 "DRASTIC" STEER AND BRAKE MANEUVER. A considerable amount of observational research is needed to describe the response patterns produced by drivers under emergency conditions. In the absence of such a description, there appear to be two pragmatic

approaches available to the safety researcher seeking to define limit performance maneuvers. In the first approach, one defines basic maneuver families on the basis of rudimentary combinations of simple control and/or disturbance inputs of systematically varying intensity. (This is the approach taken in the formulation of the five maneuvers discussed above.)

As an alternative, one can estimate reasonable bounds on the universe of all possible combinations of control inputs that might be produced in emergencies, and then seek particular combinations within this universe which may result in vehicle trajectory responses of a markedly uncontrollable character. The principal deterrent against the adoption of the latter approach in the past appears to have been inability to produce a general class of control input histories in a prescribed and precisely repeatable manner. However, a programmable mechanical controller (replacing the human controller) serves to make the approach both viable and extremely attractive.

The following sequence of control inputs, which fall within the universe of potential emergency control actions, provide a stringent test of the susceptibility of a suspension system to "jacking," "tucking," or other undesirable response: (1) a half sine wave of steering input (the first half of a lane change maneuver), and (2) a hard pulse brake input of one half second duration applied at a point in time where the vehicle's yaw response to the steer input is approaching its peak magnitude. Qualitatively, this combination of control inputs simulates a real-world emergency maneuver where the driver attempts to avoid an obstacle by simultaneous steering and braking, then releases the brakes upon perceiving the skidding resulting from wheel locking. The crucial juncture in the maneuver is the instant immediately following brake release, when the locked wheels suddenly spin up, and the magnitudes of the lateral tire forces increase from near zero to relatively high values. As the maneuver becomes more

extreme a motor vehicle will exhibit an increasingly severe
response, possibly to the point of rollover. The character of
the resulting response and the maneuver severity level at which
it occurs are considered to represent performance qualities of
distinct safety-relevance. So too, again, the influencing thereon
of service factor variations.

3.0 THE PILOT TEST PROGRAM

3.1 GENERAL

The pilot test program which is the principal subject of this report consisted of experiments corresponding to each of the limit performance maneuvers discussed in the previous section. The object of the test program was the evaluation of the test procedures and equipment, not the evaluation of the handling qualities of specific vehicles. To this end, four vehicles reflecting widely differing design philosophies and transport objectives were selected for test, thereby permitting assessment of the overall discriminatory power of the measures considered. The four vehicles (see photographs, Fig. 1) were the following:

(1) 1967 Ford Country Sedan Station Wagon -- a full size station wagon whose static directional stability varies over a wide range as a function of service factors

(2) 1970 Toyota 2000 GT Sports Coupe -- a sports car characterized by high steering gain, low height to track ratio, and a high horsepower to weight ratio

(3) 1961 Chevrolet Corvair -- a compact sedan with a rearward weight bias, and an independent rear suspension (swing axle)

(4) 1969 Mercedes 250 Sedan -- an expensive intermediate sedan with independent rear suspension whose cost reflects a substantial expenditure of performance-oriented, engineering effort

Four of the six test procedures were executed by test drivers, with the aid of passive brake and steering limiters, and two were performed using the automatic control system. The latter two tests (corresponding to rapid lane changing and "drastic" steer and

brake maneuvers) involved control inputs of so complex a nature
that a driver could not perform them with acceptable fidelity or
repeatability.

Because of severe time constraints, the testing program was
arranged to allow two parallel but essentially independent acti-
vities. The driver-control tests were performed using a "package"
of instrumentation and mechanical devices which was independent
of the package of apparatus used for the automatic-control tests.
Tests preliminary to the pilot program were conducted using two
identical 1967 Ford Station Wagons outfitted with these two
apparatus packages. The first pilot tests were also executed
with the two Fords. Then the driver-control package was sequenced
through the Toyota, Mercedes, and Corvair, respectively. In a
schedule that meshed with the driver-control sequence, the auto-
matic system was installed, and tests run, on the Corvair and then
the Toyota.

3.2   TEST EQUIPMENT

3.2.1   VEHICLE PREPARATION. Prior to testing, each vehicle
was outfitted with a complement of more or less permanent equip-
ment. Electronic wheel lockup indicators were installed on both
left wheels. These installations consisted of a small permanent
magnet attached to the brake drum or rotor assembly and a glass
reed switch attached to the backup plate or caliper assembly.
Thermocouples were also installed in the brake lining of the
two left wheel brakes.

A fifth wheel bracket was affixed to the frame and bumper
of each car.

In vehicles to be used in the automatic control tests (all
but Mercedes), a heavy duty alternator and regulator were sub-
stituted for the standard equipment. Fittings for towing the
automatically controlled vehicles to the test site were fixed to
the front frame members.

16
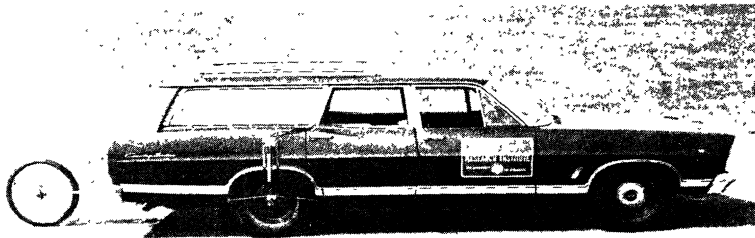
1967 FORD STATION WAGON
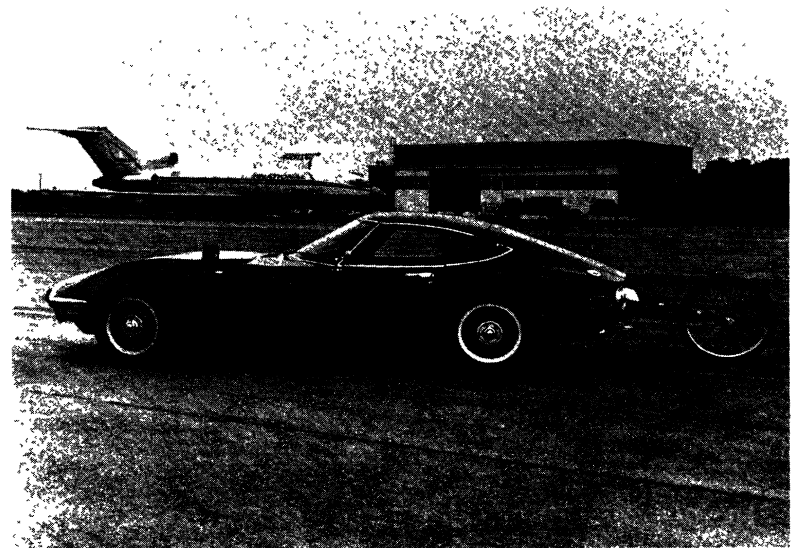
1970 TOYOTA 2000 GT

1961 CHEVROLET CORVAIR

1969 MERCEDES 250

FIGURE 1. PILOT TEST VEHICLES

Support frames were affixed to the Ford Station Wagon used for automatic-control tests and to the Corvair, in order to facilitate quick installation of outrigger arms serving to prevent rollovers (see photographs, Fig. 2). Although the Toyota was also tested with the automatic controller, it was not equipped with outriggers because of (1) little concern for the need, and (2) difficulties of application to the Monaco-type construction. The outrigger assembly was installed at a point along the frame which was directly below the c.g. of the unloaded vehicle. The assembly weighed 85 lbs and contributed about 30 slug-ft^2 to the roll moment of inertia of each vehicle. The outriggers were adjusted on each car to arrest the roll motion at a point when the tires on one side were 8 to 10 inches off the ground (as determined by a static pull test).

The Corvair and Fords were used cars and thus required extensive overhauling before testing. New brake linings, shock absorbers, and, where necessary, ball joints and wheel bearings were provided.

To guard against blowout hazards during severe cornering, tubeless tires were used with tubes installed on all test vehicles.

3.2.2 APPARATUS FOR DRIVER-CONTROL TESTS. Equipment moved from vehicle to vehicle to facilitate the driver controlled tests consisted of the following items:

1. Adjustable steering wheel stop mounted to upper steering column (see Fig. 3)

2. Adjustable brake pedal stop mounted to fire wall and dash assembly (see Fig. 4)

3. Strain gage pressure transducer installed in front brake line

4. Pressure gage with dial displayed to driver, installed in front brake line

18

INSTALLATION ON FORD STATION WAGON

INSTALLATION ON CORVAIR
FIGURE 2. OUTRIGGER INSTALLATION ON PILOT TEST VEHICLES

19
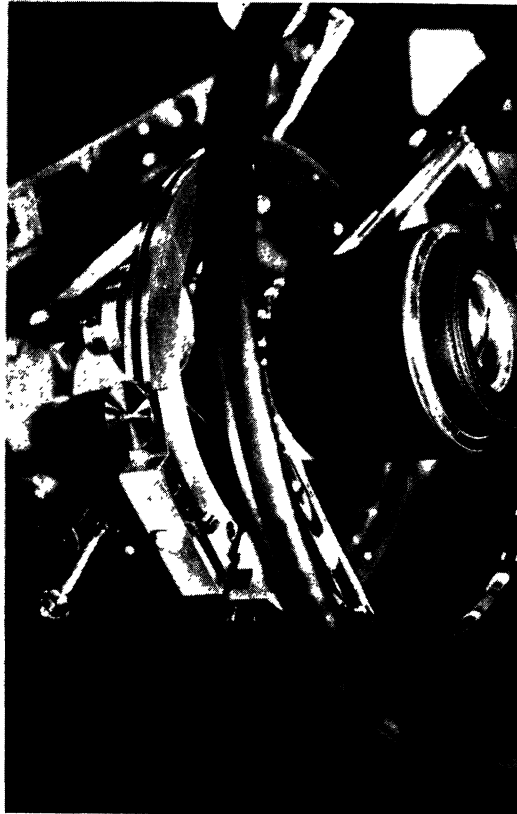
FIGURE 3. ADJUSTABLE STEERING WHEEL STOP DEVICE AND STEERING WHEEL ROTATION POTENTIOMETER INSTALLED IN MERCEDES
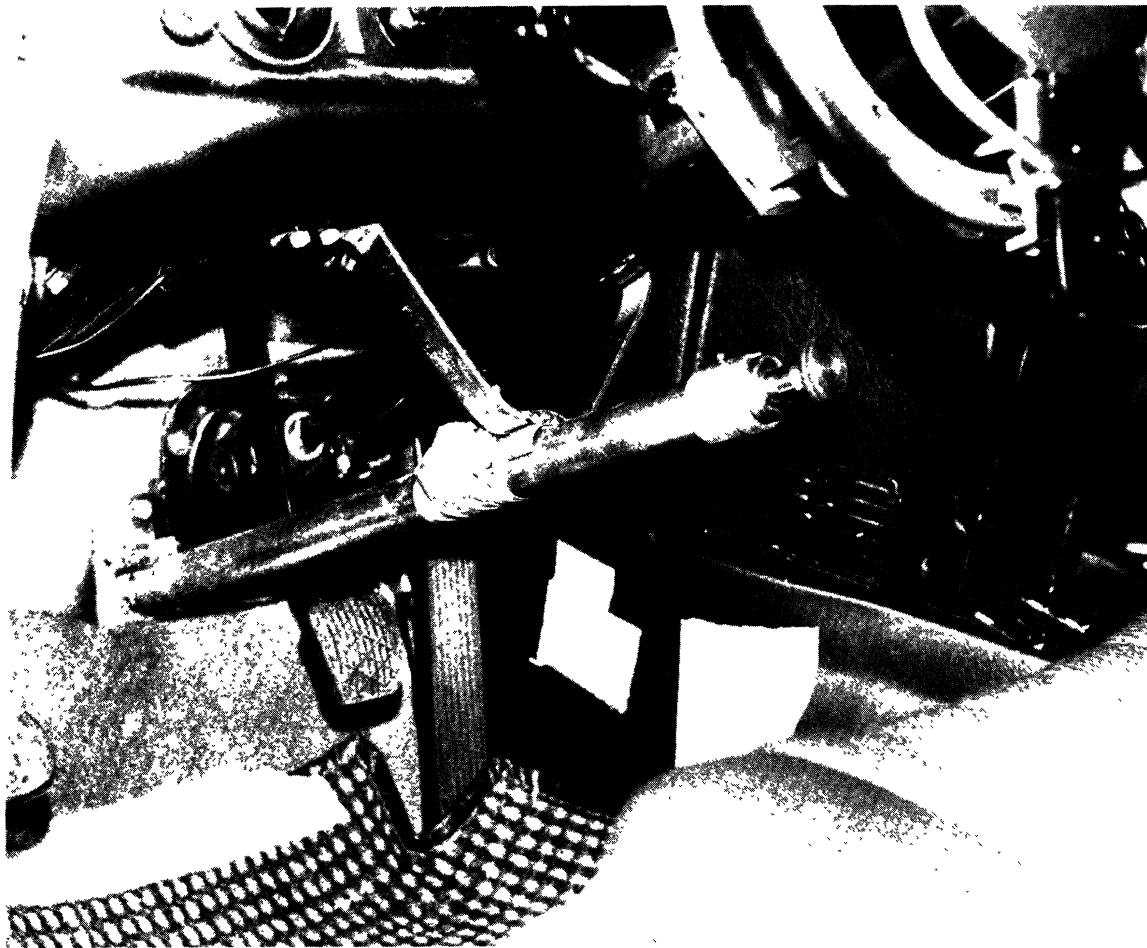
FIGURE 4. ADJUSTABLE BRAKE PEDAL STOP DEVICE INSTALLED IN MERCEDES

5. 16 channel light beam oscillograph (see Fig. 5)

6. Electronic signal conditioning package
    (see Fig. 5)

7. Fifth wheel with meter display to driver, plus
    connection to recorder

8. Brake-lining thermocouple meter for driver
    monitoring of brake temperatures

9. Transducer package consisting of vertical gyro,
    triad of accelerometers stabilized with respect
    to an earth vertical, and three rate gyros for
    measuring the components of the angular velocity
    vector (see Fig. 6)

10. Steering wheel rotation potentiometer (see Fig. 3)

The steering stop and pedal stop devices, pictured in Fig-
ures 3 and 4, were developed specifically for this program. They
were designed to permit very rapid inputs of steering and braking
to precisely set levels, without overshoot or rebound. The steer-
ing stop proved to be especially successful, permitting steering
displacements up to 700 degrees. Both devices, as well as all
of the transducers and other instrumentation, were readily trans-
ferable from vehicle to vehicle.

3.2.3 APPARATUS FOR AUTOMATIC-CONTROL TESTS. By far the
most important piece of apparatus developed for the test program
was the automatic vehicle controller. Because of its significance,
its novelty, and its complexity, this device will be described
in substantial detail.

The controller was designed to provide control inputs to the
steering wheel, brake pedal, and accelerator in three distinct
operational modes:
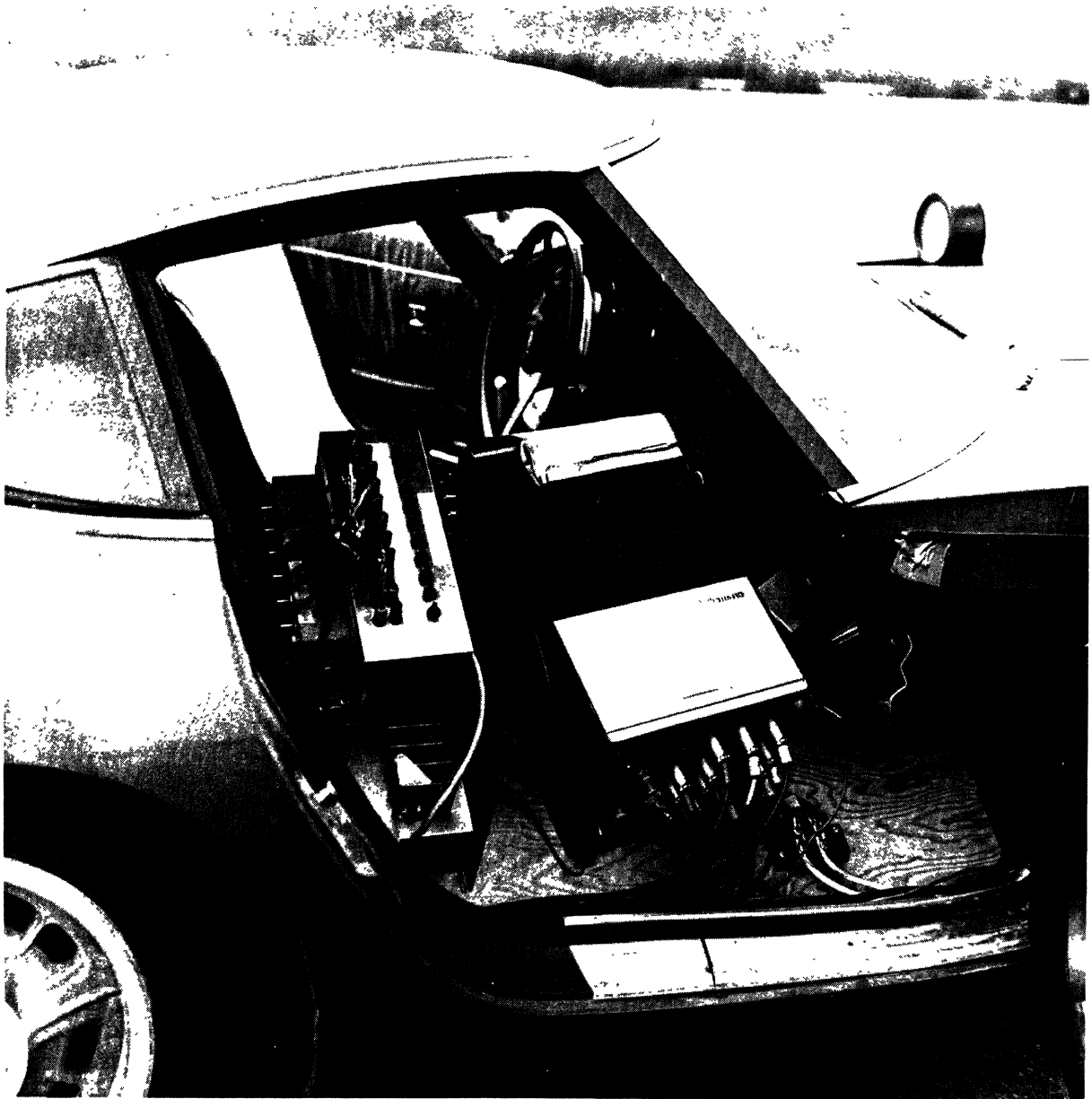
FIGURE 5. SIDE VIEW OF TOYOTA OUTFITTED FOR DRIVER-CONTROL TESTS
SHOWING OSCILLOGRAPH RECORDER AND SIGNAL
CONDITIONING EQUIPMENT
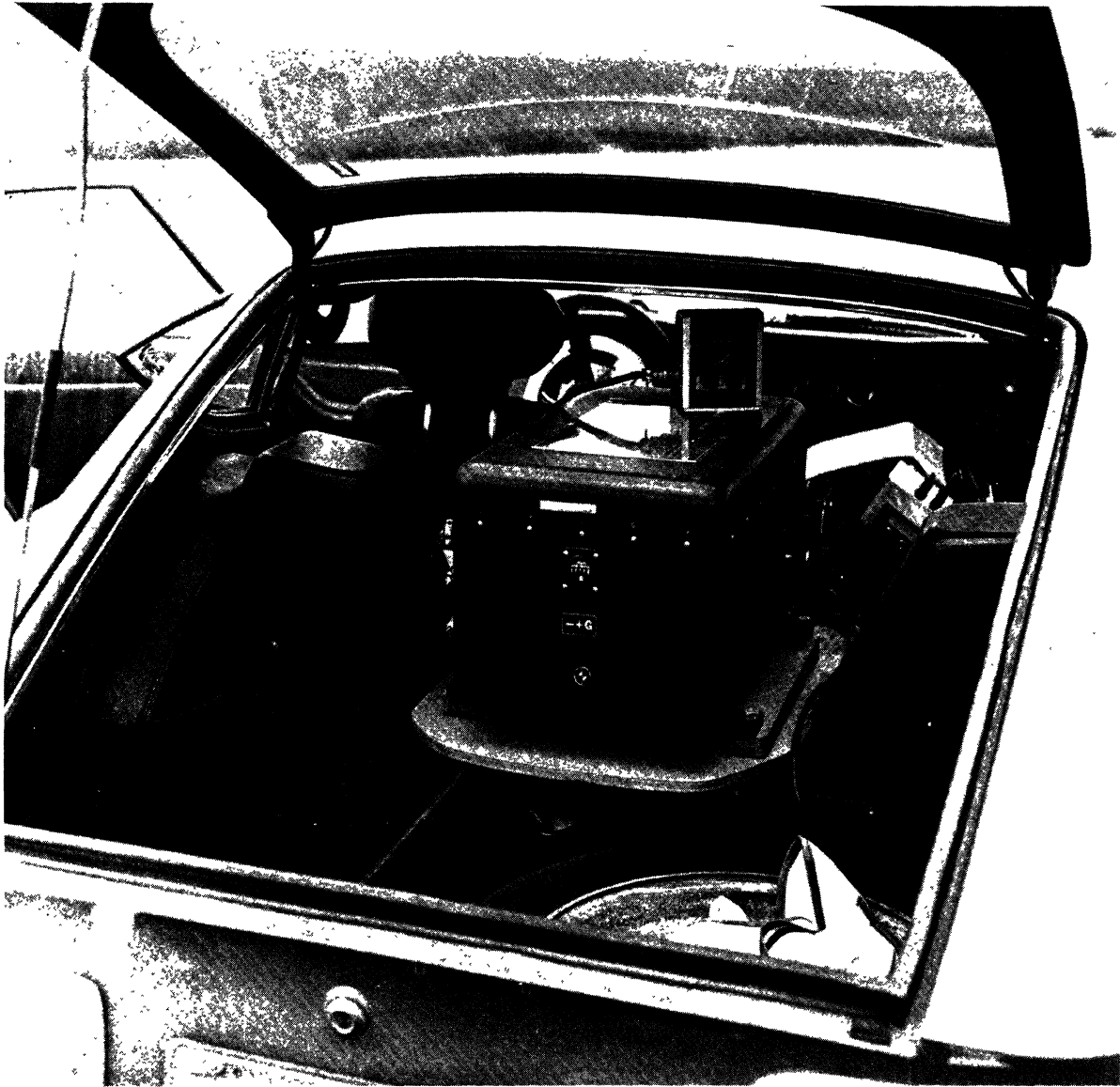
FIGURE 6. REAR VIEW OF TOYOTA OUTFITTED FOR DRIVER-CONTROL TESTS
SHOWING STABILIZED PLATFORM/ACCELEROMETER/GYRO PACKAGE

1. A drone mode, whereby the control loop on vehicle
    direction and speed is closed manually by an
    operator in a following vehicle, using a pulse
    modulating radio transmitter.

2. A program execution mode, in which the steer,
    brake, and accelerator control inputs originate
    from an on-board programmed function generator
    with no loop closure on vehicle response.

3. An abort mode in which the brakes are applied
    (and the accelerator released) spontaneously upon
    the occurrence of critical failures, or can be
    commanded by the test operator, through the trans-
    mitter link.

The controller was designed to be installable in any passenger
car. Its total weight is 260 pounds. The system is limited to
use with vehicles having automatic transmissions.

A block diagram of the vehicle control system is shown in
Fig. 7. The system consists of nine major subassemblies:

1. Radio Control Transmitter/Receiver

2. Steering Servo Amplifier and Actuator Assembly

3. Braking Servo Amplifier and Actuator Assembly

4. Accelerator Servo Amplifier and Actuator Assembly

5. Hydraulic Power Circuit

6. Function Generator

7. Master Control Logic Network

8. Abort Brake Assembly

9. Instrument Package and Recorder
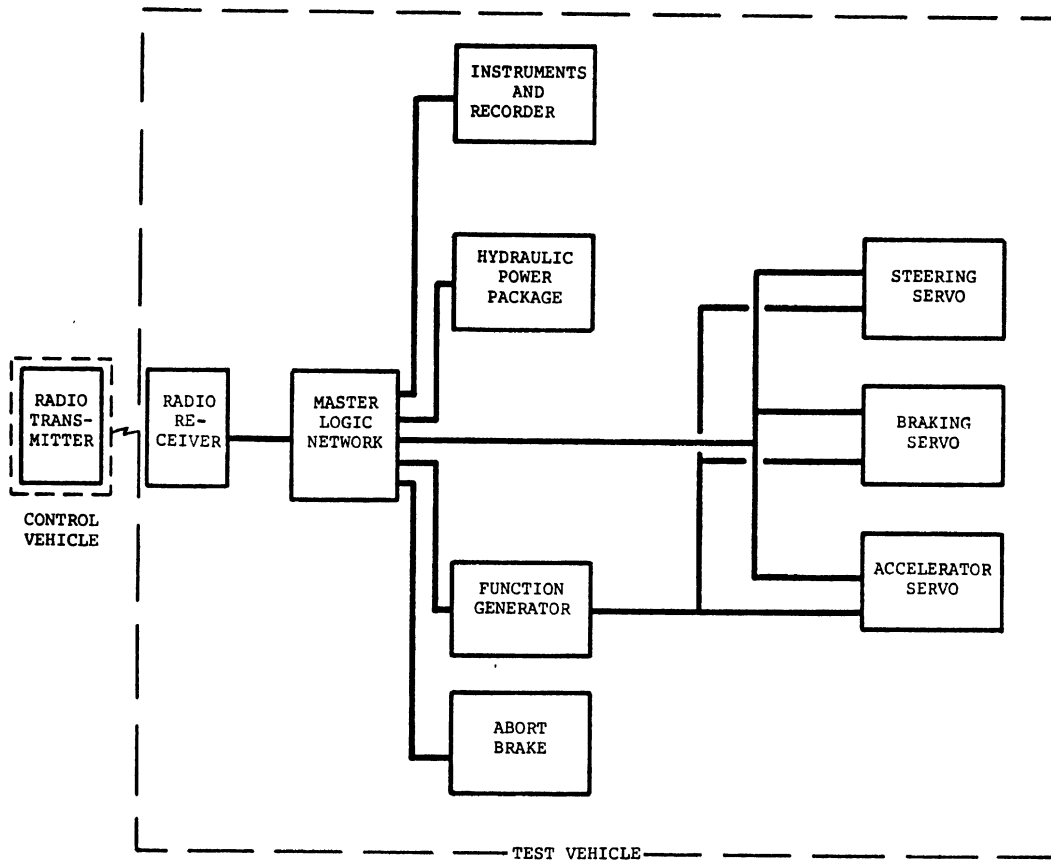
FIGURE 7. BLOCK DIAGRAM OF AUTOMATIC VEHICLE CONTROLLER

26

The radio transmitter/receiver is a 5-channel system outputting DC voltage signals for the following functions:

1. proportional steering command

2. proportional braking command

3. proportional accelerator command

4. program function generator "start/stop"

5. abort brake system on/off

The steering servomechanism is an electro-hydraulic position feedback device which controls the angular position of the steering shaft. A hydraulic motor mounted to the steering column drives a steering pulley (installed in place of the steering wheel) through a timing belt (Fig. 8).

The braking servomechanism is an electro-hydraulic position feedback system which controls the displacement of the brake pedal. A small hydraulic actuator mounted with manifold and valve assembly on the steering column, pushes on a steel plate clamped directly to the brake pedal (Fig. 8).

The accelerator servo is a DC torque motor system which uses simple pinion and rack gearing to obtain a rectilinear output (Fig. 9). This servo can either push directly on the accelerator pedal or push or pull through some other connection to the carburetor linkage.

Performance specifications for the three control servos are tabulated in Table 1. These characteristics effectively represent the performance limitations of the control system, hence the constraints on the inputs it is capable of producing.

FIGURE 8. STEERING AND BRAKING SERVOMECHANISMS INSTALLED
IN FORD STATION WAGON
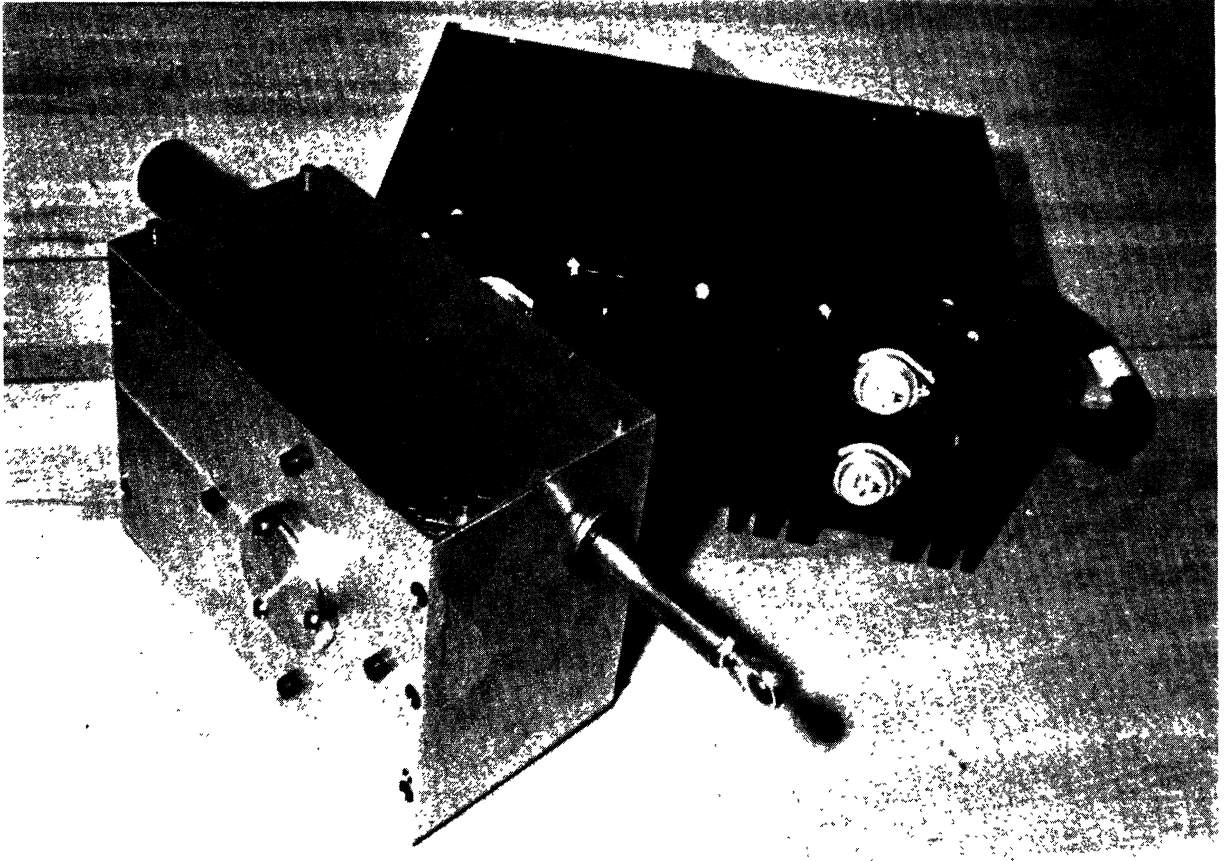
FIGURE 9. SERVOMOTOR AND GEARBOX FROM AUTOMATIC ACCELERATOR CONTROLLER

TABLE 1	
PERFORMANCE CHARACTERISTICS OF CONTROL SYSTEM SERVOMECHANISMS	

Steering Servomechanism

Total travel	$\pm$3.95 revolutions
Max. torque at 1300 deg/sec rotational speed	62 ft-lb
Stall torque	148 ft-lb
Response time (to within 5% error)	0.022 sec
Static error coefficient	380

Braking Servomechanism

Total travel	3.0 in
Max. force	400 lb
Response time (to within 5% error)	0.030 sec
Static error coefficient	290

Accelerator Servomechanism

Total travel	2.6 in
Max. force	15 lb
Response time (to within 5% error)	0.062 sec

The hydraulic power circuit (Fig. 10) provides 900 to 1400 psi hydraulic fluid to the steer and brake servos. An accumulator stores sufficient high pressure fluid to allow the steering actuator to rotate through 9 full revolutions (at the steering shaft), or the brake actuator to apply as many as five 2 1/2" stroke pedal displacements (during a single 10 second maneuver sequence). The hydraulic pump is driven by a 12 volt DC starter motor. The extreme current drawn by this motor throughout the duration of a test run necessitates the installation of a heavy duty alternator to maintain battery charge. The hydraulic power
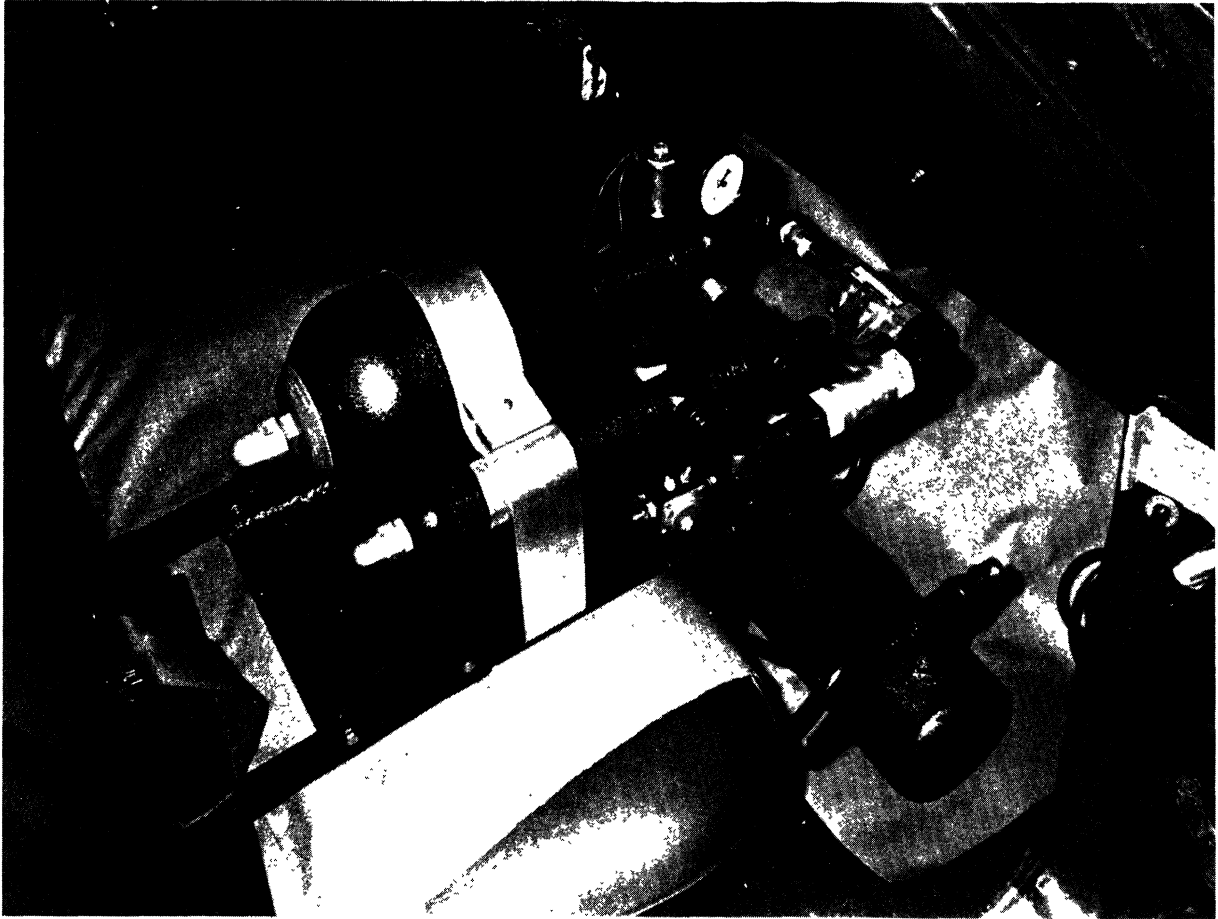
FIGURE 10. HYDRAULIC POWER CIRCUIT FOR VEHICLE CONTROLLER
INSTALLED IN FORD STATION WAGON

assembly is mounted on the floor and front seat on the passenger side of the test vehicle.

The function generator is the key component of the automatic control system. It is an electro-mechanical instrument which stores the maneuver program and, ultimately, commands the servos to execute the programmed steering, brake and accelerator control inputs. It consists of an accurate oscillator powering a synchronous motor which rotates two 100-position switch assemblies. The 100 switch contacts, encountered over a 10 second time period, control the timing of the servo input commands. One switch assembly controls the steering function timing and the other controls both brake and accelerator timing. The steering time history can assume any functional shape, analytic or nonanalytic. The brake time history is confined to a ramp-fronted step of variable ramp slope, step height, and duration.

Since the 10 sec program is distributed into 100 timing increments, the maneuver program board (Fig. 11) is arranged to allow time history selection to a 0.1 sec resolution. Thus the steering function, on the lower half of the board, has 100 discrete adjustment potentiometers. The setting on any potentiometer is verified by displaying on the digital panel meter, center left. During system operation, the internal steering function switch assembly provides each full potentiometer voltage for 50 milli-seconds followed by the average between that pot setting and the next one for the next 50 milliseconds, and so on. Filtering circuits then smooth the function. Shown in the Fig. 11 photo-graph is a half-sine wave of steering from 2.0 to 3.0 seconds, followed by a full sine wave from 5.0 to 7.0 seconds.

In the upper left and upper right of the program board are the manual selector switches which determine the time at which the accelerator or brake commands are either high (at the adjusted
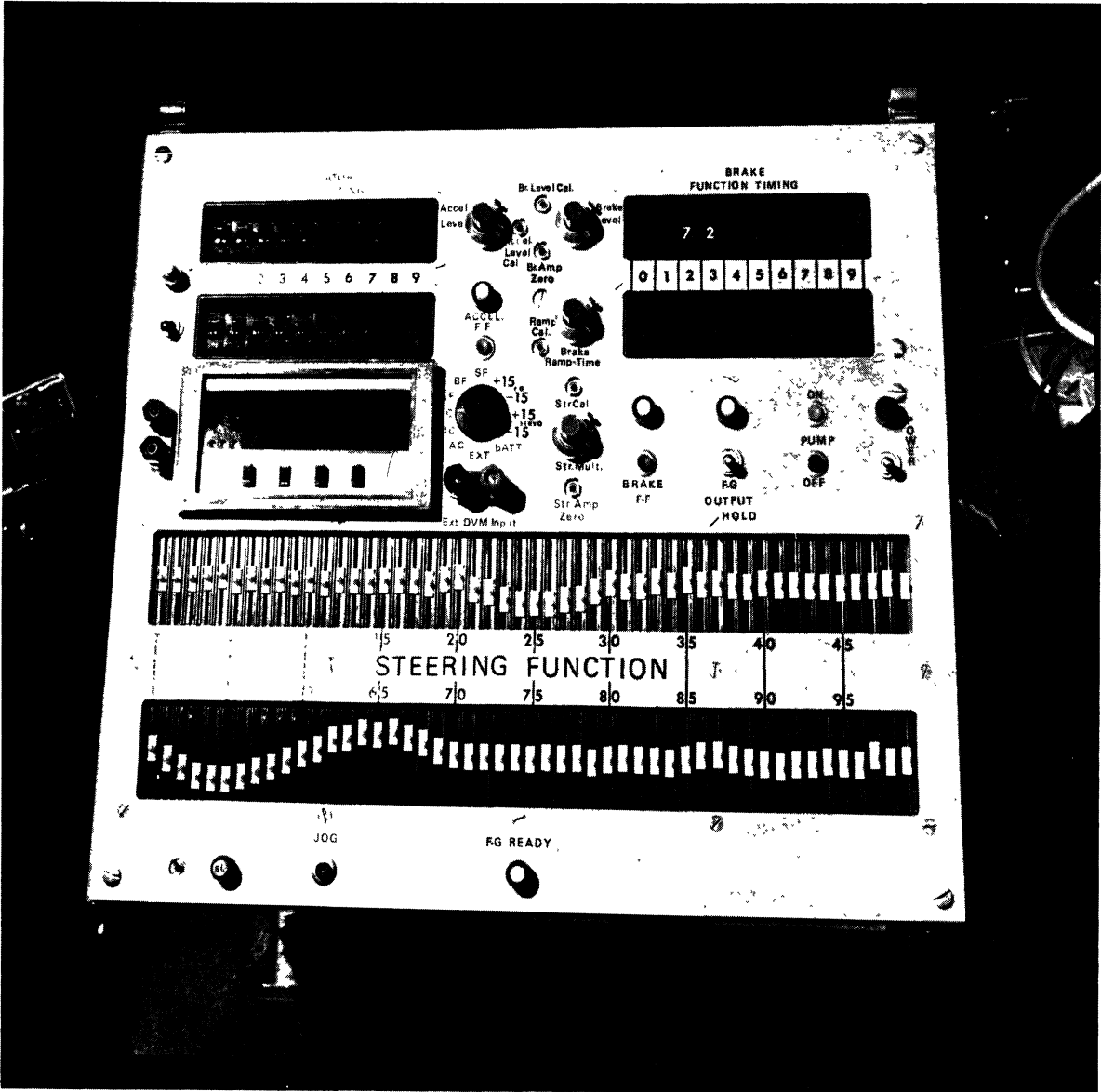
FIGURE 11. FUNCTION GENERATOR FOR AUTOMATIC VEHICLE CONTROLLER

level), or at zero. The brake switch bank (upper right) in Fig. 11, for example, is set up to have the ramp-fronted brake step begin at 2.7 seconds and re-zero (release) at 3.2 seconds.

The master logic network is an array of electronic logic elements which control the rational interlocking of system operating modes, startup procedures, and (fail-safe) abort brake activation. It performs this control function in accordance with the status of the following factors:

1. Vehicle transmission in "park" or not

2. Radio carrier being received or not

3. Abort function being commanded on or off

4. Recorder running or not

5. Function generator set or not

6. Accelerator and brake flip-flops high or low

7. Hydraulic pump motor on or off

8. Drone mode brake command high or zero

The abort brake system, shown schematically in Fig. 12, is an auxiliary fail-safe brake mechanism for providing emergency braking by application of the two front brakes. To hold the abort brake off, and allow system operation, a chain of signals must be present from the transmitter to the brake actuator's solenoid. This sustains engine manifold vacuum on the modified boost assembly, and holds the brake cocked, also allowing the standard brakes to be applied. If any signal in the chain is interrupted, the brake applies.

A further backup to the abort brake is a feature whereby the loss of radio carrier applies the servo brake as well as the abort brake. The abort function, however achieved, also causes the accelerator servo to go to idle.

34
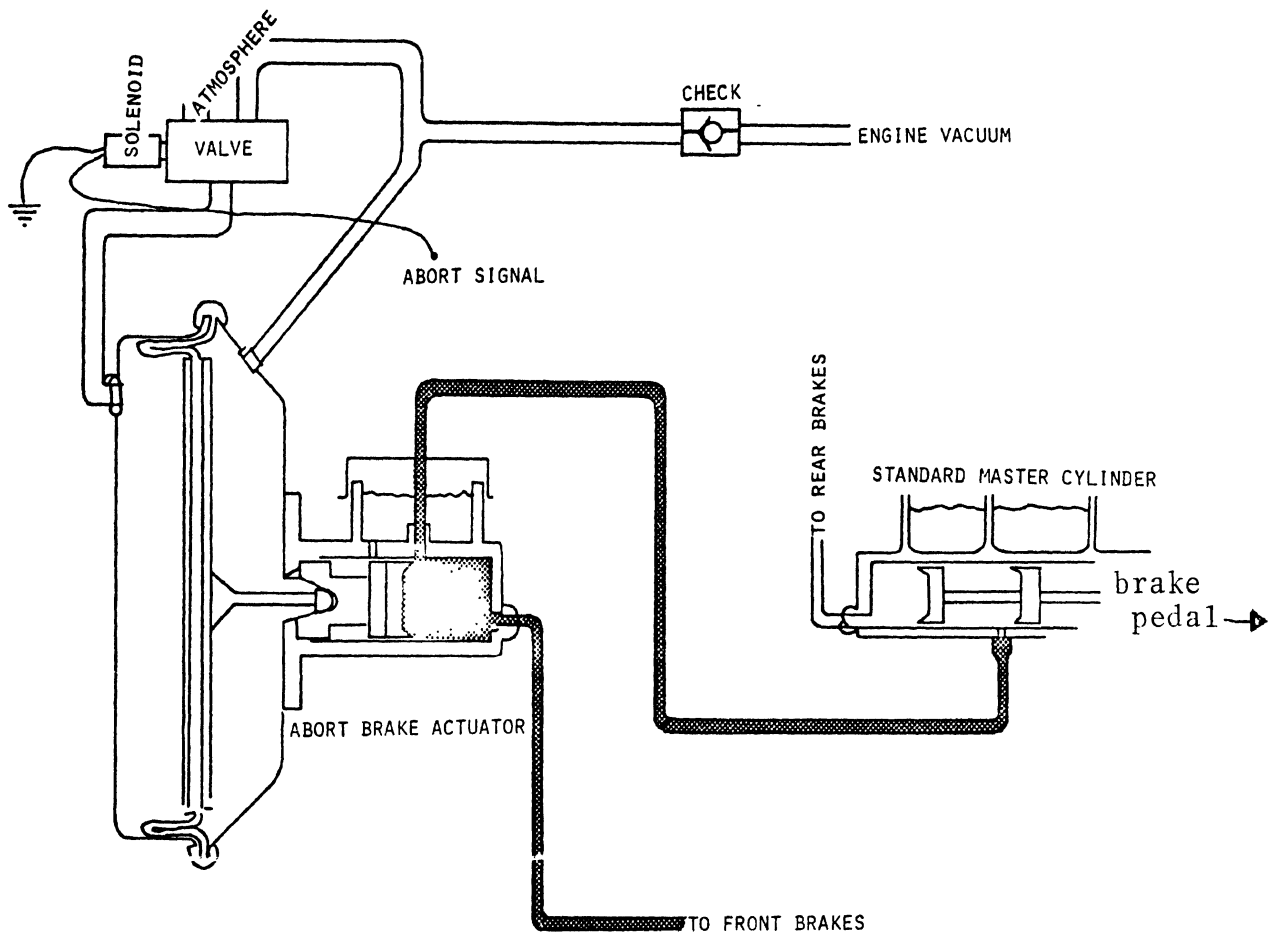
FIGURE 12. SCHEMATIC DRAWING OF ABORT BRAKE SYSTEM

A separate instrumentation package was used in the automatic-control tests. The following eight data signals were recorded on a light beam oscillograph:

1 and 2.   Left front and left rear wheel rotation (reed switches)

    3.   Front brake line pressure

    4.   Yaw rate (to 115 deg/sec)

    5.   Roll rate (to 40 deg/sec)

    6.   Position feedback from steer servo

    7.   Position feedback from brake servo

    8.   Position feedback from accelerator servo

The recorder was set up such that the chart paper would be running (at 2 in/sec) whenever the function generator was running.

The installation of the automatic controller and associated instrumentation into each of the vehicles tested was a 2-3 day task. Equipment arrangements differed somewhat from vehicle to vehicle, depending upon space available and ease of access. The packages installed in the Ford, Corvair, and Toyota, respectively, are shown in Figs. 13, 14, and 15.

3.3 TEST SITE

The pilot tests were conducted on the East Ramp of the University of Michigan Willow Run Airport. This ramp is a 3300 x 425 ft concrete-paved pad, a portion of which has been resurfaced with strips of asphalt and painted asphalt (see Fig. 16). Some straight line braking tests were performed on the painted asphalt strip, wetted down to provide a low friction coefficient surface. All other testing took place on the concrete pavement. Experiments

36

VIEW THROUGH RIGHT FRONT DOOR

VIEW THROUGH REAR DOOR

FIGURE 13. EQUIPMENT PACKAGE FOR AUTOMATIC-CONTROL TESTS
INSTALLED IN FORD STATION WAGON
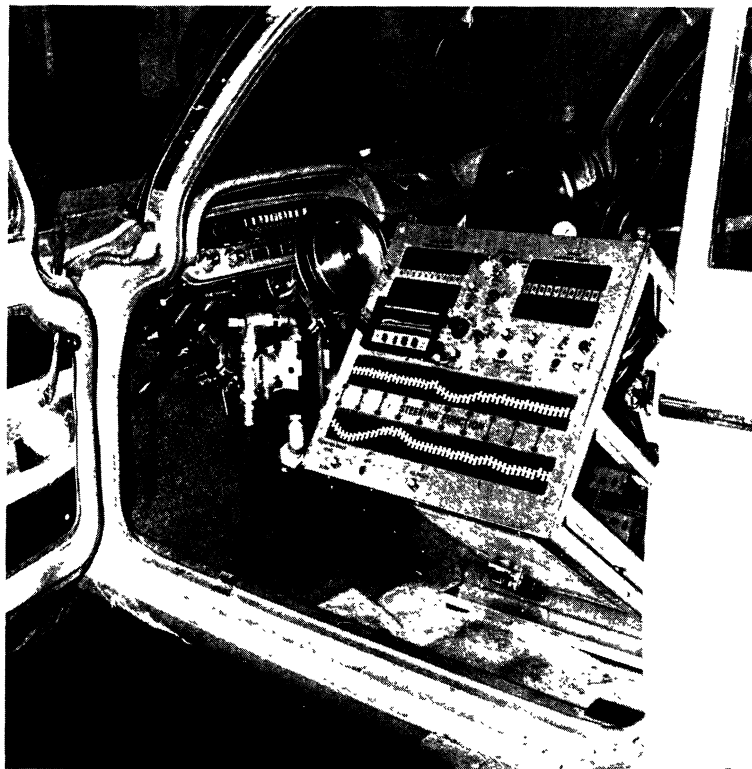
VIEW THROUGH LEFT DOOR
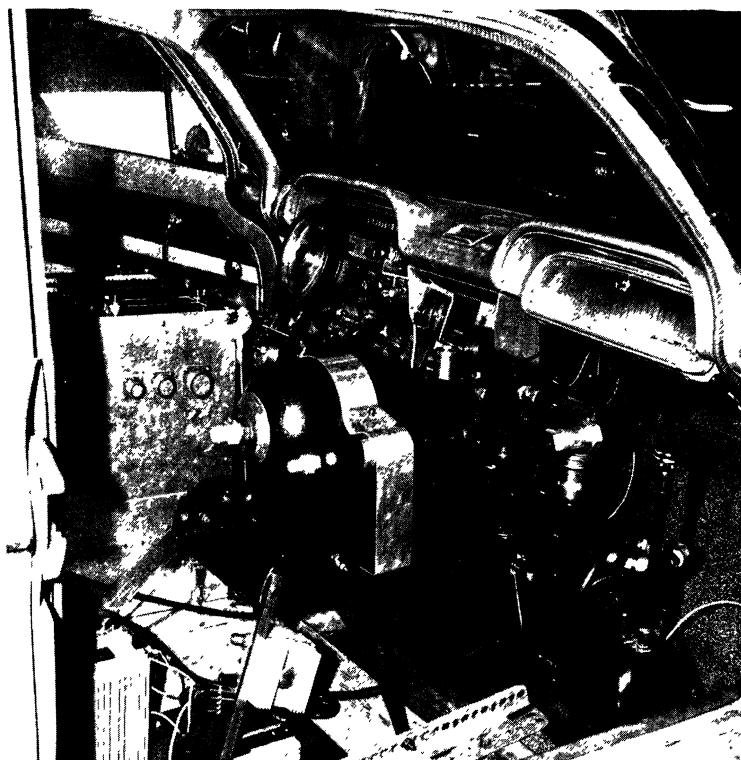
VIEW THROUGH RIGHT DOOR

FIGURE 14. EQUIPMENT PACKAGE FOR AUTOMATIC-CONTROL TESTS
INSTALLED IN CORVAIR
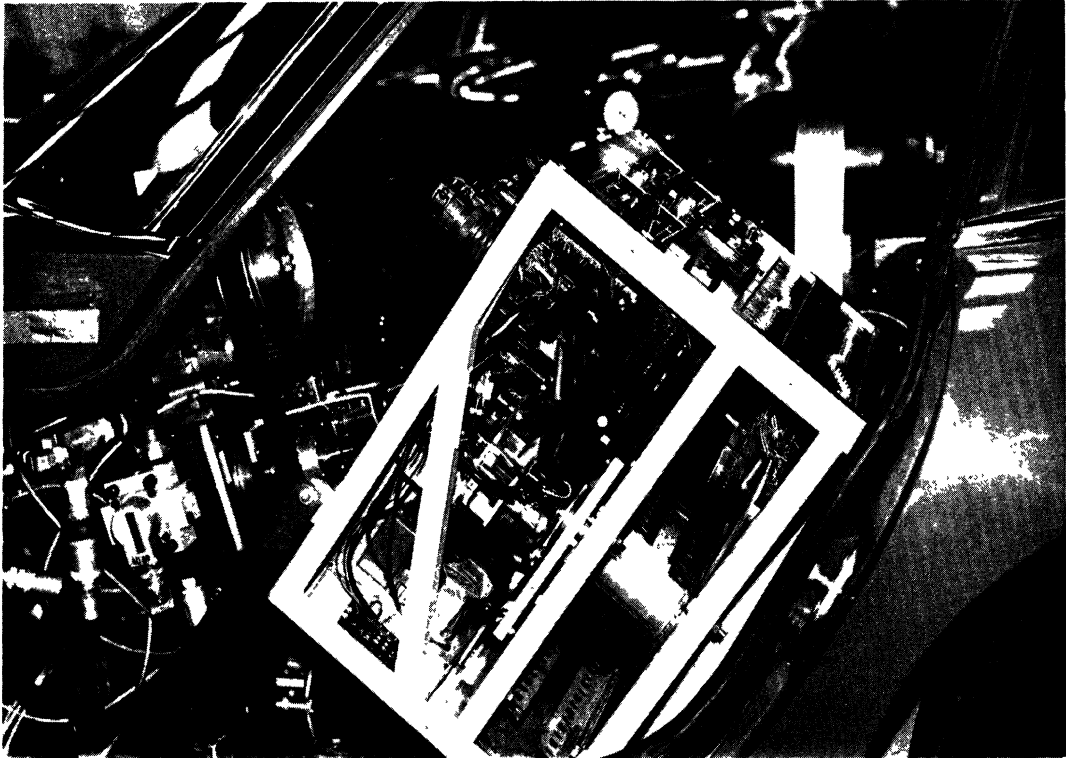
VIEW THROUGH LEFT DOOR
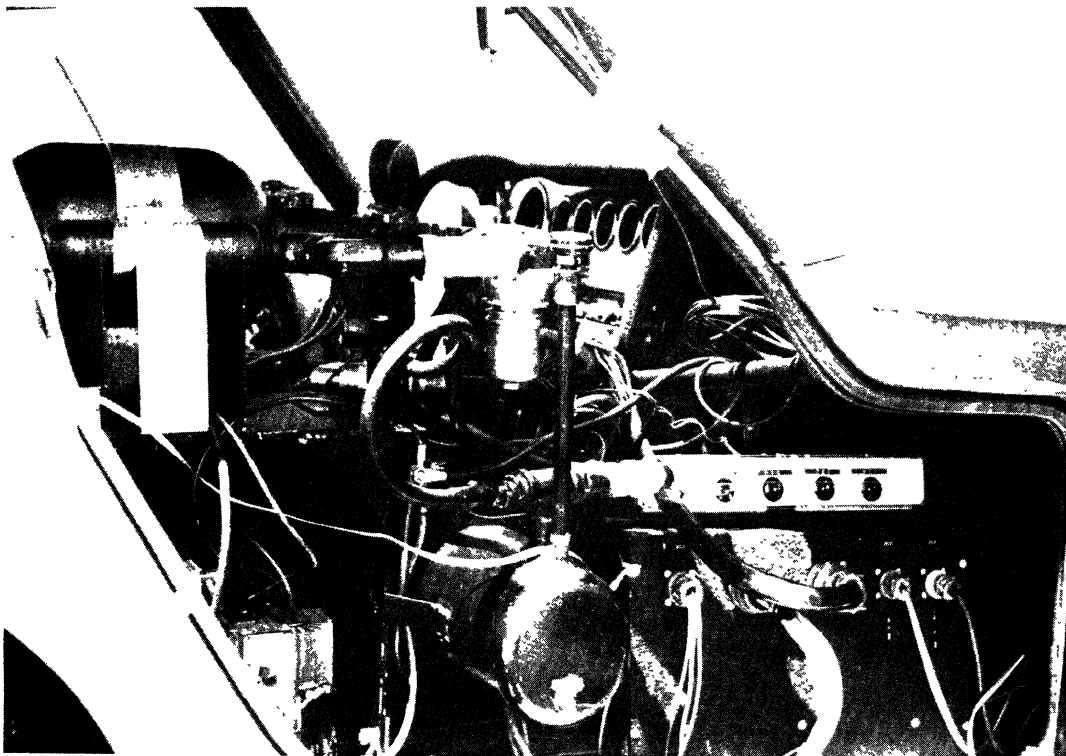
VIEW THROUGH RIGHT DOOR

FIGURE 15. EQUIPMENT PACKAGE FOR AUTOMATIC-CONTROL TESTS
INSTALLED IN TOYOTA
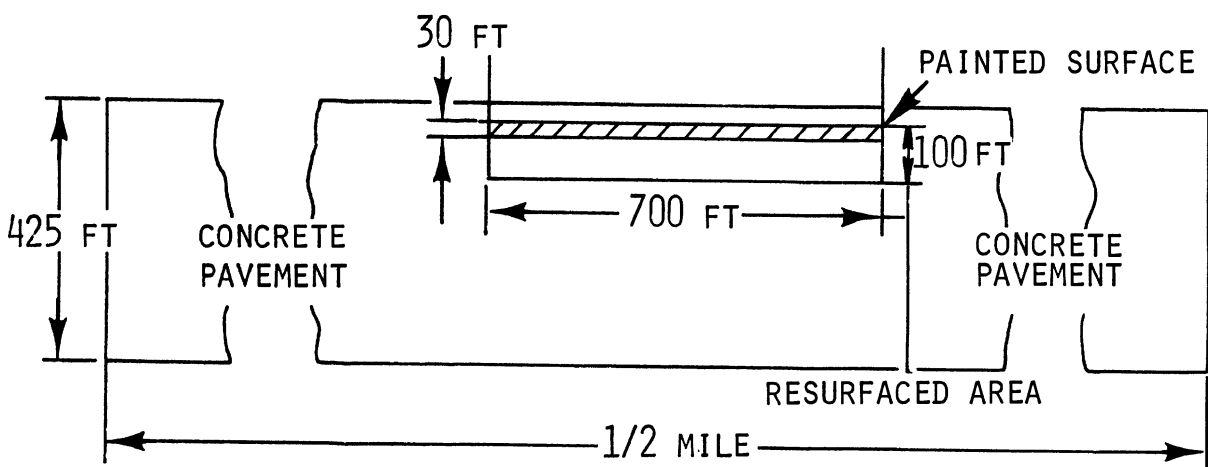
FIGURE 16. VEHICLE TEST FACILITY - - EAST RAMP, WILLOW RUN AIRPORT

in which severe maneuvers (e.g., "drastic" steer and brake) were performed at speeds of 60 mph or more required just about all of the available area for acceleration to speed, test execution, and runout.

3.4   TEST PROGRAM

In this section, we describe the program of experiments corresponding to each of the limit performance maneuvers discussed in Section 2.0.   Only test schedules and procedures are described. The test results are presented and discussed in Section 4.0 which follows.

3.4.1   STRAIGHT LINE BRAKING.   These tests involved the measurement of straight-line braking effectiveness, from an initial speed of 30 mph, with a program of brake inputs designed to permit the precise determination of deceleration at the point of incipient wheel lockup, hence braking efficiency.

Brake inputs of a quasi-step form were produced by slamming the brake pedal against the adjustable stop, set according to a calibration curve relating pedal displacement to brake line pressure (for the rolling vehicle).   In a sequence of tests for a given set of loading and pavement conditions, line pressure was first increased in increments of approximately 100 psi until a wheel lockup condition was encountered.   Tests were then made with pressures decreased in approximately 25 psi increments in order to define the lockup condition with more precision than could be done with the initial increment size.   A series of repeatability runs were then performed with line pressures set as near as possible to the lockup condition.

In each test run, the steering wheel was held fixed and pedal displacement, to the mechanical stop, was achieved in less than 0.18 seconds.   Although pedal application delay can be a significant

41

factor in stopping distance tests, its effect on the results measured here is virtually negligible because of the nature of the data reduction method (see Sec. 4.0).

Brake lining temperatures were maintained between 150° and 250° before each run. Representative data on fade characteristics of brake lining materials indicate that variability in braking effectiveness due to thermal effects is relatively moderate over this conveniently maintained temperature range (see Fig. 17).

Each test vehicle was subjected to straight line braking tests on two pavement surfaces: dry concrete and wet, painted asphalt. Tests were run on all vehicles in an "unloaded" condition (test driver plus instrumentation package). In addition, the Ford Station Wagon was tested with a load of 450 lb in the rear luggage compartment. This additional loading resulted in a front to rear weight distribution of 2335 lb/3075 lb, as opposed to 2445 lb/2515 lb when the vehicle was in the nominally loaded condition.

In each straight line braking test, the following data were recorded:

A_x — longitudinal acceleration

V — fifth wheel velocity

w_f — front lockup indicator

w_r — rear lockup indicator

P_f — front brake line pressure

3.4.2 RESPONSE TO RAPID, EXTREME STEERING. In these tests, the vehicle was subjected to a quasi-step displacement of the steering wheel, concurrent with the release of the accelerator, with the vehicle moving initially in a straight path at a speed of 30 mph.
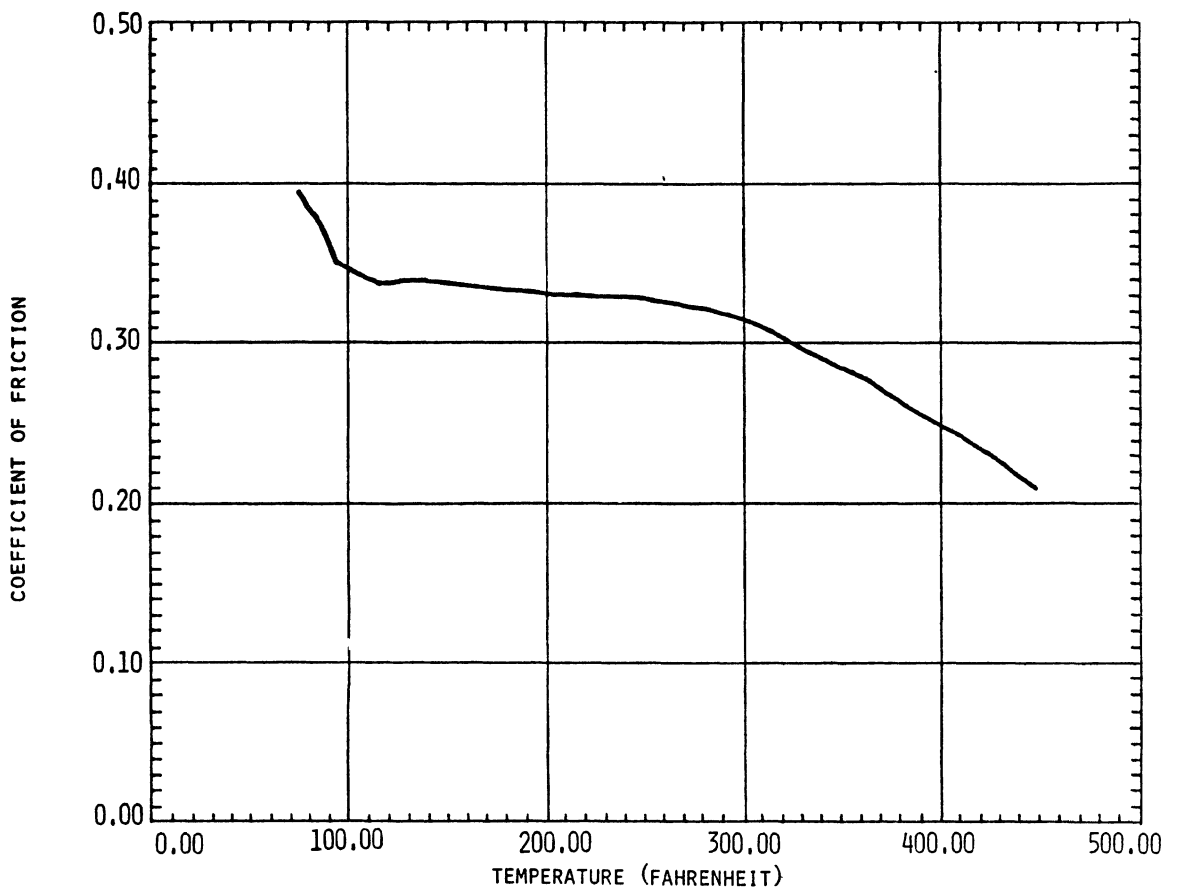
FIGURE 17. THERMAL FADE CHARACTERISTICS OF FRICTION MATERIAL AS
DETERMINED FROM DYNAMOMETER TESTS OF DISC BRAKES (FROM REF. 9)

The steer inputs were applied by slamming the wheel against the adjustable steering stop. The time required for the test driver to achieve full steering wheel displacement in a number of representative runs is shown in Fig. 18. The points illustrated represent the 3 largest steering wheel displacements used with each vehicle, plus one other displacement near 180°. The effect of variations in steering input rate was investigated by computer simulation. Figure 19 shows simulation time histories of yaw rate and lateral acceleration computed using steering inputs with 0.18 sec and 1.5 sec delay times (the computer steering delay was a first order lag with (3 τ) = 0.18 and 1.5, respectively -- see Appendix B). Although the time shift is evident in the recordings, the peak levels reached are very close.

A test sequence consisted of successive runs with systematically increasing values of normalized steer angle,

$$\Delta'_{SW} = \frac{\Delta_{SW}}{\ell N_G} \qquad (1)$$

where Δ_{SW} is the steering wheel displacement, ℓ is the vehicle wheelbase, and N_G is the overall steering ratio as determined experimentally by measuring front wheel and steering wheel displacements with the front wheels lifted clear of the ground. It can be shown from geometric considerations that Δ'_{SW} represents the zero-speed-limit value of path curvature corresponding to the steering wheel angle Δ_{SW}. Accordingly, differences in the path curvature response of vehicles operating with equal values of Δ'_{SW} are entirely attributable to the influence of dynamic effects.

Each test vehicle was subjected to quasi-step steering response tests under at least two sets of service factor conditions: (1) nominal - vehicle loaded with driver plus instrumentation, and tires inflated as per manufacturer's recommendation, and (2) off-design in a manner intended to degrade performance -- with rear-biased load, underinflated rear tires, and overinflated front tires.
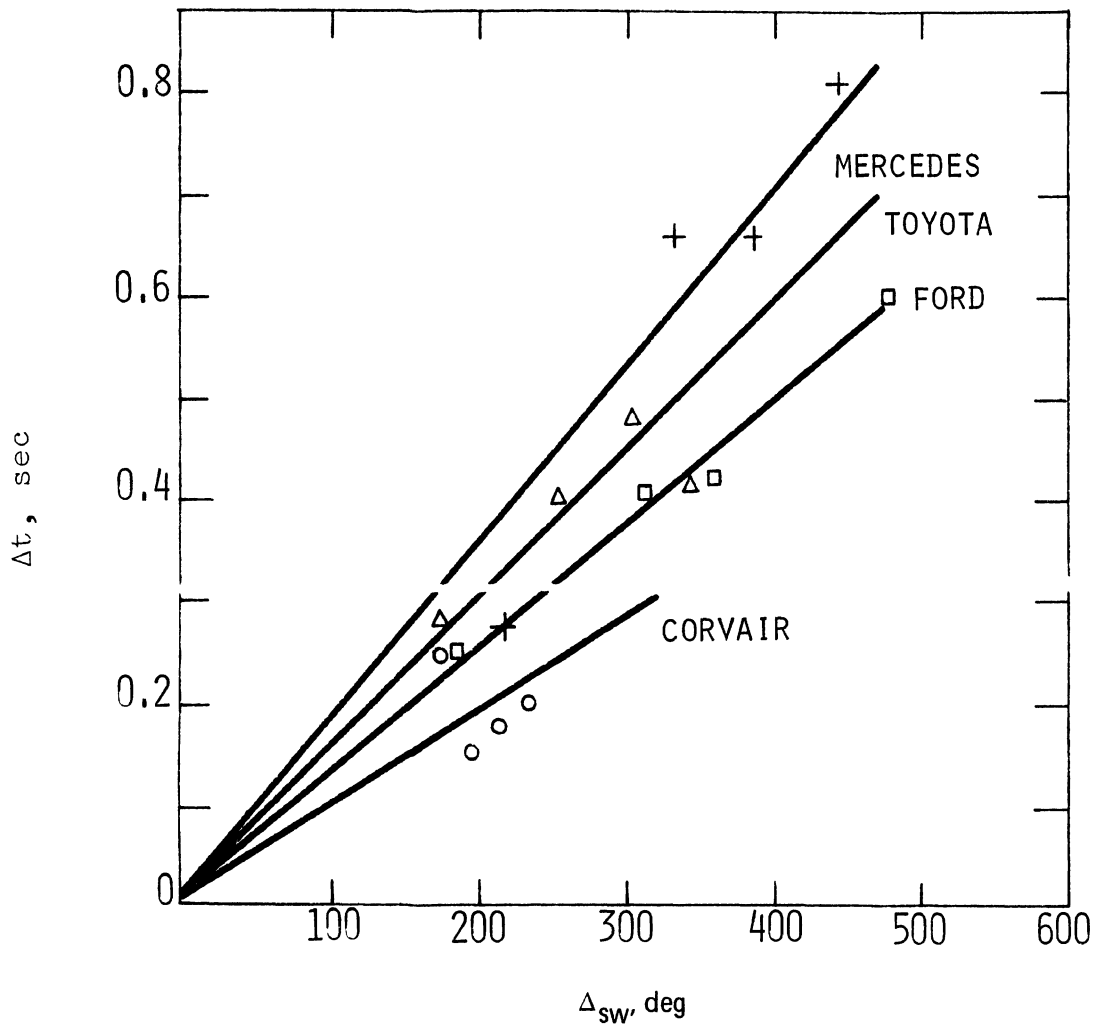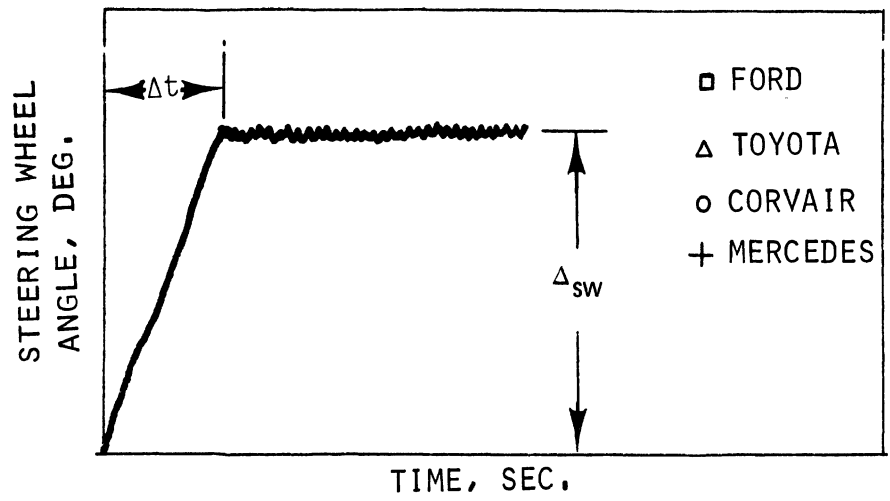
FIGURE 18. DELAY TIMES OF QUASI-STEP STEERING WHEEL INPUTS
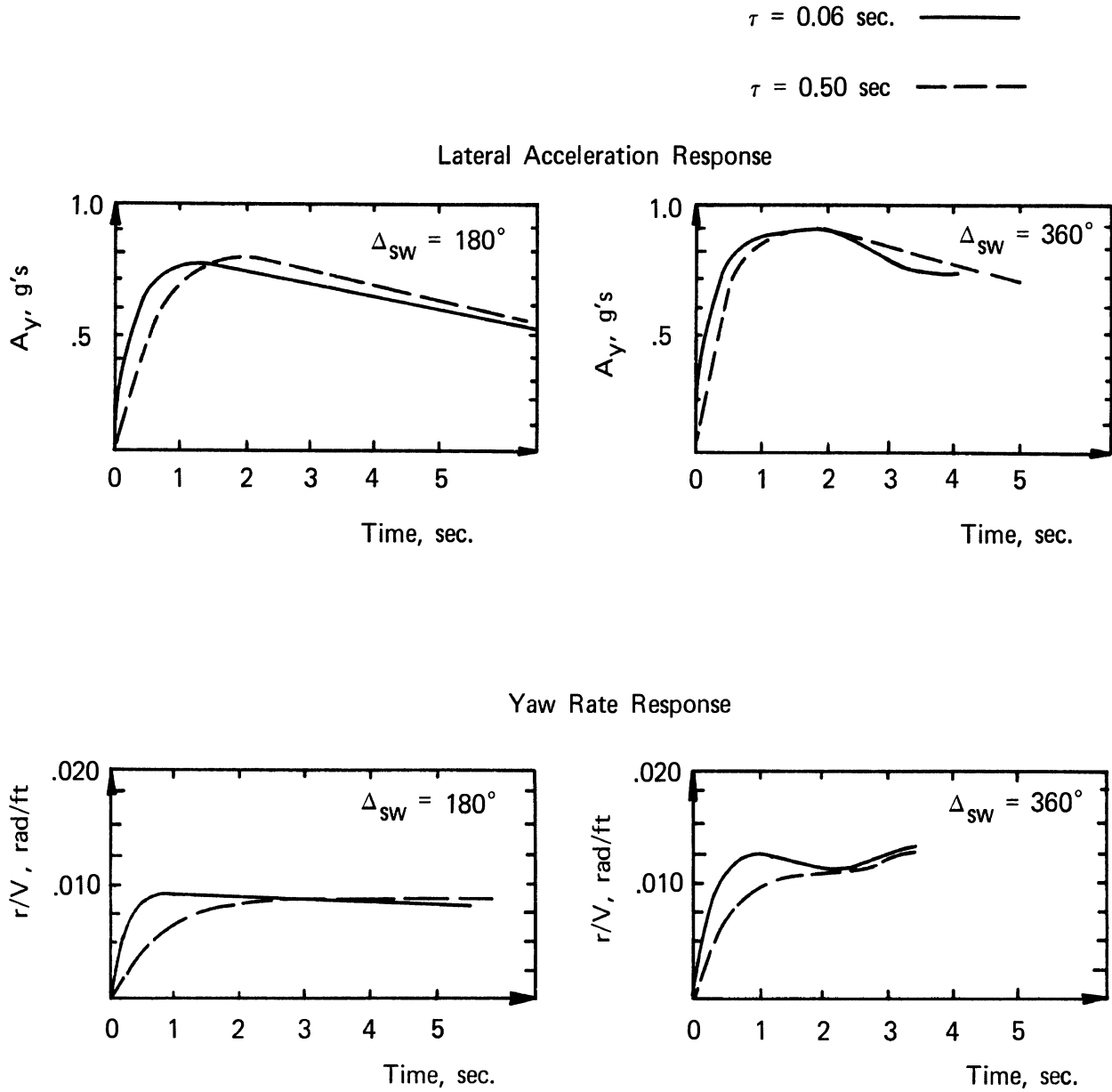
FIGURE 19, INFLUENCE OF STEER DELAY TIME ON RESPONSE TO QUASI-STEP STEERING WHEEL INPUTS - - SIMULATED FORD STATION WAGON

46

A complete listing of test conditions for the quasi-step steering response tests is given in Table 2.

TABLE 2

TEST CONDITIONS FOR QUASI-STEP STEER RESPONSE MEASUREMENTS

Vehicle	Tire Pressures, psi F	R	Carge Compartment Load, lb.	Steering Wheel Displacement, degrees, at Indicated Value of Δ'_{sw} .4	.5	.6	.7	.8	.9	1.0	1.1	1.2	1.4	1.6	2.0	2.4	2.8	3.2
Ford	28	28	0	90	112	135	157	180	203	225	248	270	315	360	450	X	X	X
	32	24	0	90	112	135	157	180	203	225	248	270	315	360	450	X	X	X
	32	24	450	X	X	X	X	X	X	X	X	270	X	360	450	X	X	X
Corvair	18	30	0	86	108	129	151	172	194	215	237	X	X	X	X	X	X	X
	28	28	0	86	108	129	151	172	194	X	X	X	X	X	X	X	X	X
Mercedes	28	34	0	55	69	83	96	110	124	138	152	165	193	220	276	331	386	442
	31	31	450	55	69	83	96	110	124	138	152	165	193	220	276	331	386	442
Toyota	27	27	0	43	54	65	76	87	98	108	119	130	152	174	217	260	304	347
	30	24	180	43	54	65	76	87	98	108	119	130	152	174	217	260	304	347

In each step steering test, the following data were recorded:

A_y - lateral acceleration

V - fifth wheel velocity

r - yaw rate

δ_{sw} - steering wheel angle

3.4.3 BRAKING IN A TURN. These tests involved the same procedure as the straight line braking tests, but the initial condition (instead of being a straight course equilibrium) was a 30 mph steady turn producing a nominal lateral acceleration of 0.3 g. The steering wheel displacement required to establish the steady turn was held fixed throughout the maneuver. The

47

brake inputs were incremented following the same procedure described for the straight line tests (see Section 3.4.1). The test program included the service factor variations tabulated in Table 3.

TABLE 3

SERVICE FACTOR CONDITIONS: BRAKING IN TURN TESTS

Vehicle	Tire Pressures, psi		Load in Cargo Compartment lb	(Fixed) Steering Wheel Angle, deg.
	Front	Rear		
Ford	28	28	0	69.9
	32	24	450	74.5
Toyota	27	27	0	55.4
	30	24	180	40.0
Corvair	18	30	0	75.7
	28	28	0	75.7
Mercedes	28	34	0	73.2
	31	31	450	62.7

The following data were recorded:

A_y - lateral acceleration

r - yaw rate

V - fifth wheel velocity

δ_{sw} - steering wheel angle

P_f - brake line pressure

w_f - front lockup indicator

w_r - rear lockup indicator

3.4.4 TURNING ON A ROUGH SURFACE. Roadholding tests were performed by driving the test vehicle, initially in a steady turn, across a prefabricated rectangular grid of steel pipe constituting a fixed disturbance of road roughness (see Figure 20). The accelerator was released just prior to contact with the grid; the steering wheel was held fixed throughout the maneuver.

Tests were conducted at speeds selected to assure that the corresponding range of pipe/tire contact frequencies would circumscribe the range of fundamental wheel hop frequencies for the test vehicles. This range was established by estimating upper and lower limits representing, respectively,

> (1) the lightest front end unsprung mass resting on an over-inflated tire;

> (2) the heaviest solid rear axle unsprung mass resting on an under-inflated tire.

The respective estimates were 69.5 ft/sec (48 mph) and 24.2 ft/sec (16 mph). The overall speed range was arbitrarily divided into four equal increments. Thus tests were made with five different values of initial speed; V_o = 16, 24, 32, 40, 48 mph. Simplified vibration analyses of the automobile suspension-unsprung mass system indicate that typical "widths" of resonance peaks are broad relative to these speed increments. This assures that no significant resonance phenomenon passes undetected by the test procedure.

Each vehicle was subjected to roadholding tests with tires inflated at each of two different sets of inflation pressures: (1) according to manufacturer's recommendation, and (2) over-inflated by a constant increment at all four tires. The Ford station wagon was also tested with uniformly under-inflated tires. A complete listing of test conditions established for the roadholding tests is given in Table 4.

VEHICLE PATH

30 feet

4.4'

1 3/4"

1/4"

FIGURE 20. ROAD ROUGHNESS SIMULATOR CONFIGURATION

50
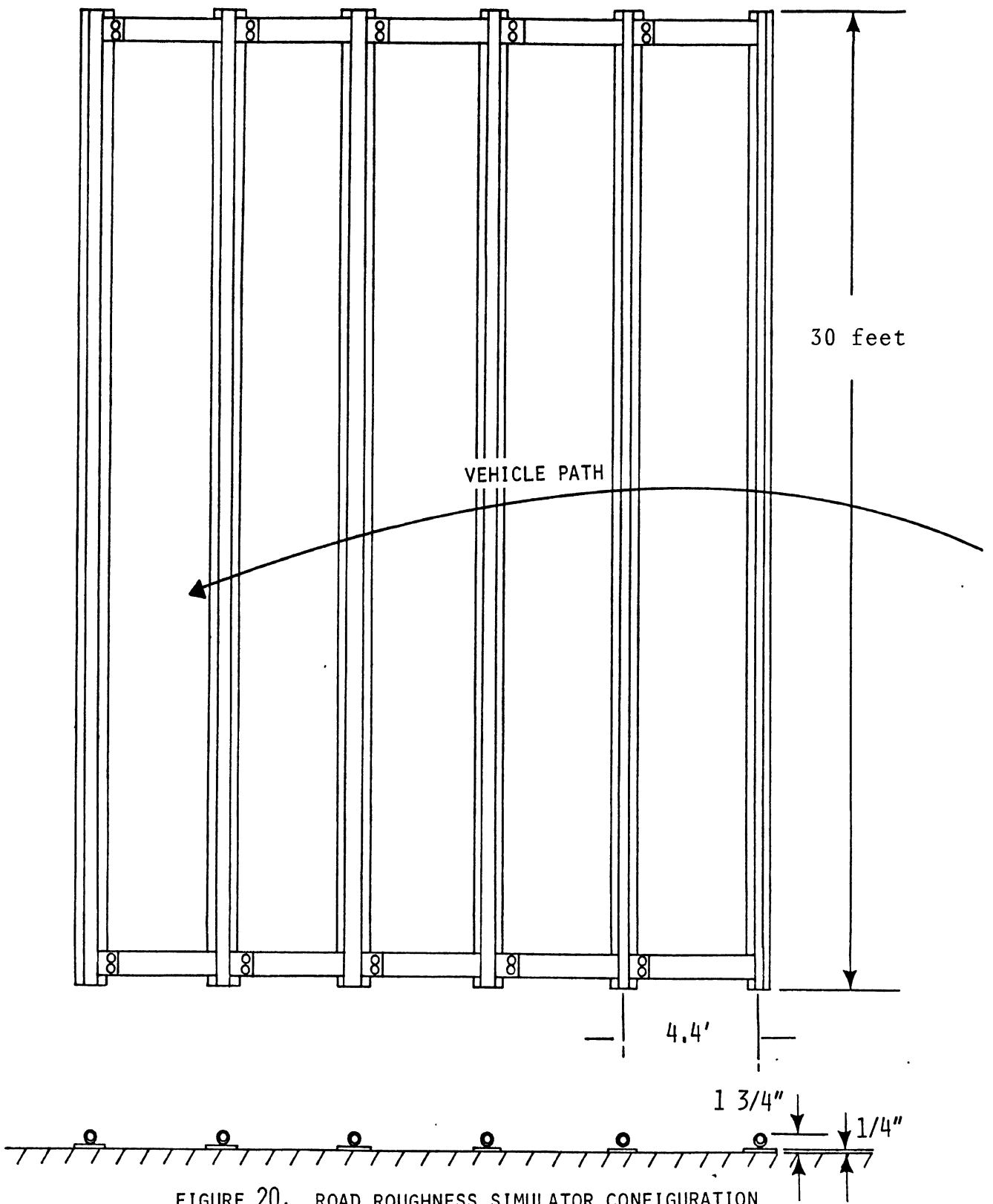
TABLE 4

TEST CONDITIONS FOR ROADHOLDING TESTS

Vehicle	Tire Pressures, psi		(Fixed) Steering Wheel Angle (deg) at Indicated Velocity				
	Front	Rear	16 mph	24 mph	32 mph	40 mph	48 mph
Ford	28	28	400	178	100	64.3	44.5
	37	37	400	178	100	64.3	44.5
	24	24	400	178	100	64.3	44.5
Corvair	18	30	300	120	85	54	X
	25	37	368	163	92	52	X
Mercedes	28	34	393	173	98	63	44
	35	41	320	139	80	51	36
Toyota	27	27	204	107	60	38	27
	31	31	204	107	60	38	27

The steering wheel angles were selected to produce initial (steady) values of lateral acceleration (A_{yo}) approximately equal to 0.4 g. Actual measured values of A_{yo} in fact varied substantially about this reference value. Exploratory tests showed, however, that the influence of initial acceleration, A_{yo}, on the normalized results was small over the range of deviation encountered.

Not surprisingly, the roadholding test data were character-ized by a considerable amount of oscillatory "noise", and dis-tinctly unfavorable signal to noise ratios. To reduce the level of measurement error arising as a consequence of this effect, multiple experiments were performed, and the results were aver-aged, for each set of test conditions. The average number of replications per test condition was 2.8.

In each roadholding test, the following data were recorded:

A_y - lateral acceleration

V - fifth wheel velocity

r - yaw rate

δ_{sw} - steering wheel angle

3.4.5 RESPONSE TO SINUSOIDAL STEER INPUT. The test vehicles were subjected to sinusoidal steer inputs with a fixed period of 2 seconds and systematically varied amplitudes. The 2 second wave period was established as representative of driver performance in emergency lane change maneuvers, on the basis of a limited program of driver-vehicle testing. Exploratory experiments indicated that vehicle response to sinusoidal steering was not qualitatively different over the range of input wave periods observed in the driver-vehicle tests.

Tests were conducted at nominal initial speeds of 30, 40, 50, and 60 mph. (Actual test speeds varied somewhat from the nominal values.) At each speed, runs were made with steer inputs of progressively increasing magnitude (following the release of the accelerator) until one of two limiting conditions was encountered, at which point the speed was incremented to the next higher level. Specifically, the speed was incremented if (1) the steer amplitude called for by the incrementing scheme exceeded 360°, or (2) the negative yawing velocity caused by left steer was observed to remain negative following the initiation and completion of the right steer portion of the input wave form. The first limit corresponds to the peak magnitude of steering wheel displacement considered likely in a real-world emergency lane-change (based on the driver-vehicle tests); the second limit represents a limit performance condition we define as a "divergent response".

The procedure for incrementing steering amplitude was designed to provide inputs of systematically increasing severity while minimizing the total number of runs required to map the response space. The steer amplitudes used were computed from the following formula:*

$$\Delta_{SW} = \frac{0.4(1 + i)N_G g \ell}{V_o^2} \qquad (2)$$

In equation 2, the index variable, i, was assigned integer values to calculate Δ_{SW} for each initial speed (V_o), according to the scheme illustrated in Table 5. Tests were first run at V_o = 30 mph with steer amplitudes computed (from equation 2) with i = 1, 2, ..., as indicated. When i_a was reached, corresponding to a steer amplitude greater than 360° at V_o = 30 mph, V_o was incremented to 40 mph and i_a was used (in equation 2) to calculate the first Δ_{SW} at that velocity. Indices i_b and i_c were likewise shifted to the higher velocity brackets.

Test runs with each car were conducted until the limit (divergent) response was observed, at i = i_{crit}. Runs were then made at steer/speed conditions calculated using i_{crit} for all test velocities higher than the velocity at which the limit was first observed. If i_{crit} did not produce critical response at each higher velocity, then successive runs were performed at i_{crit} + 1, i_{crit} + 2, etc., within each velocity, until the limit was again achieved. If i_{crit} did produce limit response at higher velocity, then further runs were made at i_{crit} - 1, i_{crit} - 2, etc., until a nondivergent response was obtained.

---

*It should be noted that this expression is related to the steady state lateral acceleration gain of the neutral steer vehicle [10].

TABLE 5

SCHEME FOR INCREMENTING STEERING WHEEL AMPLITUDE
IN SINUSOIDAL STEER TESTS

Initial Velocity, V_o, mph			
30	40	50	60
i Δ_{sw} (from eq. 2)	i Δ_{sw} (from eq. 2)	i Δ_{sw} (from eq. 2)	i Δ_{sw} (from eq. 2)
1 Δ_{sw1}			
2 Δ_{sw2}			
. .			
. .			
. .			
i_a $\Delta_{sw} > 360°$ →	i_a Δ_{sw_a}		
	i_{a+1} $\Delta_{sw_{a+1}}$		
	. .		
	. .		
	. .		
	i_b $\Delta_{sw} > 360°$ →	i_b Δ_{sw_b}	
		i_{b+1} $\Delta_{sw_{b+1}}$	
		. .	
		. .	
		. .	
		i_c $\Delta_{sw} > 360°$ →	i_c Δ_{sw_c}
			i_{c+1} $\Delta_{sw_{c+1}}$
			. .
			. .
			. .
		Highest value of i applicable for this vehicle →	i_{d-1} $\Delta_{sw_{d-1}}$
			i_d $\Delta_{sw} > 360°$

Sinusoidal-steering response tests were performed with the same combinations of service factors as the quasi-step steering response tests (see Table 2). All eight data signals produced by the automatic-control test instrumentation package were recorded during each test, viz:

p - roll rate

r - yaw rate

w_f - front lockup indicator

w_r - rear lockup indicator

P_f - front brake line pressure

δ_{sw} - steering wheel angle

δ_{BP} - brake pedal displacement

δ_a - accelerator displacement

3.4.6 RESPONSE TO "DRASTIC" STEER AND BRAKE INPUTS. The test vehicles were subjected to steering and braking inputs of the form illustrated in Figure 21. The steer input was a half sine wave of 1.0 second duration. The brake input, a quasi-pulse of 0.5 second duration, was initiated at time t_1 corresponding to the instant of 95% peak yaw rate response to a sinusoid of magnitude Δ_{sw_a}, as determined from the results of the sinusoidal steer tests (see Table 5 and Figure 21).

The ramp front of the brake input was adjusted to provide a 0.050 second delay to reach peak displacement. The corresponding application rates were compatible with driver performance observed in emergency braking maneuvers simulated on the skid pad.

The braking input level was held fixed throughout a test sequence with a given vehicle. For each vehicle, the brake pedal displacement, Δ_{BP}, was determined by making measurements of the relationship between pedal force, pedal displacement, and front brake line pressure. Δ_{BP} was taken to be that pedal displacement producing a line pressure corresponding to a pedal force of 250 lb, or 1300 psi, whichever was lower.
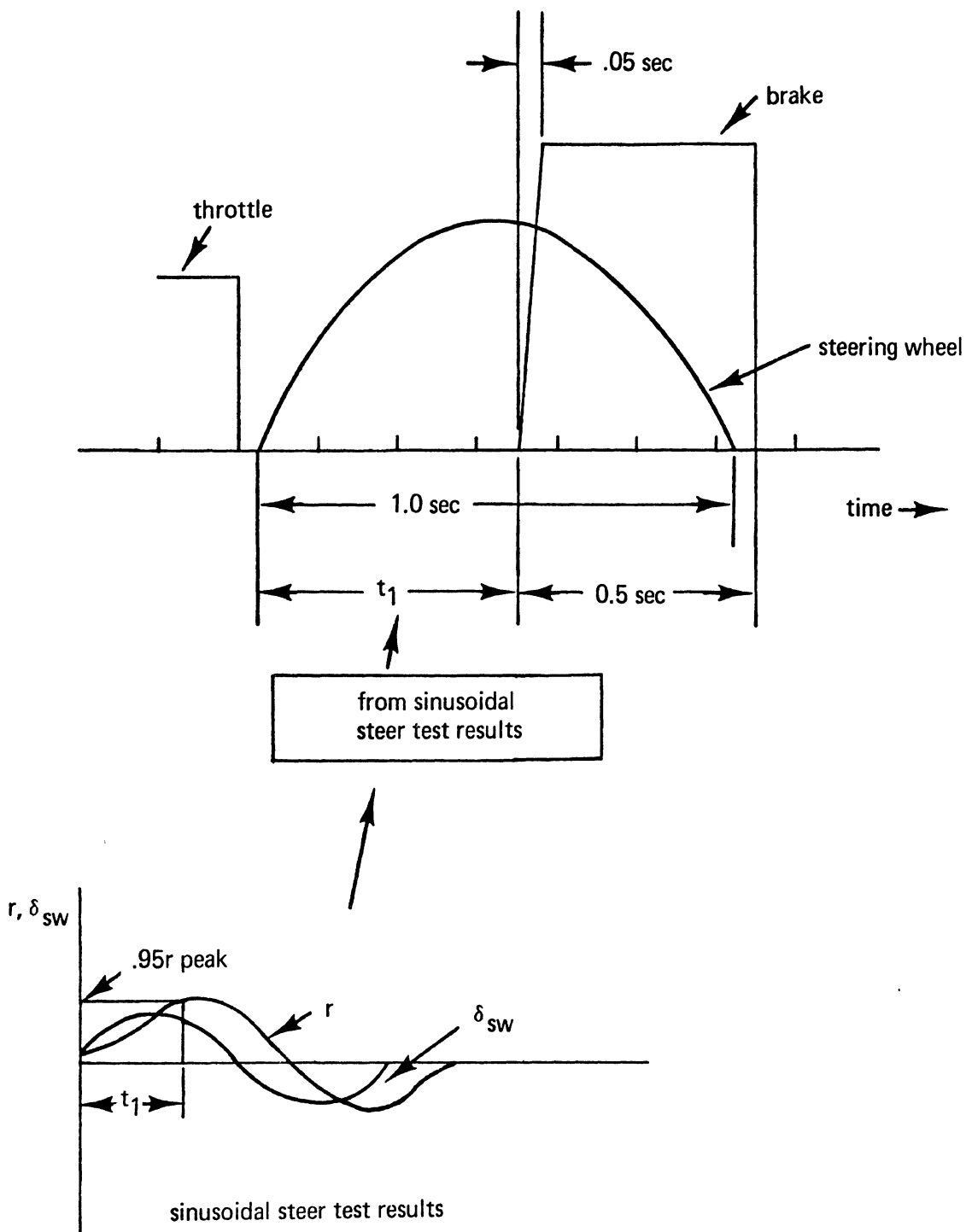
FIGURE 21. CONTROL INPUTS FOR "DRASTIC" STEER AND BRAKE MANEUVER

Thirteen hundred psi is the maximum brake system pressure allowable for the automatic controller's abort brake assembly. A pedal force of 250 lb corresponds approximately to the maximum capability of the 20th percentile male and the 80th percentile female, as estimated from static tests performed on a sample population of drivers [11]. In every test, the magnitude of the brake input was sufficiently great to produce wheel locking.

A complete listing of test conditions for the "drastic" steer and brake maneuver tests is given in Table 6. The test values of steering amplitude were varied according to equation 2, as in the case of the sinusoidal steering tests. The scheme for incrementation, however, was much less complete than the sinusoidal steering test procedure outlined in Table 5. Strong efforts were made to reduce the total number of runs because of the severe mechanical stresses imposed on the test

TABLE 6

TEST CONDITIONS FOR "DRASTIC" STEER/BRAKE RESPONSE MEASUREMENTS

Vehicle	Front	Rear	Load lb.	Nominal Speed mph	1	3	4	5	6	7	8	9	10	11	12	13	14	15	17	19	20	21	23	24	28	34
Ford	28	28	0	40	x	x	x	x	339	x	x	x	x	x	x	x	x	x	x	x	x	x	x	x	x	x
"	28	28	0	50	x	x	x	x	x	249	280	311	342	x	x	x	x	x	x	x	x	x	x	x	x	x
"	28	28	0	60	x	x	x	x	x	x	x	x	x	259	x	x	x	x	x	x	x	x	x	x	x	x
"	32	24	450	40	x	x	x	x	339	x	x	x	x	x	x	x	x	x	x	x	x	x	x	x	x	x
"	32	24	450	50	x	x	x	x	x	249	x	x	342	x	x	x	x	x	x	x	x	x	x	x	x	x
"	32	24	450	60	x	x	x	x	x	x	x	x	x	259	302	345	x	x	x	x	x	x	x	x	x	x
Toyota	27	27	0	30	x	x	x	249	x	332	x	x	x	x	x	x	x	x	x	x	x	x	x	x	x	x
"	27	27	0	40	x	x	x	x	x	x	x	x	256	303	349	x	x	x	x	x	x	x	x	x	x	x
"	27	27	0	50	x	x	x	x	x	x	x	x	x	x	x	x	x	239	269	x	x	328	359	x	x	x
"	27	27	0	60	x	x	x	x	x	x	x	x	x	x	x	x	x	x	x	x	200	x	x	250	300	360
"	30	24	0	40	x	x	x	x	x	x	x	x	x	x	x	x	344	x	x	x	x	x	x	x	x	x
"	30	24	0	50	x	x	x	x	x	x	x	x	x	x	x	x	x	x	x	x	x	x	x	359	x	x
"	30	24	0	60	x	x	x	x	x	x	x	x	x	x	x	x	x	x	x	x	x	x	x	x	300	x
"	30	24	180	40	x	x	x	x	x	x	x	x	x	x	x	x	344	x	x	x	x	x	x	x	x	x
"	30	24	180	50	x	x	x	x	x	x	x	x	x	x	x	x	x	x	x	x	299	x	359	x	x	x
Corvair	18	30	0	30	165	x	x	x	x	x	x	x	x	x	x	x	x	x	x	x	x	x	x	x	x	x
"	18	30	0	40	x	x	231	277	324	x	x	x	x	x	x	x	x	x	x	x	x	x	x	x	x	x
"	18	30	0	50	x	x	x	x	x	x	x	295	324	x	x	x	x	x	x	x	x	x	x	x	x	x
"	28	28	0	30	x	329	x	x	x	x	x	x	x	x	x	x	x	x	x	x	x	x	x	x	x	x
"	28	28	0	40	x	x	231	277	x	x	x	x	x	x	x	x	x	x	x	x	x	x	x	x	x	x

vehicles during these maneuvers.* Emphasis was placed on
· identifying limit conditions, hence tests at low and moderate
maneuver severity levels were restricted to a minimum.

All eight data signals produced by the automatic-con-
trol instrumentation package (see list, Section 3.4.5) were
recorded during each test.

---

*Tire wear and wheel alignment were incessant problems and
had to be monitored diligently. Structural failures were en-
countered periodically as well, notably in running gear and
suspension components, necessitating extensive mechanical repairs
to restore the vehicle to its original operating state. The
most spectacular failure involved the shearing of a rear axle,
resulting in loss of a wheel; the damage incurred by the test
vehicle from running on three wheels was considerable.

4.0 RESULTS AND DISCUSSION

4.1 STRAIGHT LINE BRAKING

A typical set of raw data traces from a straight line braking test is presented in Figure 22. To derive braking effectiveness/efficiency results from these data, four distinct pieces of information must be extracted:

(1) whether or not front wheels lock

(2) whether or not rear wheels lock

(3) effective brake line pressure

(4) effective longitudinal acceleration

The first two pieces of information are found easily from the wheel lockup indicator traces. The third, effective brake line pressure, is also relatively straightforward to evaluate; the pressure-time curve has a characteristic shape (generally with pressure falling off gradually throughout the course of a constant-pedal displacement run), and it is merely necessary to establish a systematic procedure for picking off an effective pressure value and adhere to it consistently. Our practice has been to employ the first quasi-steady-state value (554 psi in the run shown in Figure 22).

The evaluation of an effective longitudinal acceleration from the braking test data is not such a straightforward matter. Generally speaking, longitudinal acceleration varies considerably during the course of a stopping maneuver as a result not only of brakeline pressure variations but also of variations in brake lining friction due to changing speed and temperature [9]. When wheel locking is involved, similar variations in tire-road friction are also a factor [12].

It appears most meaningful to define braking effectiveness in terms of an effective longitudinal acceleration evaluated by

Test vehicle: Mercedes
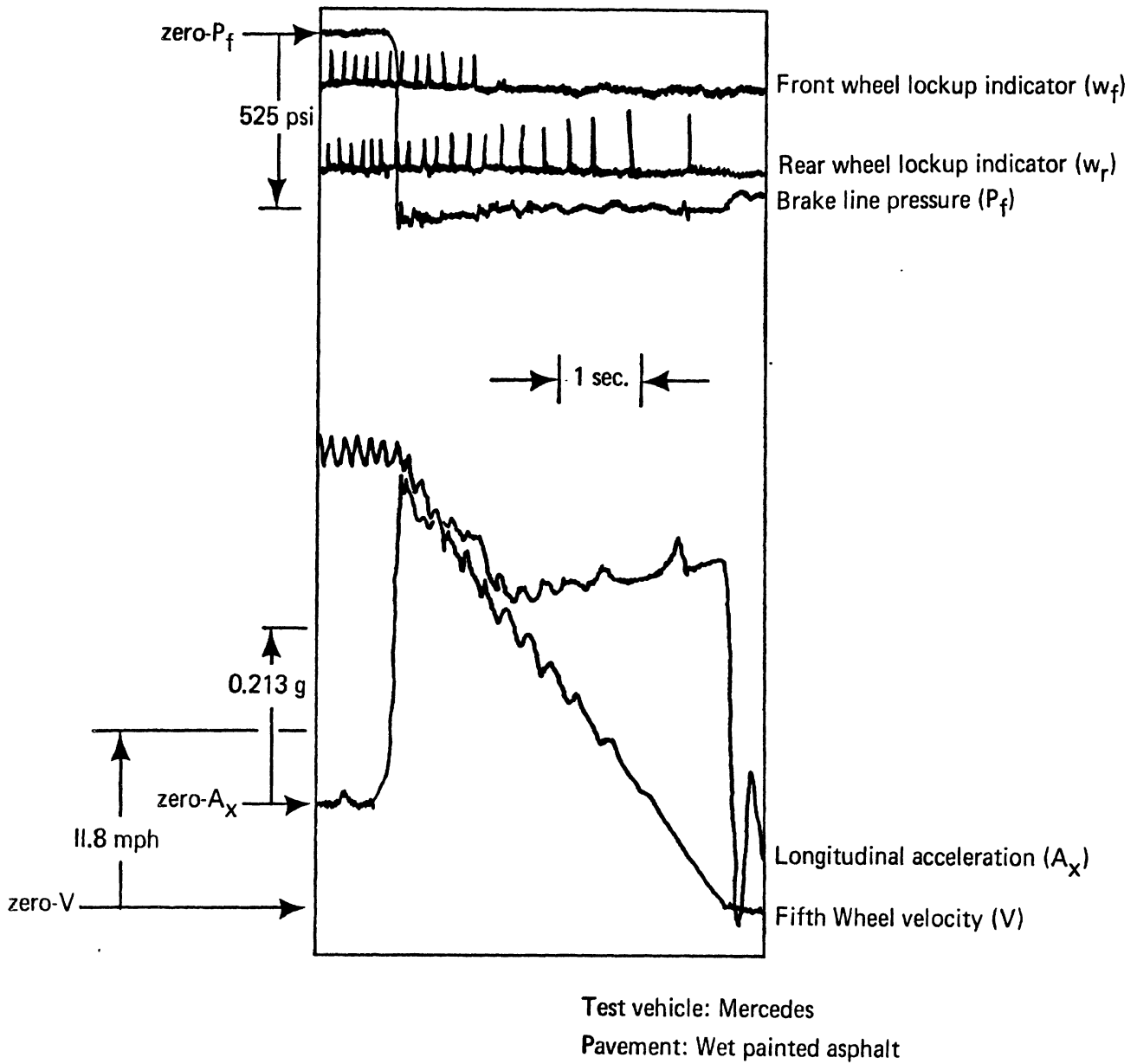Pavement: Wet painted asphalt

FIGURE 22. TYPICAL RECORDING FROM STRAIGHT-LINE BRAKING TEST

some sort of averaging process, rather than at any distinct point during the stopping trajectory. The simplest objective procedure for forming such an average is by graphical differentiation of the velocity-time history. Discrepancies between averages so formed and corresponding results obtained through planimeter averaging of acceleration-time curves have been found to be negligible. We have accordingly employed the graphical differentiation procedure to analyze the pilot test results. To eliminate the effects of the extreme transients at the beginning and end portions of the maneuver, we have evaluated the average over the speed range $10 \text{ mph} \leq V \leq 25 \text{ mph}$.

Let $_{25}\Delta t_{10}$ denote the time interval required for the vehicle to decelerate from 25 to 10 mph. The quantity

$$\bar{A}_x = \frac{15\left(\frac{\text{miles}}{\text{hour}}\right) \times 1.467}{32.2 \times {}_{25}\Delta t_{10}} \tag{3}$$

represents the effective deceleration in g units. For the data shown in Figure 22, $_{25}\Delta t_{10}$ is 2.22 seconds (evaluated by fairing the velocity-time curve), and $\bar{A}_x$ is 0.309 g.

Braking effectiveness data derived from the test time histories by application of the described procedure are presented in Figure 23. Stops in which wheel locking was encountered are so indicated. Examination of the figure reveals that the maximum deceleration achievable without wheel locking can either be greater or less than the maximum achievable with locking (depending mainly on the relative magnitude of "peak" and "sliding" friction coefficients for the tire-pavement combination involved [12]). The procedure followed in establishing peak non-wheel-locking deceleration is different for the two cases. When the highest value measured is from a non-locking stop (e.g., Toyota), that value is used (e.g., 0.88 for the Toyota on the dry concrete).
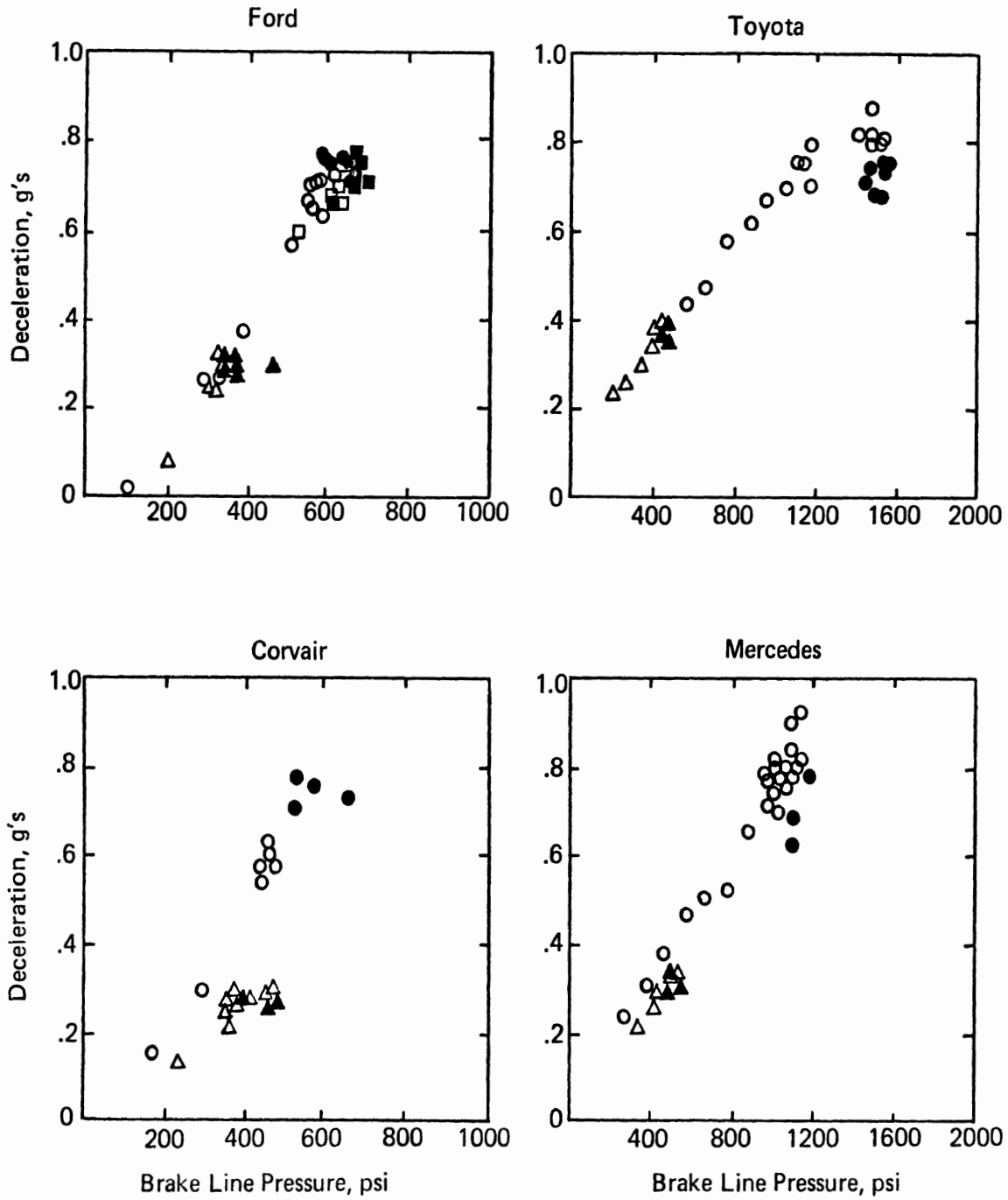
FIGURE 23. BRAKING EFFECTIVENESS DETERMINED FROM STRAIGHT-LINE BRAKING TESTS

When the highest deceleration involves a locking condition
(e.g., Corvair on dry concrete), the value used is the
average of the peak non-locking value and the next higher
measurement (e.g., 1/2 × (0.64 + 0.71) = 0.68 for the
Corvair on dry concrete).

Values of maximum deceleration achievable without
wheel locking, established for each test configuration as
described above, are tabulated in Table 7. Also indicated
for each configuration is the axle (front or rear) at which
wheel locking was first encountered.

TABLE 7 PEAK DECELERATION ACHIEVABLE WITHOUT WHEEL LOCKING: STRAIGHT LINE BRAKING TESTS				
Vehicle	Pavement	Cargo Compartment Load, lb.	$(A_x)_{max}$, g's	Wheels Which Locked First
Ford	Dry Concrete	0	0.75	Rear
"	"	450	0.72	Front
"	Wet Painted Asphalt	0	0.33	Rear
Toyota	Dry Concrete	0	0.88	Front
"	Wet Painted Asphalt	0	0.41	Front
Corvair	Dry Concrete	0	0.68	Rear
"	Wet Painted Asphalt	0	0.31	Rear
Mercedes	Dry Concrete	0	0.92	Front
"	Wet Painted Asphalt	0	0.35	Front

Conversion of the peak deceleration data given in Table 7
into the form of braking efficiencies requires that they be
normalized (divided) by appropriate values of friction coeffi-
cient. Two basically different approaches may be taken in the
definition of such values. On the one hand, we can attempt to
characterize the frictional interaction prevailing between tire
and road under the actual test conditions. This approach would
require that shear force measurements be made for each specific

tire-pavement combination tested. Braking efficiencies computed on the basis of such data (which we will denote as "classical braking efficiencies" because of their historical origin [3]) would provide a meaningful assessment of the degree to which the vehicle has been engineered to exploit the traction properties of the particular tires with which it is outfitted. They would say nothing, however, about the absolute level of braking effectiveness produced by the total tire-vehicle system.

To obtain an absolute measure of braking efficiency, it is necessary to normalize the deceleration data on the basis of reference friction values which are independent of the properties of the tires on the vehicle under test. In light of the objectives of the present study, an absolute braking efficiency measure appears to be appropriate. We have accordingly normalized the test data on the basis of nominal friction coefficients obtained from traction measurements on a single, arbitrarily selected tire (Goodyear Polyglas H78-15 with 1000 lb normal load, 24 psi inflation pressure). The nominal coefficients, corresponding to zero-speed-limit values [8] for dry concrete and wet painted asphalt surfaces, respectively, are $\mu_o = 1.02$ and $\mu_o = 0.46$. Braking efficiencies computed on this basis for each test vehicle configuration are given in Table 8.

TABLE 8 ABSOLUTE BRAKING EFFICIENCIES		
Vehicle Configuration	Absolute Braking Efficiency $\mu_o = 0.46$	$\mu_o = 1.02$
Ford, empty	0.72	0.74
Ford, loaded	-	0.71
Toyota	0.89	0.86
Corvair	0.67	0.67
Mercedes	0.76	0.90

Considered in toto, the test results presented in Figure 23 and synthesized in Tables 7 and 8 appear to provide a meaningful assessment of a safety-relevent aspect of vehicle performance. Substantial differences in the maximum ability of the vehicle to decelerate without gross degradation of stability and/or controllability have been perceived and quantified. In order to interpret and extrapolate further, however, it is necessary to consider how such results are influenced by variations in such important operating conditions as speed, pavement friction, and service factors.

Let η_o denote the absolute braking efficiency as defined above, i.e.,

$$\eta_o = \frac{(\bar{A}_x)_{max}}{\mu_o} \tag{4}$$

where $(\bar{A}_x)_{max}$ is the maximum deceleration achievable without wheel locking and μ_o is the nominal friction coefficient whose value is unique for a given pavement. Let η denote the corresponding classical braking efficiency,

$$\eta = \frac{(\bar{A}_x)_{max}}{\mu} , \tag{5}$$

where μ is an effective peak friction coefficient defined for the particular tire-road combination tested. If we assume (1) that peak friction for a given tire-road combination is a monotonically decreasing function of translational velocity, (2) that temperature effects are negligible, and (3) that deceleration does not vary significantly during the maneuver, then the value of μ may be evaluated from tire traction measurements of the form shown in Figure 24, performed at speed V_o , the initial velocity for the braking maneuver.

Solving equations 4 and 5 for $(\bar{A}_x)_{max}$, equating the results, and rearranging gives

Wet Concrete Pavement
Tire Size H78-15
Bias Belted Construction
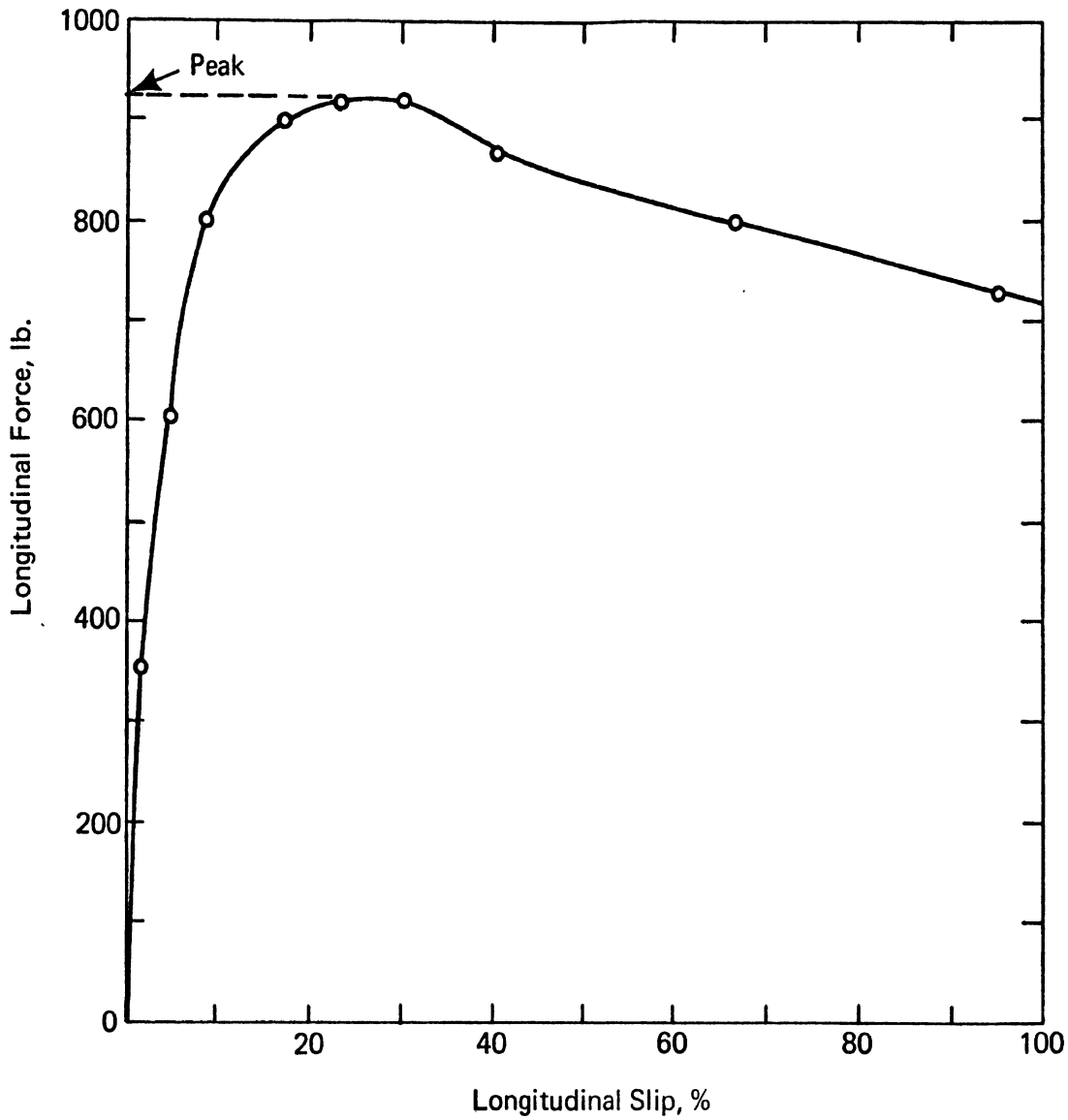Inflation Pressure 24 psi
Normal Load 1000 lb
Speed 30 mph

FIGURE 24. LONGITUDINAL FORCE VERSUS LONGITUDINAL SLIP AS MEASURED WITH THE HSRI MOBILE TIRE TESTER [13]

66

$$\eta_o = \frac{\mu}{\mu_o} \eta \qquad\qquad (6)$$

Given the definition of the straight line braking maneuver and of braking efficiency as a quasi-static property (i.e., defined with respect to a finite time interval over which deceleration is considered constant), it follows that the influence of speed on η is negligible. This conclusion is supported by simulation results performed using the hybrid model described in Appendix B. Further, μ_o is by definition constant for a given pavement surface. Thus the influence of speed on absolute braking efficiency is a direct function of its influence on the peak coefficient of tire-road friction, μ. Although this effect can certainly be a significant one (particularly in the case of wet pavement when hydroplaning is a possibility), it is more appropriately measured directly, through tire traction tests (such as those illustrated in Figure 24), than through vehicle tests which are confounded by many other factors.

In tests preliminary to the pilot program, measurements were made of braking effectiveness at both 30 and 50 mph. The data obtained at the higher speed were characterized by considerably more scatter. This led to the decision to perform the pilot tests with V_o = 30 mph .

The influence of pavement friction on braking efficiency is both important and complex. For a given pavement surface, two factors are of significance: (1) the frictional compatibility of the vehicle's tires with the given surface (μ/μ_o in equation 6), and (2) the degree to which brake, chassis, and suspension properties, and operating conditions are matched to equalize brake torque/vertical load ratios at each axle (η in equation 6). Although the second factor is governed by a systematic relationship, the first is not; the friction levels produced by two different tires (in this case, the test vehicle tire and the nominal reference tire) on different pavements cannot

be related a priori on the basis of existing technology. For the long term, attempts should be made to develop a comprehensive procedure for evaluating absolute braking efficiency as a function of pavement friction, by means of a systematic program of tire traction testing on a series of different surfaces plus a limited number of vehicle tests to establish classical braking efficiency. Such an undertaking is beyond the scope of the present program. An interim procedure wherein straight line braking tests are repeated on as many different pavement surfaces as practicable appears to be a reasonable, pragmatic approach. The decision to conduct pilot tests on two surfaces was based on practical time and money considerations.

Traditional analyses of vehicle braking performance [e.g., 3] indicate that the influence of realistic tire inflation pressure variations on braking efficiency is not significant. Simulation runs with appropriately varied values of circumferencial tire stiffness (see Appendix B) indeed demonstrate the negligibility of associated tire compliance effects. However traction data obtained recently [12] on severely overloaded/underinflated tires indicate that significant degradation in effective friction coefficients may be produced under such circumstances. Should further testing indicate that realistic off-design combinations might significantly affect braking efficiency results through this mechanism, straight line braking tests with multiple values of inflation pressure will be indicated. Pending such a development, it appears appropriate to conduct tests using only nominal inflation pressures.

The influence of vehicle loading condition on braking efficiency is very important. Generally speaking, when pavement conditions are such that the first wheels to lock on
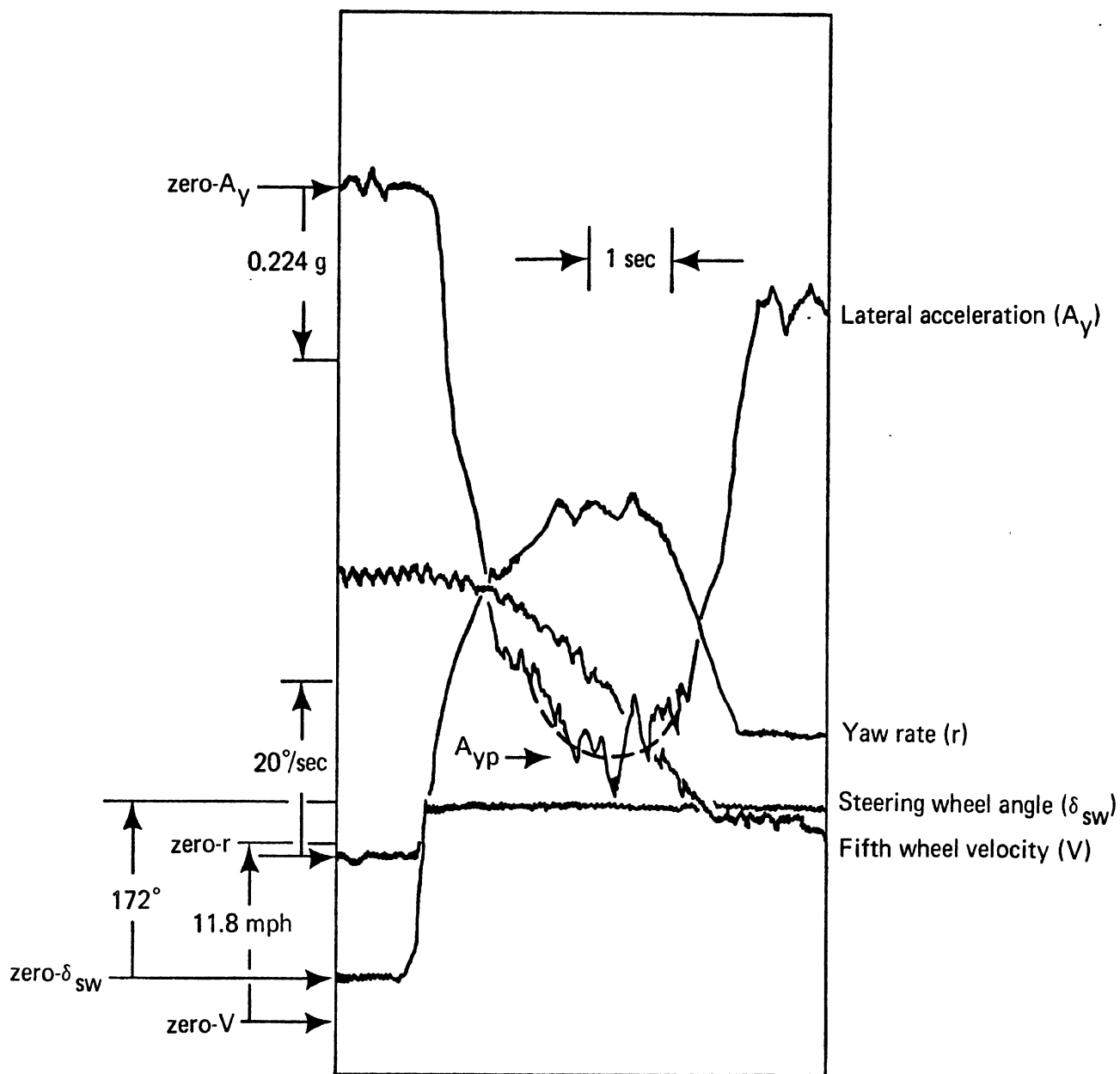
the nominally loaded vehicle are the front wheels, any load variation producing a C.G. shift either rearward or downward tends to degrade braking efficiency. If the rear wheels lock first when the vehicle is unloaded, braking efficiency is degraded by moving the C.G. either forward or up. Performance-degrading conditions for a comprehensive straight line braking evaluation should be derived from service factor data accordingly (see Appendix A).

4.2 RESPONSE TO RAPID, EXTREME STEERING

A typical set of time histories from a step steering response test is presented in Figure 25. Unlike the case of the braking test discussed previously, we are unable to structure a quasi-static interpretation of these data, since we cannot define an effective lateral acceleration comparable to $\bar{A}_x$ in the previous case. We instead focus attention on the peak value of the fundamental lateral acceleration transient, A_{yp} , as estimated graphically by fairing the raw acceleration-time history (see Figure 25).

Plots of A_{yp} versus steering wheel displacement are presented for each vehicle configuration tested, in Figure 26. These plots obviously constitute an analog to the braking effectiveness plots (Figure 23) discussed and analyzed earlier. There is one important difference, however. The steering maneuver is not characterized by a distinctly recognizable limit condition such as the occurrence of wheel locking. The limit responses of "spinout" and "driftout" occur, but it is not straightforward either to identify or to quantitatively characterize these limit phenomena on the basis of the objective data that are obtained.

Qualitatively, the limit responses produced in the step steering maneuver involve a tire reaching a saturation condition wherein the prevailing level of tire-road friction effectively bounds the maximum achievable lateral force.

FIGURE 25. TYPICAL RECORDING FROM STEP STEERING RESPONSE TEST

70

	Loaded?	No	Yes
Tire Inflation			
Nominal		o	—
Off-design		□	△

Ford (N_G = 22.8)

Toyota (N_G = 14.4)

A_{yp}, g's

Corvair (N_G = 23.8)

Mercedes (N_G = 15.3)

A_{yp}, g's

Steering Wheel Displacement, deg.
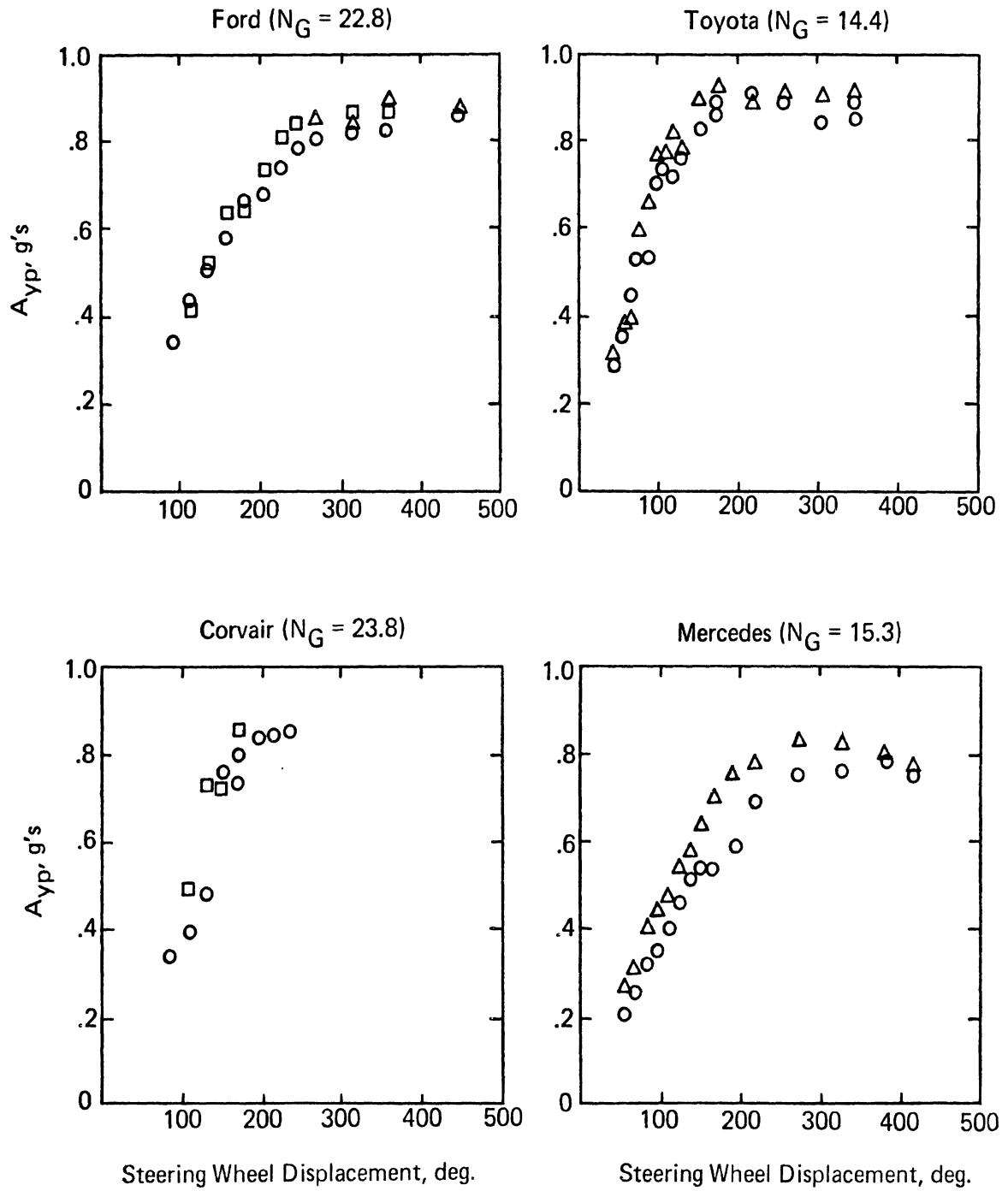
Steering Wheel Displacement, deg.

FIGURE 26. PEAK LATERAL ACCELERATIONS ATTAINED IN STEP STEERING RESPONSE TESTS

Hence an increase in the tire sideslip angle does not produce an increased force. The relative extent to which front and rear tires are affected by this phenomenon dictates the general nature of the limit response. When saturation is encountered at the rear axle, there obtains an effective deficiency in the yaw moment offsetting that produced by the steered front tires, and the vehicle experiences a sharp increase in yaw rate, or "spinout." Conversely, when the force deficiency appears at the front axle, the effectiveness of the front tires in producing yaw rate decreases and the vehicle "drifts out" of the turn.

To quantify these limit steering responses on the basis of the data at hand, we defined the normalized yaw rate

$$r' = \frac{r\ell}{V} \cdot \frac{N_G}{\Delta_{SW}} \tag{7}$$

The peak fundamental values of this response parameter, designated as r'_p , appear to represent a significant description of the nature and severity of the limit response observed. Values of r'_p computed for each of the pilot step steering response tests are shown plotted versus the corresponding values of A_{yp} in Figure 27. This graph provides a much more comprehensive basis for interpretation of the data than does the previous presentation (Figure 26). Discrimination of vehicle configurations experiencing spinout (e.g., Corvair, off-design Toyota) is positive.

A promising approach towards a quantitative categorization of these results would appear to involve the following steps: (1) identification of an acceptable upper bound on r'_p based on correlation with subjective evaluations by expert drivers or, ideally, on analytical or statistical relationships with real-world accident data, and (2) stip-
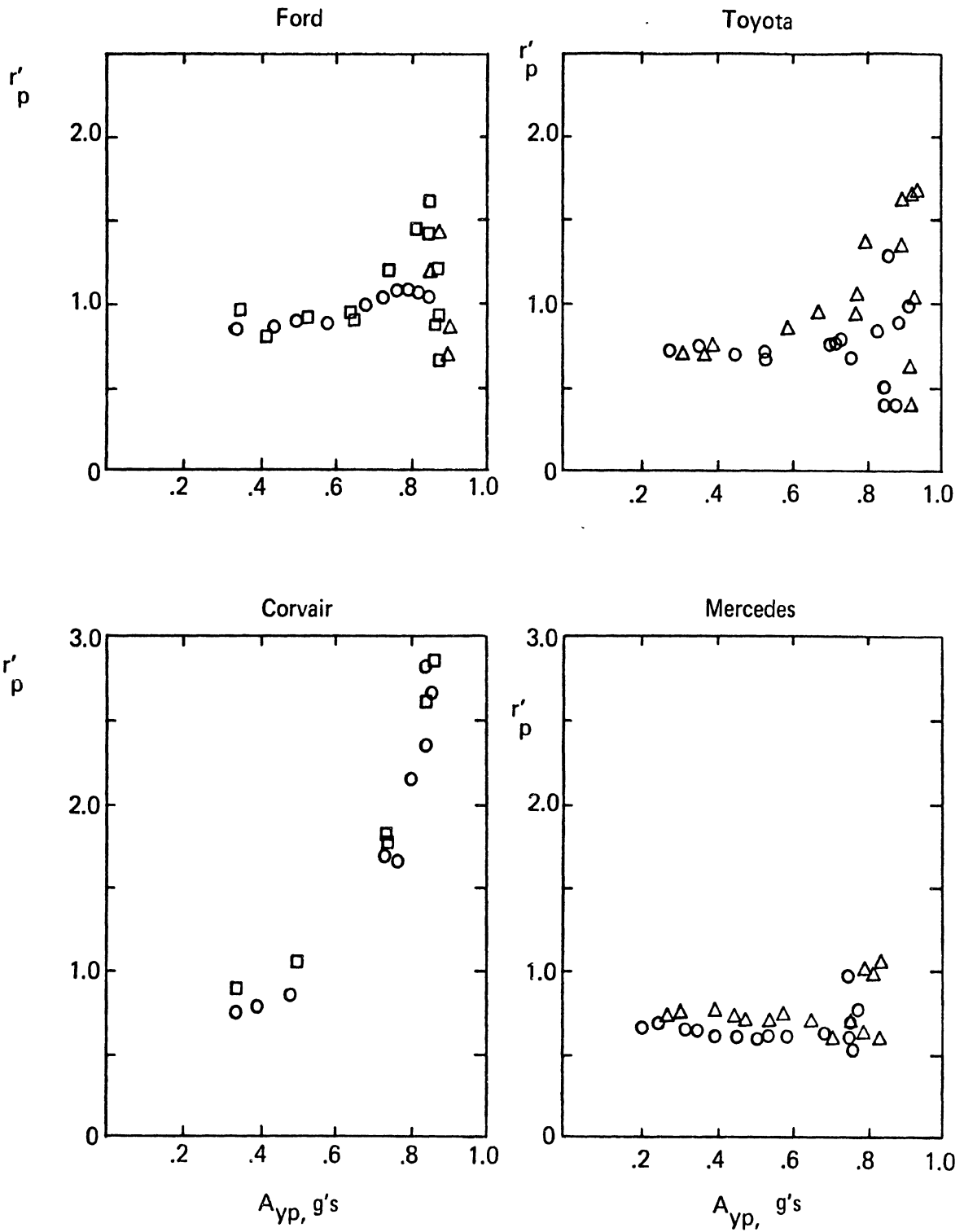
FIGURE 27. NORMALIZED PEAK YAW RATE VERSUS PEAK LATERAL ACCELERATION-STEP STEERING RESPONSE TESTS

73

ulation of a vehicle rating for the maneuver in terms of a
peak lateral acceleration (normalized to account for pre-
vailing pavement friction) corresponding either to (a) the
lowest value of A_{yp} at which r'_p equals the acceptable upper
bound or, in the event r'_p is always less than this bound,
(b) the highest value of A_{yp} achieved. Attempts to imple-
ment such a quantitative procedure on the basis of only the
limited data currently in hand are not considered warranted.

A small number of step steering maneuvers were performed
during the preliminary tests, at higher speeds than 30 mph.
These maneuvers proved to be extremely hard on the test
vehicles, resulting in significant differences in performance
from run to run unless maintenance and repairs were virtually
continuous. The pilot tests were accordingly restricted to
30 mph. Computer simulations were performed to investigate
the influence of speed on the important response character-
istics. Although the results certainly were affected quan-
titatively, it was concluded that the phenomenological aspects
of the maneuver basically were not changed and, therefore, that
the performance assessments derived from the 30 mph tests would
also be meaningful (in a relative sense) for the same maneuver
performed at higher speeds.

Simulation studies indicated that a similar situation
prevails with respect to the influence of pavement friction.
Although the friction level determines the acceleration
levels at which limit conditions are reached, the basic
character of (1) the response and (2) the effects thereon of
vehicle properties appears to be unaffected by a variation
in friction level. By and large, the quantitative influence
of vehicle suspension characteristics appears to be greater
on higher friction surfaces where load transfer effects are
more pronounced. Thus, experiments on a dry pavement sur-
face may be expected to maximize the discriminatory power
of the test procedure.

Variations in service factors significantly influence
the results of the step steering response test. As might
be expected, changes in both load and tire pressure dis-
tributions which tend to degrade the static stability (i.e.,
reduce the static margin [10]) are found, both from sim-
ulation studies and from the results of the pilot tests
(see Figure 27), to increase the tendency for spinout.
Conversely, service factor variations which increase the
static margin tend to inhibit spinout and produce a greater
tendency to drift.

4.3 BRAKING IN A TURN

These tests are a generalization of the straight line
braking tests discussed in Section 4.1. The raw data recorded
include each of the signals needed for an evaluation of braking
efficiency, w_f , w_r , P_f , and V (see Figure 22), plus the
directional response variables, δ_{sw} , r , and A_y. The steering
wheel displacement, δ_{sw} , is held fixed throughout the duration
of the experiment. The deviation from the nominal circular
trajectory produced as the level of braking (deceleration)
is increased to a limit condition is reflected in increasingly
drastic time histories of r and A_y .

Braking effectiveness curves derived from the braking-in-
a-turn test data by application of the procedure described in
Section 4.1 are presented in Figures 28 and 29, respectively,
for test vehicles with nominal and off-design service factors.
Directional response aspects of the results are depicted in
Figure 30, where the peak normalized yaw rate, r'_p (derived
as in the step steering response tests), is plotted versus
effective longitudinal deceleration, $\overline{A}_x$.

For those vehicle configurations which are characterized
by initial locking of the rear wheels, producing spinout (i.e.,
Ford, Corvair), the r'_p versus A_x plots provide an effective
demonstration of how directional response is affected significantly

75

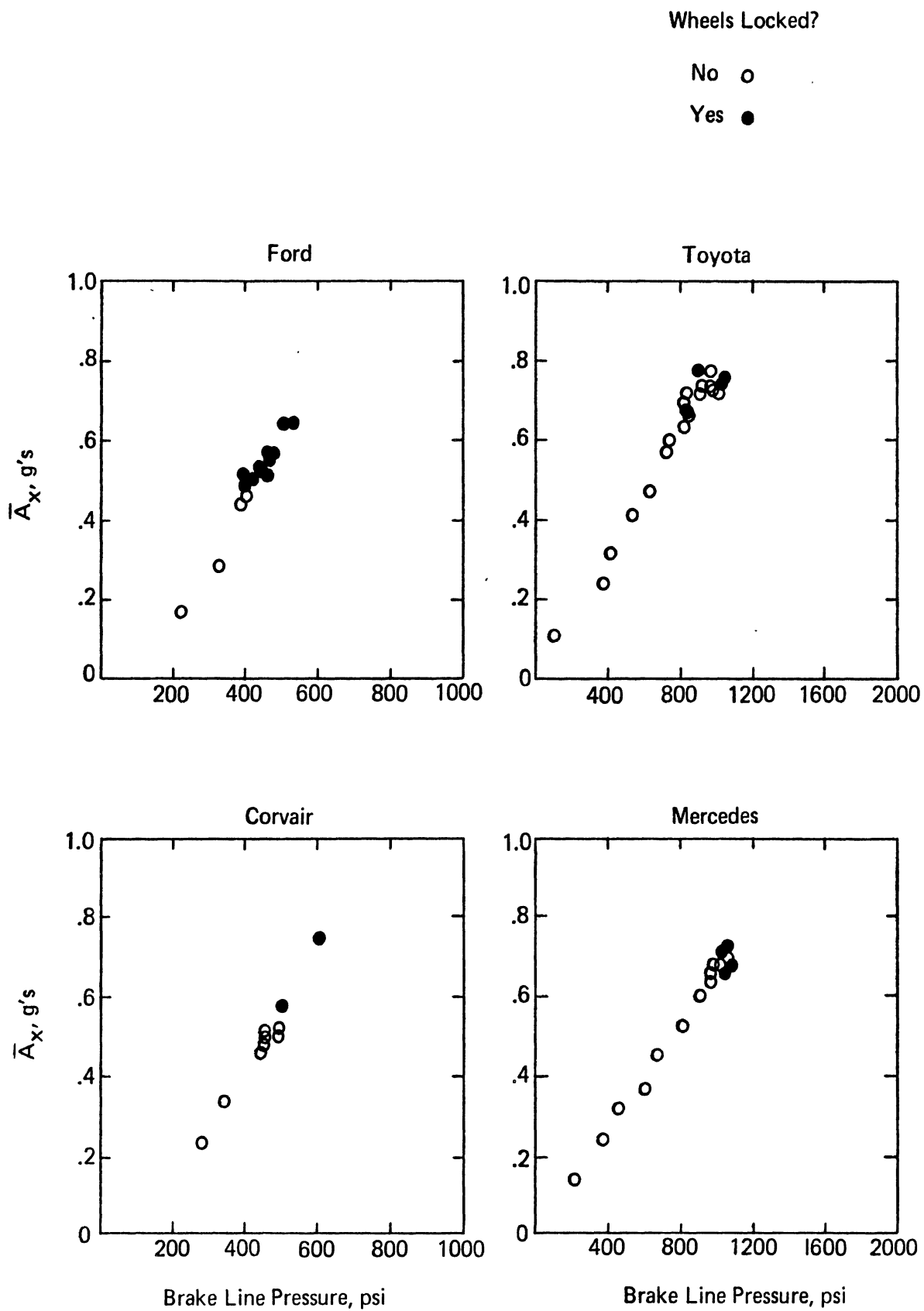FIGURE 28. BRAKING EFFECTIVENESS IN TURNING TESTS;
NOMINAL SERVICE FACTORS
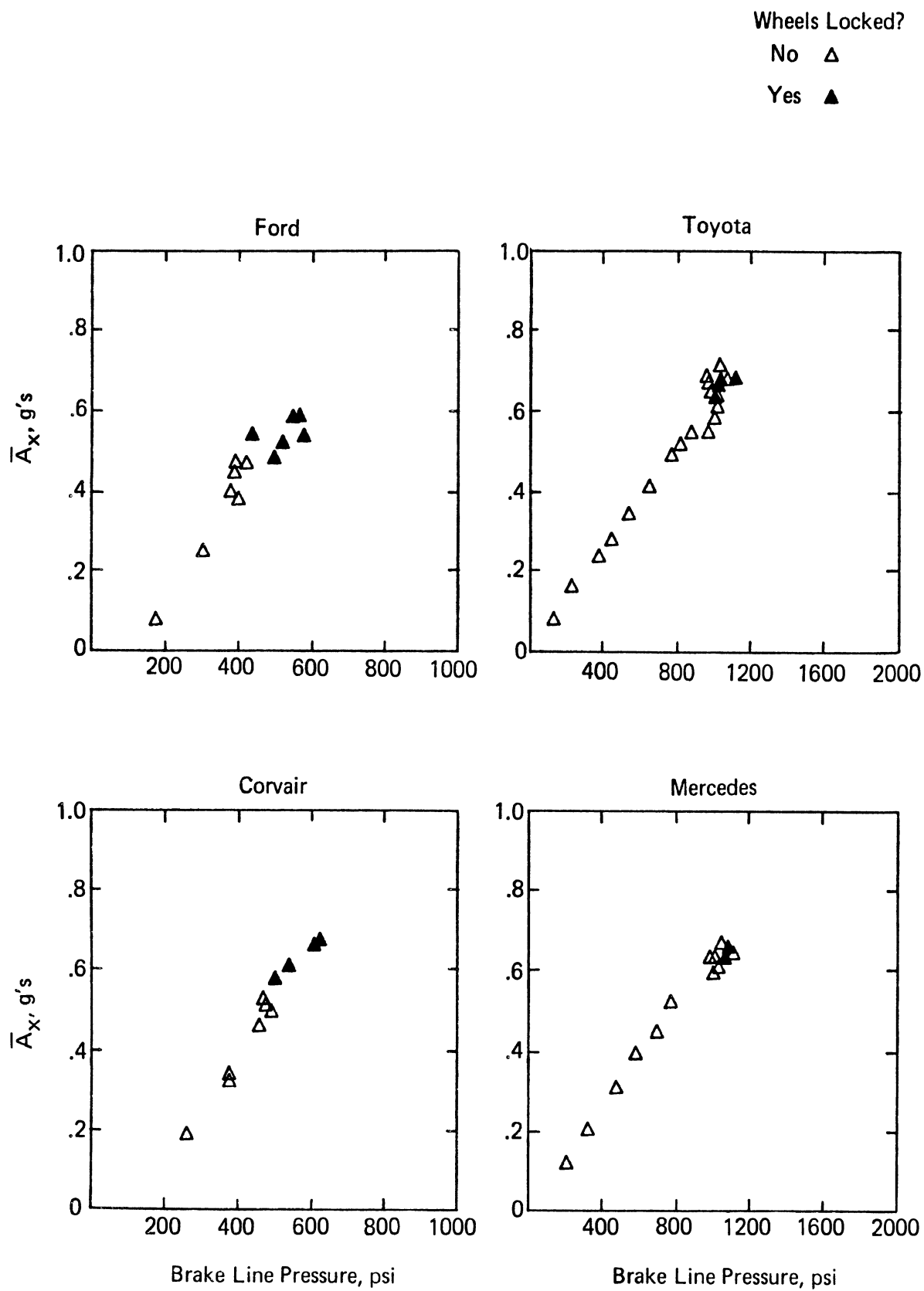
FIGURE 29. BRAKING EFFECTIVENESS IN TURNING TESTS:
OFF-DESIGN SERVICE FACTORS

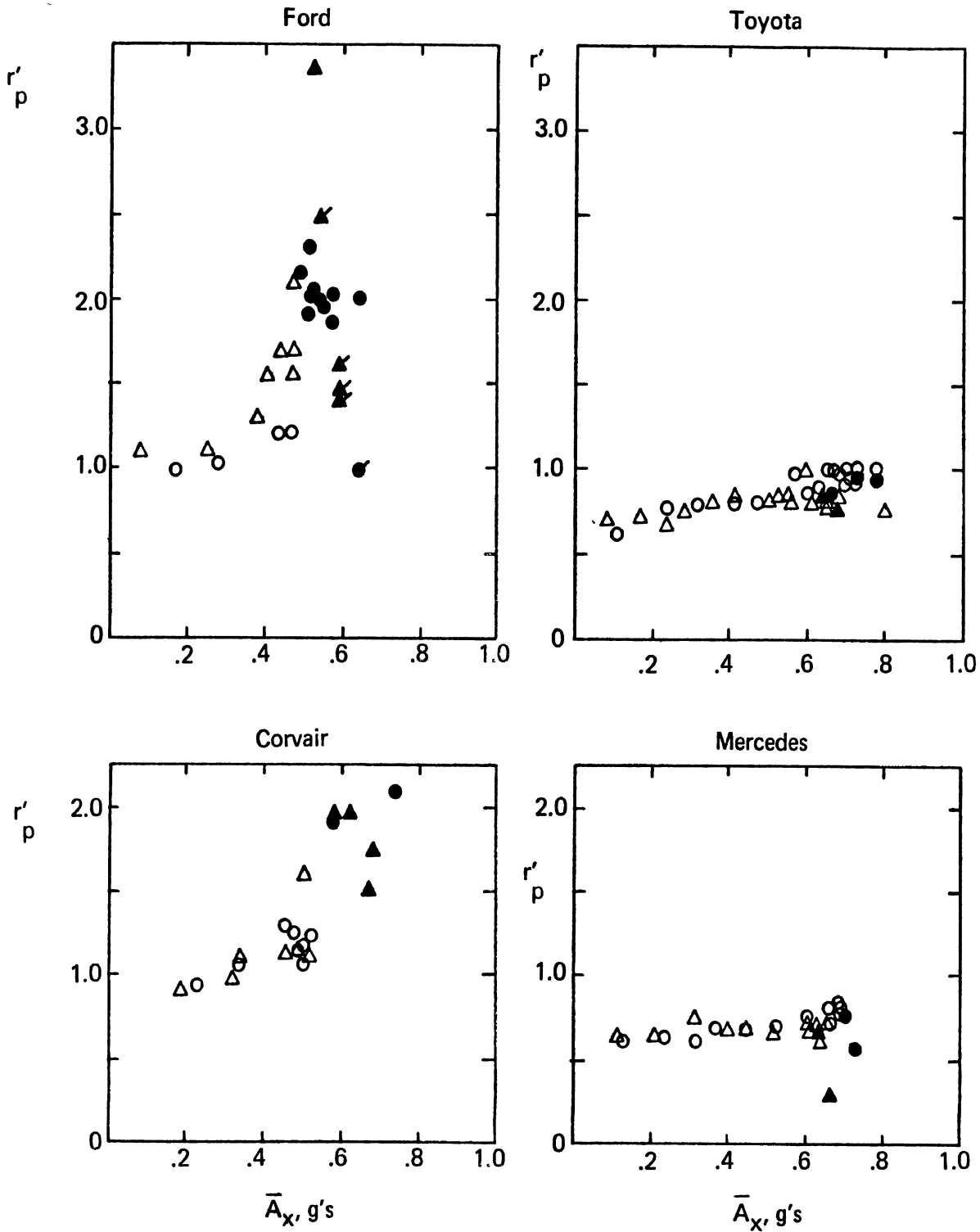| Service Factors	Wheels Locked?		
	No	Yes	All
Nominal	o	●	☞
Off-Design	△	▲	↙

FIGURE 30, NORMALIZED PEAK YAW RATE VERSUS LONGITUDINAL DECELERATION AS PRODUCED BY BRAKING IN A STEADY TURN

78

by braking even at longitudinal accelerations substantially lower than the wheel locking limit. In light of this effect, it appears that braking efficiency values based on accelerations at the lockup limit may not represent a properly conservative basis for specifying and/or regulating performance in this maneuver. Some scheme based on stipulation of an acceptable upper bound for r'_p , such as described in the previous section, appears a promising possibility for this application as well.

In cases where wheel locking is first encountered at the front axle (Toyota, Mercedes), there is no increase in yawing velocity as a result of braking. Consequently there is no peak yaw rate and r'_p , as plotted, merely corresponds to the initial turning rate. Although efforts have been made to quantitatively categorize driftout response by graphically differentiating the yaw-rate time history, these attempts have not been successful. Pending the development of some acceptable quantitative measure of driftout prior to lockup (e.g., a satisfactory means for measuring the sideslip velocity of a motor vehicle under dynamic conditions), it appears desirable to employ braking efficiency as one index of performance in this maneuver and r'_p versus $\bar{A}_x$ as a second index of performance.

4.4 TURNING ON A ROUGH SURFACE

Reduced data from the roadholding tests are plotted in Figures 31 and 32, in the form of the peak decrements in lateral acceleration and yaw rate ΔA_y and Δr , normalized with respect to the initial steady values of lateral acceleration and yaw rate, A_{yo} and r_o . It will be noted that neither data presentation is generally characterized by clearly defined and systematic responses having a resonant character (we are obviously dealing here with rather well-damped systems). For some vehicles,
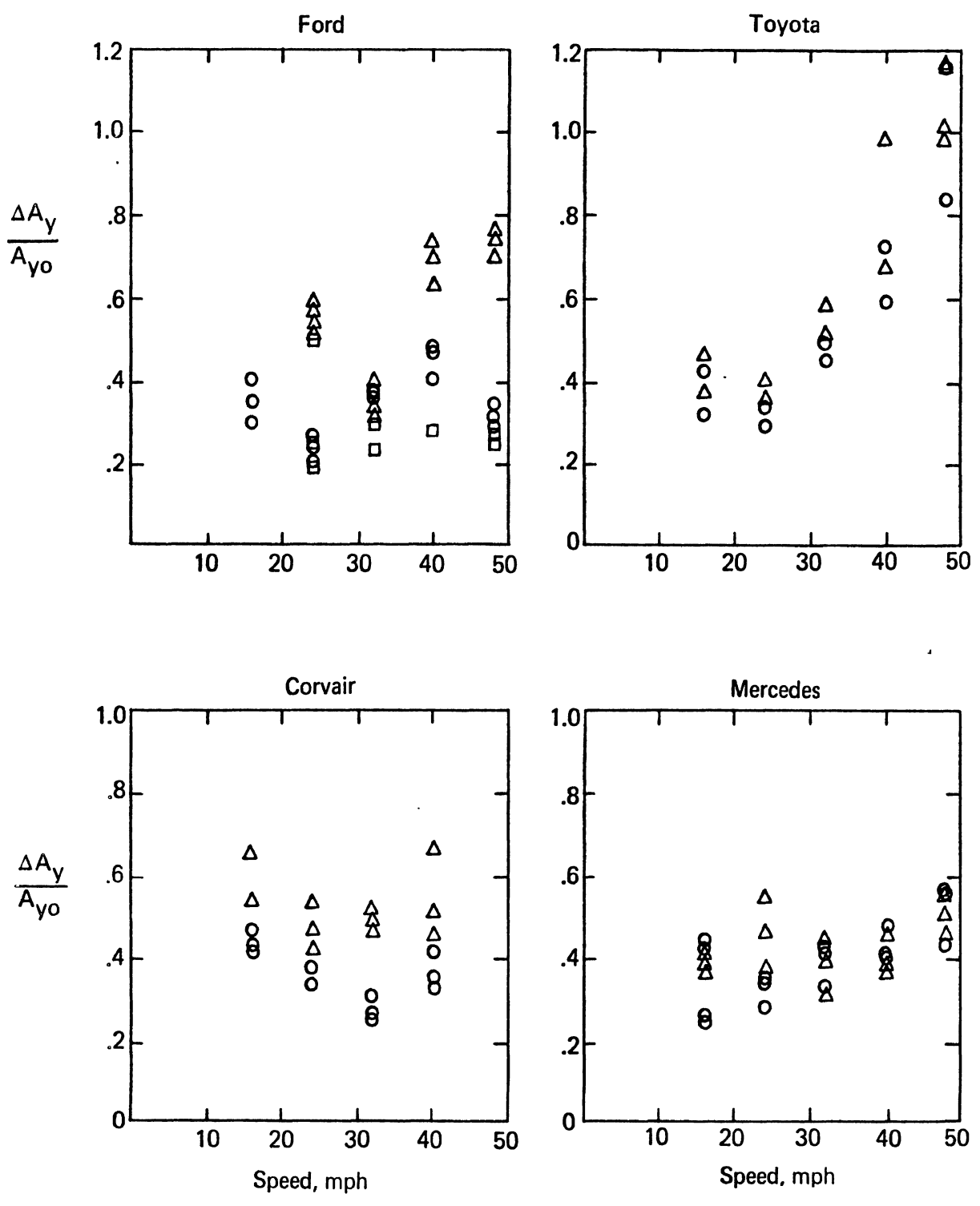
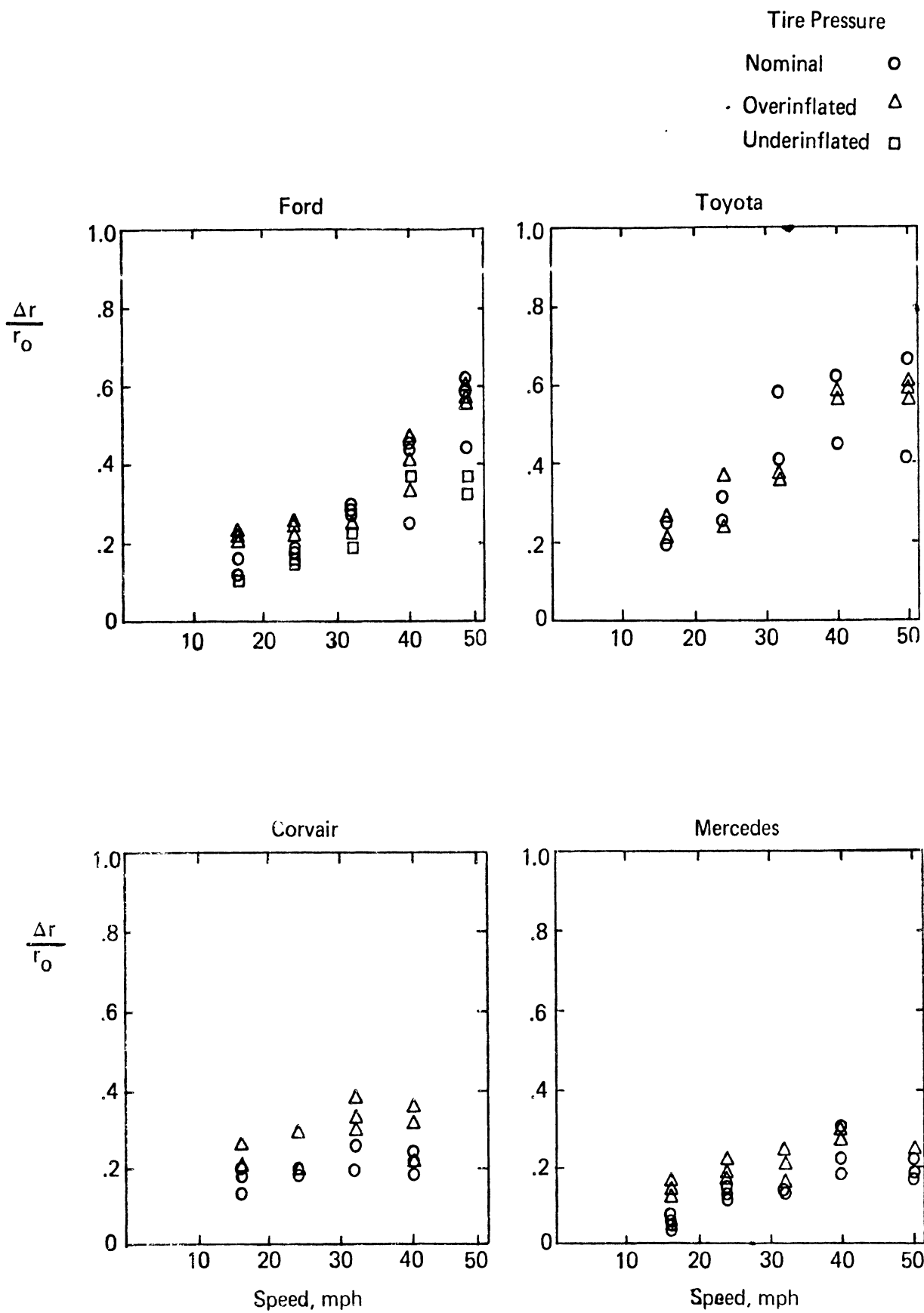FIGURE 31. LATERAL-ACCELERATION DECREMENT CAUSED BY ROAD ROUGHNESS
IN A STEADY TURN

FIGURE 32. YAW-RATE DECREMENT CAUSED BY ROAD ROUGHNESS IN A STEADY TURN

the results as plotted increase monotonically over the speed range covered (e.g., $\Delta r/r_o$ for Ford), or have minima but no maxima (e.g., $\Delta A_y/A_{yo}$ for Corvair). These characteristics make it impossible to quantitatively interpret the data without being somewhat arbitrary. It is clear, however, that there are significant differences among the data obtained for the different test configurations (and this conclusion can be reached on a purely statistical standpoint), and further that these data differences reflect real differences in the degree to which the basic directional response is affected by the roughness disturbance. Therefore, given the pragmatic nature of the overall approach, some arbitrariness in the quantitative interpretation of the data is considered warranted.

The roadholding test data prove to be qualitatively consistent. For example, increased tire inflation pressure invariably degrades performance, whether measured in terms of acceleration or yaw rate. This trend accords with expectation on two grounds: (1) higher pressure intensifies the disturbance forcing function by opposing the fixed height disturbances with "stiffer springs," and (2) higher pressure produces a decrease in the equivalent damping ratio of the wheel hop system. It follows that any test procedure to evaluate the roadholding ability of a motor vehicle should include measurements with tires overinflated to realistic levels (see Appendix A).

There is consistency, too, with respect to the relative performance of the four vehicles tested. If we (arbitrarily) elect to quantify performance on the basis of the peak measured value (as obtained by averaging replications) of either (1) the lateral acceleration decrement $(\Delta A_y/A_{yo})_p$, or (2) the yaw rate decrement $(\Delta r/r_o)_p$, we find that the rank order of the four specimens is the same for both performance measures (see Table 9).

82

	TABLE 9		
	ROADHOLDING PERFORMANCE MEASURES		
Vehicle	$(\frac{\Delta A_y}{A_{yo}})_p$	$(\frac{\Delta r}{r_o})_p$	Ranking
Ford	.74	.57	3
Toyota	1.06	.59	4
Corvair	.60	.34	2
Mercedes	.52	.28	1

4.5 RESPONSE TO SINUSOIDAL STEER INPUTS

A representative sample of raw data from the sinusoidal steering tests is presented in Figure 33. The curves shown are time histories of steering wheel angle (δ_{sw}) and vehicle yaw rate (r) as produced by a 50 mph test of the Ford station wagon, with nominal loading and tire pressures, and a steering amplitude of 311°. By any criterion, and specifically in terms of the relevant hypotheses of this program (Section 2.3.5), this was a severe maneuver. The yaw rate response produced was markedly asymmetrical, resulting in a gross heading change ($\Delta\psi$) of 36.5°, as determined by integrating the r-t curve with a planimeter. Qualitatively speaking, however, this response was significantly less drastic than a limit response.

Reduced data from all the sinusoidal steering pilot tests are presented in Figure 34 in the form of plots of gross heading change ($\Delta\psi$) versus normalized steering amplitude,

$$\Delta_{sw}^* = \frac{\Delta_{sw} V_o^2}{N_G g \ell} \tag{8}$$
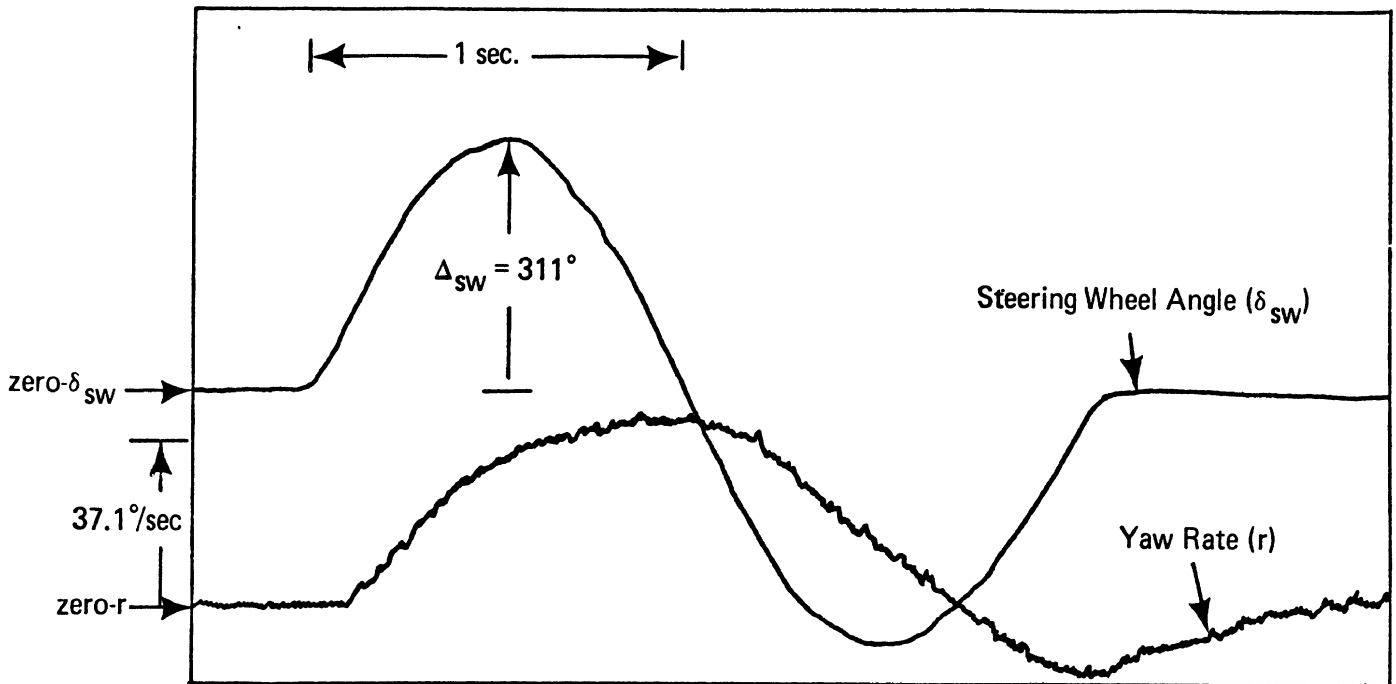
Test vehicle: Ford
Tire Pressure : 28 psi
Velocity: 50 mph

FIGURE 33. TYPICAL RECORDING FROM SINUSOIDAL STEERING RESPONSE TEST

Nominal Velocity, mph	30	40	50	60
Vehicle Empty, Tire Inflation Nominal	○	△	□	◇
Vehicle Empty, Tire Inflation Off-Design	◓	▲	◪	◗
Vehicle Loaded, Tire Inflation Off-Design	●	▲	■	◆

Points with X: Divergent Response

Ford

$\Delta\psi$, deg

Δ^*_{SW}

Toyota

$\Delta\psi$, deg
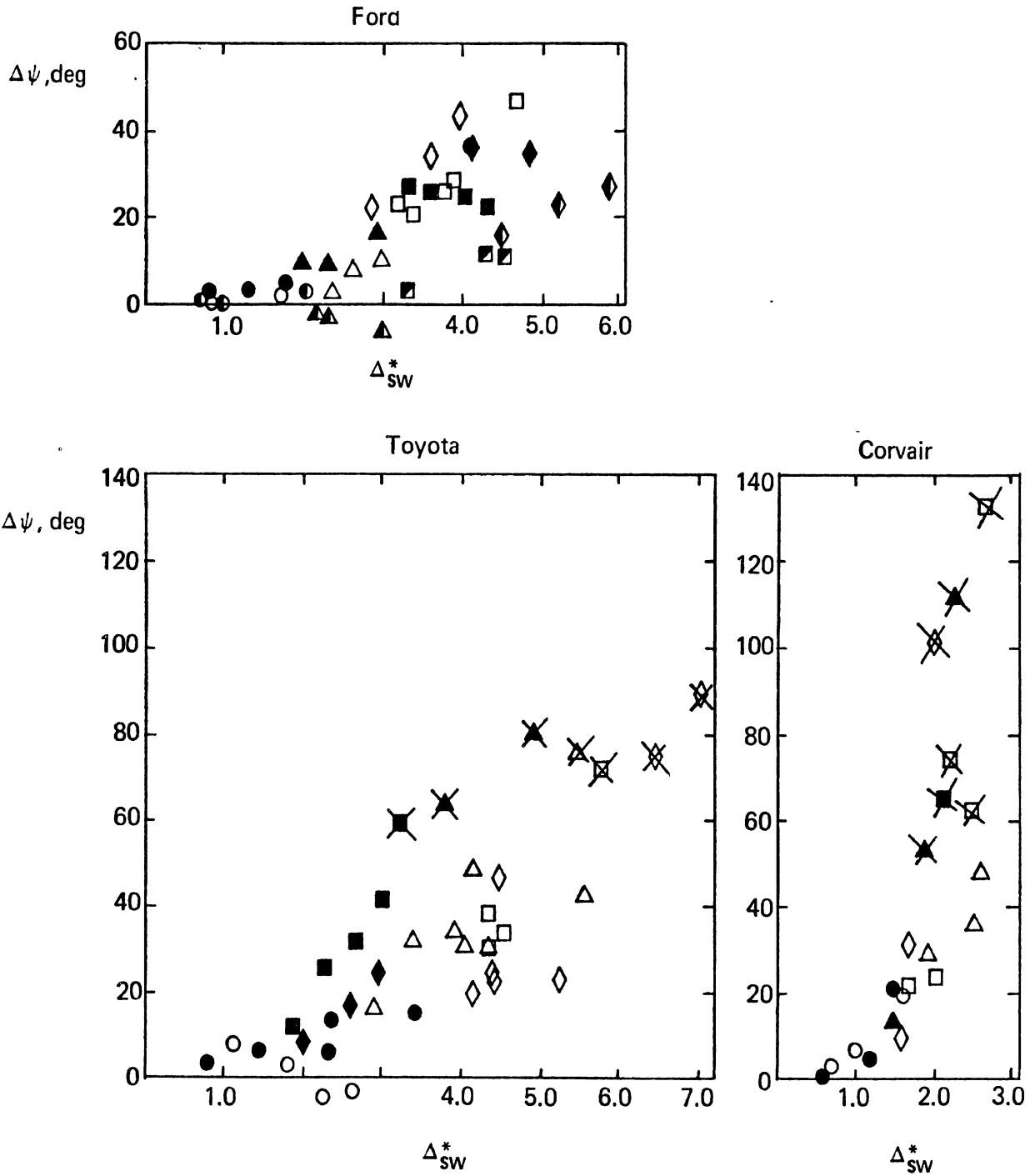
Δ^*_{SW}

Corvair

Δ^*_{SW}

FIGURE 34. GROSS HEADING CHANGE VERSUS NORMALIZED STEER AMPLITUDE
PRODUCED IN THE SINUSOIDAL STEER MANEUVER

Of the three vehicles tested, two (Corvair and Toyota) experienced limit (or "divergent") responses within the allowed range of steering wheel displacement (i.e., 360 degrees) whereas the third (Ford) did not. In order to make some quantitative statements with respect to factors affecting the limit response, we note (see Figure 34) that there is a definite association between gross heading change and the occurrence of a divergent response. For the vehicles tested, a divergent response occurs whenever the gross heading change is greater than 50 degrees, with the response being nondivergent whenever the heading change is less than 50 degrees. Let us define the normalized steer amplitude required to produce a gross heading change of 50 degrees as $(\Delta^*_{sw})_{lim}$.

When the data plotted in Figure 34 are interpolated to determine $(\Delta^*_{sw})_{lim}$, the findings tabulated in Table 10 are obtained. On the basis of these results, (and other data obtained from exploratory tests with the Corvair in a different off-design condition), it appears reasonable to conclude that the influence of test speed on the limit response variable $(\Delta^*_{sw})_{lim}$ is not systematic. Hence the normalization scheme employed (equation 8) constitutes an effective procedure to account for the speed effect, and it is meaningful to consider the average values tabulated in the last column of Table 10 as indicative of the limit performance in this maneuver. Response-limit boundaries constructed on the basis of this premise are presented in Figure 35. Also plotted on this figure are data points from all of the limit (i.e., divergent) and near-limit test runs. The degree of precision with which the above described procedure defines the limit boundary is apparent.
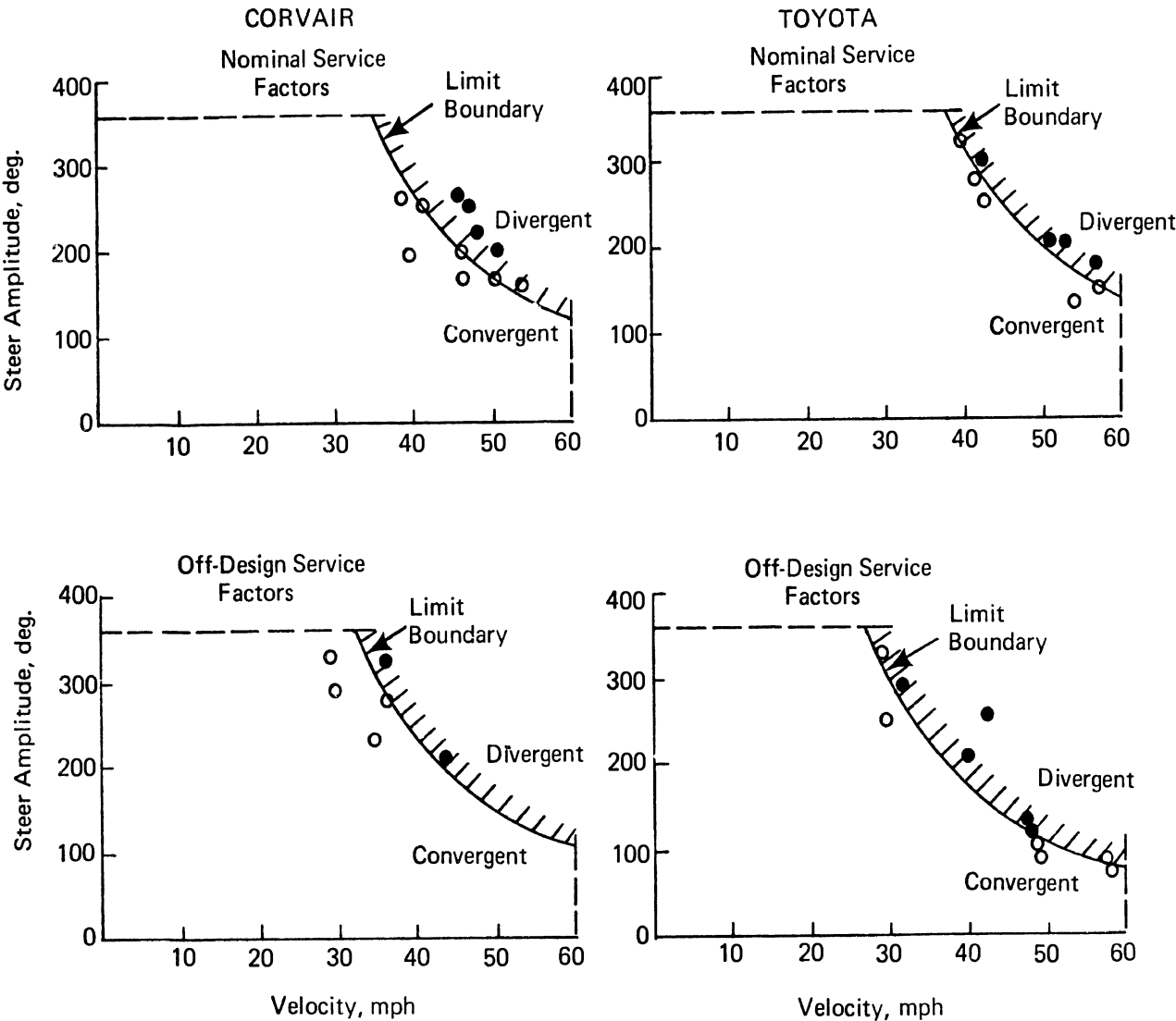
CONVERGENT TEST DATA o
DIVERGENT TEST DATA •

CORVAIR

Nominal Service Factors

TOYOTA

Nominal Service Factors

Off-Design Service Factors

Off-Design Service Factors

FIGURE 35. LIMIT-RESPONSE BOUNDARIES -- SINUSOIDAL STEERING
RESPONSE TESTS

TABLE 10

**LIMIT NORMALIZED STEER AMPLITUDE $(\Delta^*_{sw})_{lim}$; SINUSOIDAL
STEERING RESPONSE TESTS**

Test Configuration \ Nom. Velocity, mph	40	50	60	Avg.
Toyota, Nominal Service Factors	5.5	5.1	5.7	5.4
Toyota, Off-design Service Factors	2.6	3.2	–	2.9
Corvair, Nominal Service Factors	2.7	2.3	1.8	2.3
Corvair, Off-design Service Factors	1.9	2.0	–	2.0

The influence of service factor variations on the limit response depicted in Figure 35 is substantial. Not surprisingly, variations in loading and tire inflation pressures which tend to reduce static margin tend also to reduce the level of maneuver severity required to produce divergent response to sinusoidal steer inputs. This effect should certainly be considered in designing a test schedule for evaluating the emergency lane changing performance of a particular vehicle configuration.

4.6 RESPONSE TO "DRASTIC" STEER AND BRAKE INPUTS

A representative sample of raw data from the drastic "steer/brake" response tests is presented in Figure 36. The sequence of events depicted in this set of time histories may be described as follows:

1. The vehicle, initially proceeding along a straight path at a speed of 50 mph, was subjected to a half sine wave steering wheel input which produced a yaw-roll response of a characteristic form.

Rear wheel lockup indicator

Front wheel
lockup indicator

$280\,\delta_{sw}$

zero-δ_{sw}

Steering Wheel Angle (δ_{sw})

26°/sec

zero-r

Yaw Rate (r)

zero-p

Roll Rate (p)

25.9 deg/sec (p)

1 sec

Brake Line Pressure (P_f)

zero-P_f
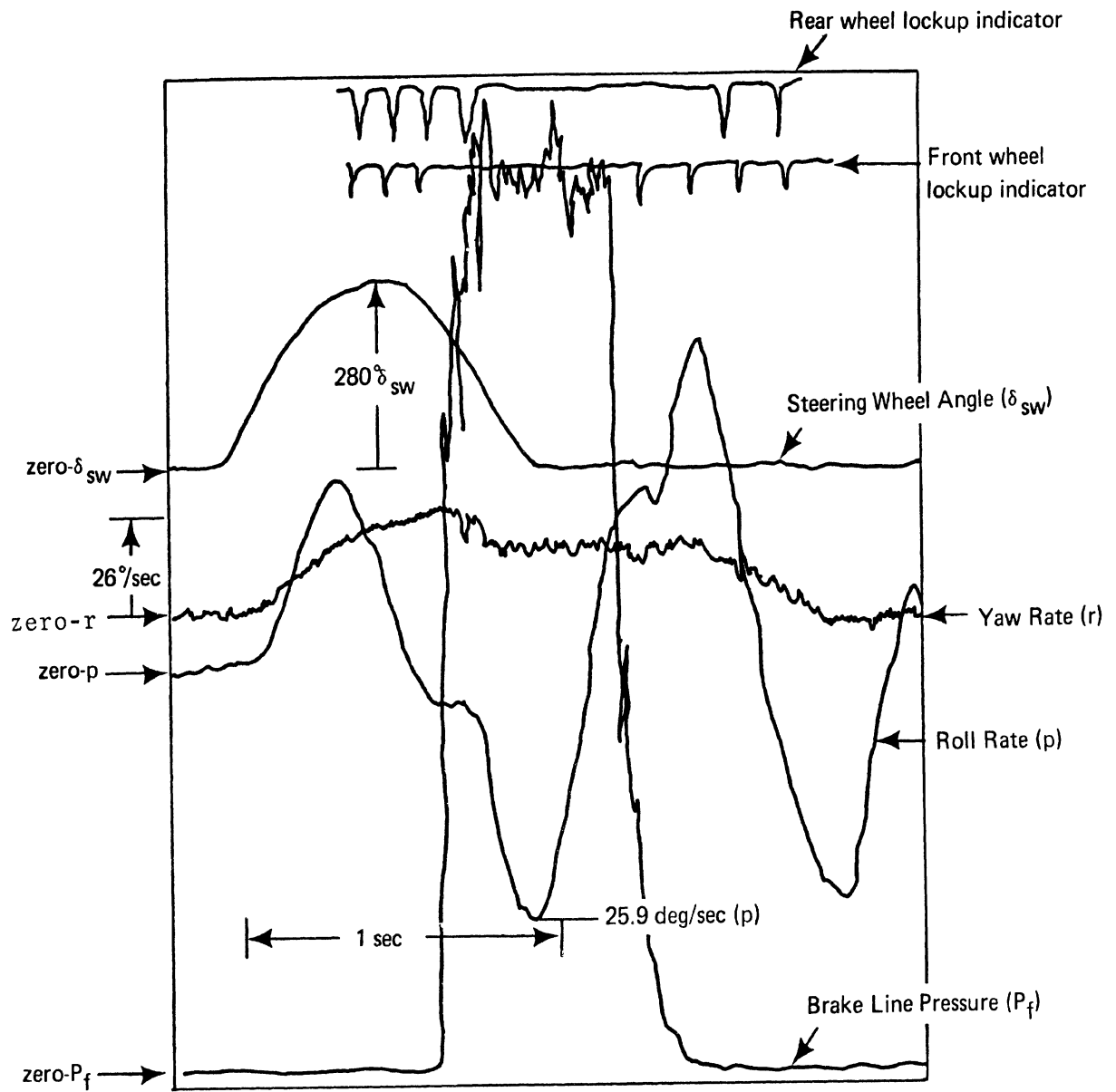
Test vehicle: Ford
Tire pressure: 28 psi
Velocity : 50 mph

FIGURE 36. TYPICAL RECORDING FROM DRASTIC STEER AND BRAKE MANEUVER

89

2. At a point in time where the vehicle's yaw rate response had just about reached a maximum, a severe step of brake input was applied. This input caused the vehicle's wheels to lock and perceptibly perturbed the yaw and roll response.

3. After one half second, the brake input was suddenly released. The vehicle's wheels resumed rolling. The associated sudden increments in lateral force and roll moment produced little change in yaw rate but a very substantial augmentation of the rate of rolling. (It will be noted that the relative phase of control actions and response variables is extremely significant).

The limit response condition defined for this maneuver corresponds to the case where the rolling motion following release of the brake is so great as to cause the vehicle to roll over. Of the three vehicles tested, this limit response was encountered only with one, the Corvair.*

Rollover limit response was observed in three separate runs with the Corvair operated in a nominal service factor condition.** The control inputs in these runs were so similar (see Table 11) that it is not possible to identify any sort

---

*Because of the presence of the roll-limiting outriggers (see Section 3.2.1), the test vehicle could not in fact roll completely over. In tests wherein the result "rollover" is reported, there is no doubt that the vehicle would have overturned if not so restrained (see Figure 37).

**An apparent rollover was also encountered in one of the tests with off-design tire pressures, but the vehicle was severely damaged during the tests and the extent to which the damage might have contributed to the rollover is not known. The severity of the control inputs ($V_o = 37.8$ mph, $\Delta_{SW} = 277°$) in this questionable test was significantly less than in the rollover tests with nominal tire pressures.
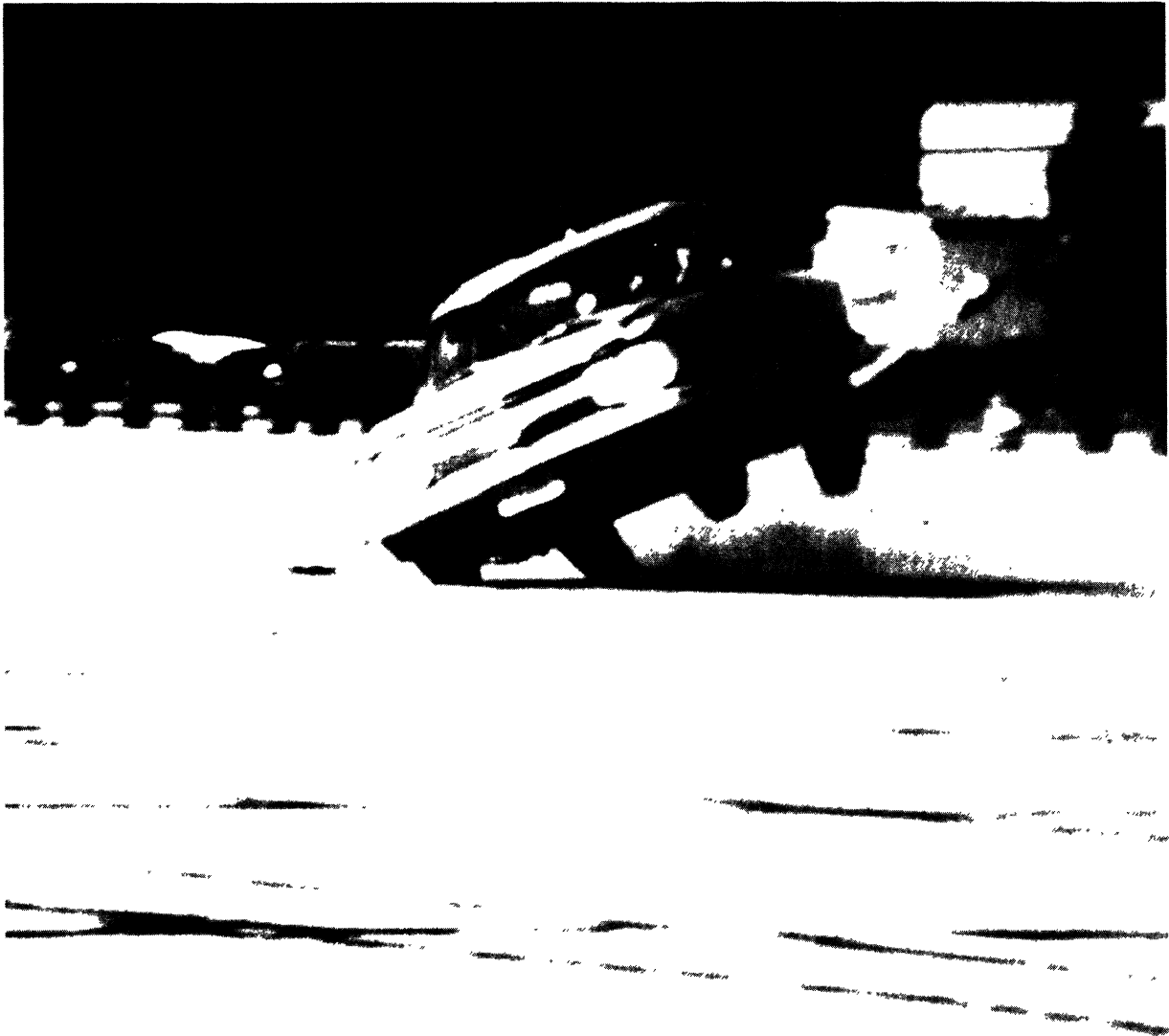
FIGURE 37. VEHICLE IN DRASTIC STEER AND BRAKE MANEUVER
RESTRAINED FROM ROLLING OVER BY OUTRIGGER

of limit response boundary such as was done in the preceeding section for the sinusoidal steering response test results. Nevertheless, the positive identification of a single limit response point is considered to constitute a thoroughly adequate demonstration of the discriminatory power of this unique test procedure.

TABLE 11		
TEST CONDITIONS IN DRASTIC STEER/BRAKE RESPONSE TESTS WHERE LIMIT (ROLLOVER) PERFORMANCE WAS ENCOUNTERED		
Initial Velocity mph	Steering Amplitude deg.	Δ_{sw}^* (See eq. 8)
47.2	324	3.92
47.7	324	4.00
47.2	324	3.92

In the tests with off-design tire pressures, the severity of motions in response to comparable sub-limit control inputs was uniformly greater than in the tests with nominal pressures. This finding (supported by the quasi-finding mentioned in the second footnote on the previous page) demonstrates the desirability of tests with off-design service factors when evaluating motor vehicles with the drastic steer and brake maneuver.

5.0 CONCLUDING REMARKS

The specific objectives of the study have been achieved. A set of performance characteristics postulated to reflect the pre-crash safety quality of the motor vehicle have been defined. Methods of testing and data analysis have been demonstrated which provide objective and discriminating procedures for measuring these safety-relevant characteristics. Particularly notable is the development of an automatic controller which permits the conduct of severe handling tests heretofore impossible because of the limitations of the human controller

With respect to the ultimate goal of the study, viz., implementation of a vehicle handling performance standard, much work remains to be done. A logical first step is the conduct of a more general test program to measure the performance characteristics defined here for a much broader cross-section of passenger vehicles. The purpose of such a program would be threefold:

1. To refine and augment the developed procedures with the aid of additional test experience and data.

2. To more precisely define the precision and discriminatory power of the proposed performance measures.

3. To produce a data base defining the performance characteristics of the passenger vehicle population, which would serve as a basis for accident causation studies and, ultimately, for the establishment of minimum performance requirements.

Summary descriptions of the procedures developed in this program are given below. They are intended to constitute a recommendation for the format of handling tests to be per-

formed in an expanded pilot program. It is implicit in their
definition that these tests would be supplemented by a compre-
hensive program of tire traction measurements. The summary
is not intended to be self-contained - - it means little in
the absence of much of the material presented in the body of
this report.

Recommended Vehicle Handling Measurements

1. Straight line braking effectiveness -- to
   the limit of tire-road adhesion -- two pave-
   ment conditions; dry concrete and wet, painted
   asphalt -- two loading conditions.

2. Response to step steering input -- to the
   limit of tire-road adhesion -- to characterize
   the breakaway condition in terms of peak lateral
   acceleration and continuity of yaw response --
   two service factor conditions: nominal and off-
   design.

3. Braking effectiveness from a steady-turn initial
   condition -- to provide a generalized braking ef-
   ficiency characterization involving a measure of
   the deviation of vehicle trajectory (from its
   nominal circular path) produced by braking -- to
   the limit of tire-road adhesion -- two service
   factor conditions: nominal and degraded.

4. Response to simulated road roughness in a steady
   turn -- to assess degradation in turning per-
   formance as the frequency of disturbance encounter
   is varied over a range including fundamental
   wheel hop frequency -- two tire inflation pres-
   sures: nominal and overinflated.

5. Response to sinusoidal steer input -- to quantify (1) degree of deviation from a trajectory whose final and initial paths are parallel, and (2) evidence of oscillatory or unstable behavior -- as a function of maneuver severity over a range comparable to emergency lane changing -- two service factor conditions: nominal and degraded.

6. Response to simultaneous half-sine steering input and pulse brake input -- to quantify vehicle tendency to roll over as maneuver severity is varied over a range comparable to emergency obstacle-avoidance situations -- two service factor conditions: nominal and degraded.

The above recommendation does not imply that the scope of a second generation pilot program should be restricted exclusively to the procedures that have been developed. In certain respects, these procedures need refinement. For example, the development of a reliable procedure to measure vehicle sideslip angle under dynamic conditions would facilitate the interpretation of several of the tests. It must also be assumed that additional procedures, of at least equivalent safety relevance, could surely be developed. It appears that we have just begun to scratch the surface of a virtually limitless domain of investigations that are made possible with the aid of an automatic controller. Other combinations of steering and braking time histories could and should be programmed on the function generator and evaluated. By the same token, additional potentially relevant tests suitable for driver control should also be explored (e.g., response to aerodynamic inputs; response to roadholding during braking).

It should be noted that the performance measures defined in this study provide a meaningful focus for new analytical work and simulation activity. Mathematical models of the mechanics of the motor vehicle should be extended and refined to permit accurate simulation of these maneuvers. The existence of refined simulations would facilitate sensitivity analyses to guide the efforts of designers and researchers, and to provide new depths of understanding of the pre-crash dynamics of the roadway-vehicle system.

APPENDIX A

REPRESENTATIVE SERVICE FACTOR DATA

An important feature of the testing procedures described in this report is the conduct of experiments under multiple service factor conditions. This Appendix illustrates the derivation of appropriate off-design conditions, on the basis of representative tire usage data obtained in a comprehensive survey conducted under the auspices of the National Bureau of Standards [14, 15].

The results of the NBS survey included distributions of the following variables, as measured for a total sample population of 4502 vehicles (18008 tires):

1. Cold tire inflation pressure (corrected for temperature effects as per [16]), by location of tire on vehicle, p_i

2. Rated inflation pressure, p_R

3. Vertical tire loading, by location of tire, L_i

4. Type of vehicle (sedan, coupe, station wagon, truck, etc.)

From these data, one can construct distributions of the following functions, for each type of vehicle, as illustrated in Figures A-1 through A-3.

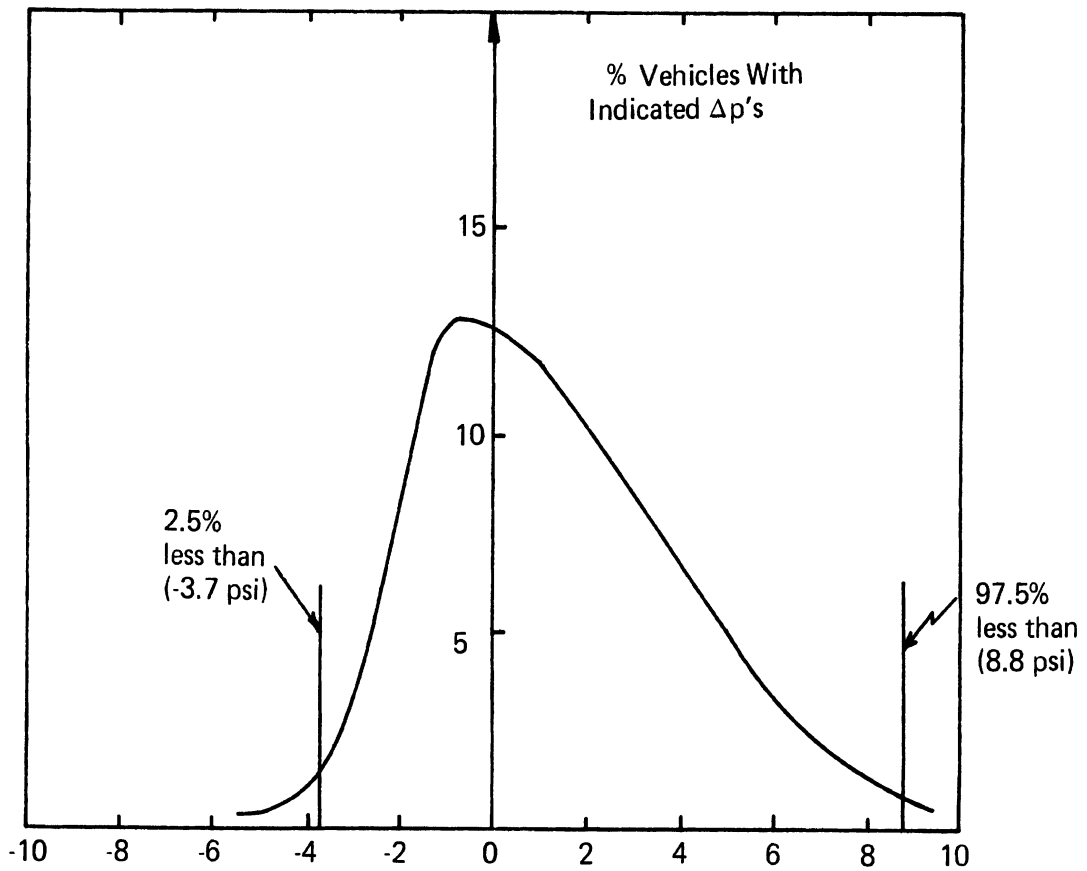1. Average tire pressure minus rated pressure,

$$\Delta p_{avg.} = \frac{1}{4} \sum_{i=1}^{4} p_i - p_R \qquad (A-1)$$

2. Average front tire pressure minus average rear tire pressure,

$$\Delta p_{f-r} = \frac{1}{2} (p_1 + p_2 - p_3 - p_4) \qquad (A-2)$$

Type Vehicles: Station Wagons
Size of Sample: 209

% Vehicles With
Indicated Δp's

15

2.5%
less than
(-3.7 psi)

97.5%
less than
(8.8 psi)

10

5

-10   -8   -6   -4   -2   0   2   4   6   8   10

$$\Delta p_{avg} = \frac{1}{4} \sum_{i=1}^{4} p_i - p_r, \text{ psi}$$

FIGURE A-1.   REPRESENTATIVE SERVICE FACTOR DATA; AVERAGE TIRE
PRESSURE MINUS RATED TIRE PRESSURE

98

Type Vehicles: Sedans
Size of Sample: **1045**

% Vehicles with
Indicated Δp's

20

10

99%
less than
(7.6 psi)

-10   -8   -6   -4   -2   0   2   4   6   8   10

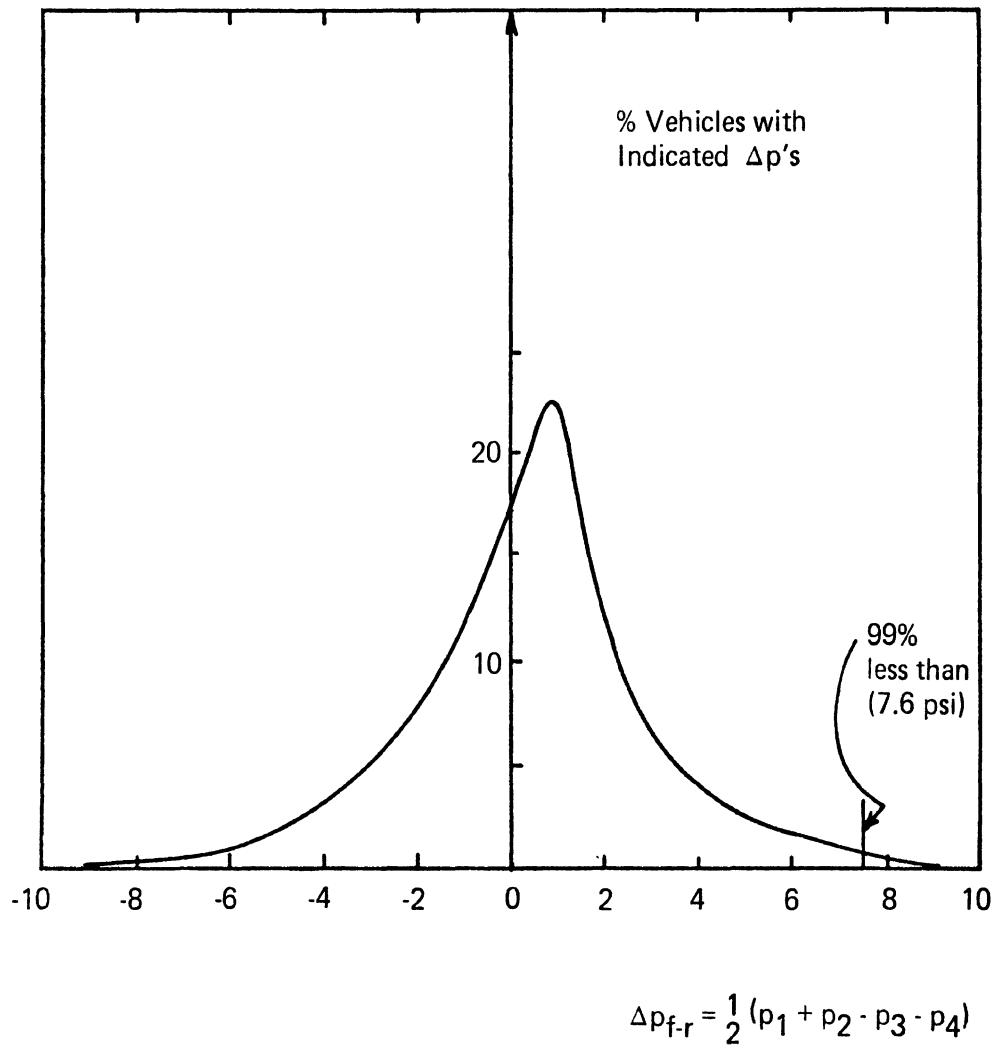$$\Delta p_{f\text{-}r} = \frac{1}{2} (p_1 + p_2 - p_3 - p_4)$$

FIGURE A-2.   REPRESENTATIVE SERVICE FACTOR DATA; AVERAGE FRONT
TIRE PRESSURE MINUS AVERAGE REAR TIRE PRESSURE

99

Type Vehicles: Sedans
Size of Sample: 1966

% Vehicles With
Indicated a/ℓ

$$\frac{a}{\ell} = \frac{L_3 + L_4}{L_1 + L_2 + L_3 + L_4}$$
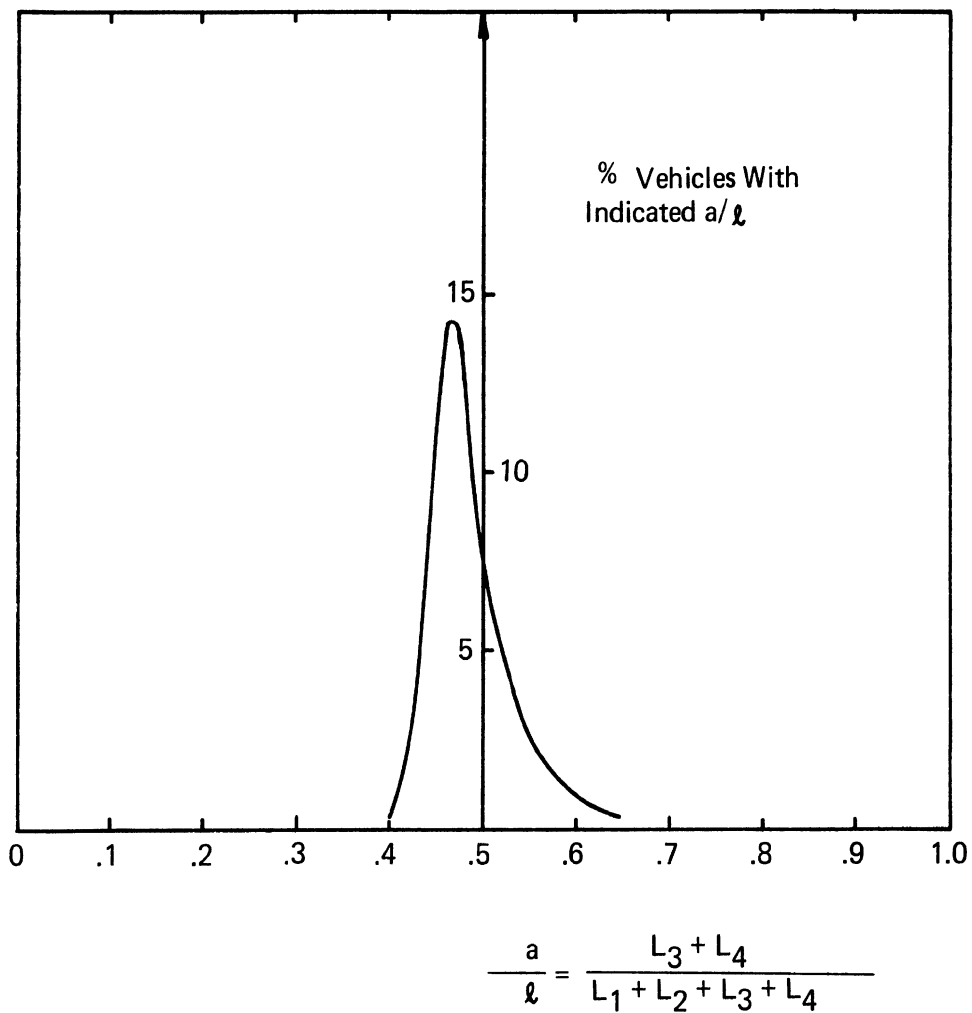
FIGURE A-3. REPRESENTATIVE SERVICE FACTOR DATA; DISTANCE,
CG TO FRONT AXLE, DIVIDED BY WHEELBASE

3. Distance, C.G. to front axle, divided by wheelbase,

$$\frac{a}{\ell} = \frac{L_3 + L_4}{L_1 + L_2 + L_3 + L_4} \tag{A-3}$$

In order to establish from these data reasonable off-design conditions for evaluating vehicle performance, it is necessary to stipulate reasonable vehicle population percentages corresponding to reasonable limits of service factor variability for vehicles in use. For illustrative purposes, we have indicated in Figures A-1 through A-3 bounds corresponding to particular assumed percentages of included population.

Representative applications of the illustrated bounds for establishing off-design vehicle handling test conditions include the following:

1. Upper bound of Δp_{avg} (see Figure A-1): Measurements with realistically overinflated tires for roadholding evaluation

2. Upper bound of Δp_{f-r} (see Figure A-2): Measurements with realistically decreased static margin

3. Lower bound of Δp_{f-r} (see Figure A-2): Measurements with realistically increased static margin

4. Upper bound of a/ℓ (see Figure A-3): Measurements with realistically decreased static margin; condition tending to stimulate front wheel locking

5. Lower bound of a/ℓ (see Figure A-3): Measurements with realistically increased static margin; condition tending to stimulate rear wheel locking.

APPENDIX B

VEHICLE PERFORMANCE SIMULATION

The iterative, trial and error process which was employed to define and rationalize the test conditions for the pilot program involved a substantial amount of computer simulation in addition to vehicle testing. This Appendix describes the mathematical models employed, and compares the simulation results with experiment to illustrate the qualitative agreement considered adequate for the purposes of this study.

VEHICLE DYNAMICS

The simulation model employed in this study may be characterized as a modified horizontal planar model, in that the vehicle is assumed basically to consist of a rigid mass constrained to move on a horizontal plane. Differential equations approximating the pitching and rolling dynamics of the sprung mass (relative to the horizontal plane) are employed to compute pitch and roll angles for use in the calculation of tire normal loads and kinematics (pitch- and roll-steer and camber), but are assumed uncoupled from the yaw plane dynamics.

The motion of the vehicle in the horizontal plane is described in terms of velocity components in a body fixed x-y-z coordinate system with origin at the vehicle's center of gravity (see Figure B-1). Application of Newton's second law for forces along the x and y axes and moments about the z-axis, respectively, yields

$$m(\dot{u} - r\,v) = F_x, \tag{B-1}$$

$$m(\dot{v} + r\,u) = F_y, \tag{B-2}$$
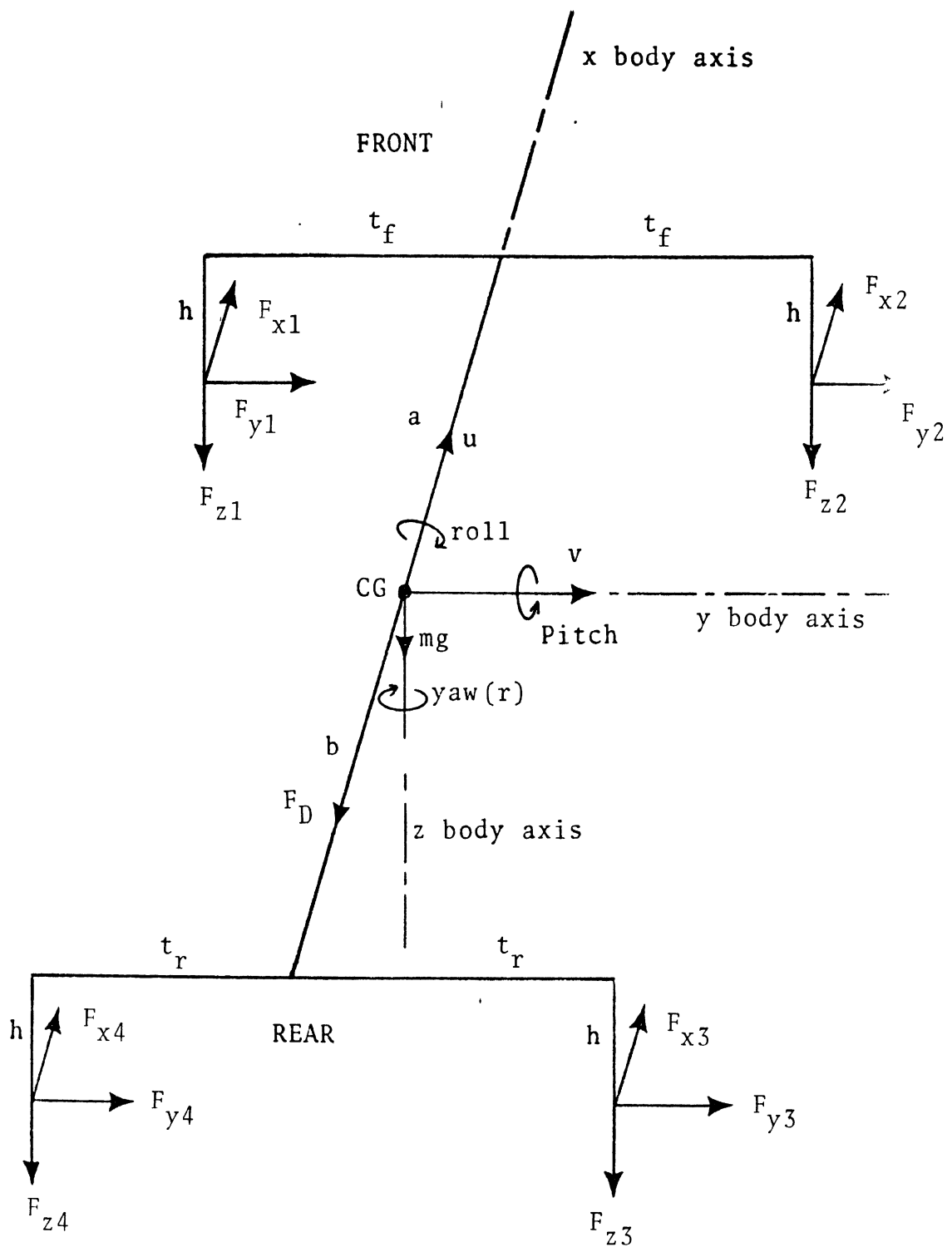
$$I_z \dot{r} = T_z. \tag{B-3}$$

FIGURE B1. VEHICLE GEOMETRY

m is the mass of the vehicle, I_z is its yaw moment of inertia, F_x is the total longitudinal force on the vehicle, F_y is the total lateral force on the vehicle, and T_z is the total torque acting on the vehicle about the vertical (z) axis through its C.G.

The roll and pitch dynamics of the sprung mass are approximated by the following equations:

$$I_{xs}\ddot{\phi} + 2\,\zeta_\phi\,\omega_{n\phi}\,I_{xs}\,\dot{\phi} + \omega_{n\phi}^2\,I_{xs}\,\phi = T_{xh} \qquad (B-4)$$

$$I_{ys}\ddot{\theta} + 2\,\zeta_\theta\,\omega_{n\theta}\,I_{ys}\,\dot{\theta} + \omega_{n\theta}^2\,I_{ys}\,\theta = T_{yh} \qquad (B-5)$$

I_{xs} and I_{ys} are, respectively, the roll and pitch moments of inertia of the sprung mass; T_{xh} and T_{yh} are torques due to forces in the horizontal plane acting on the sprung mass about the x and y axes, respectively; $\omega_{n\phi}$, ζ_ϕ, $\omega_{n\theta}$, and ζ_θ are roll natural frequency, roll damping, pitch natural frequency and pitch damping, respectively, as determined in the laboratory through tests involving pure rolling or pure pitching motions only.

The modified horizontal planar model represented by equations B-1 through B-5 can be derived from more comprehensive vehicle dynamics representations [e.g., 17] by neglecting all terms which are comparatively small for passenger car maneuvers on smooth level pavement.

APPLIED FORCES AND MOMENTS

The external forces considered to act on the vehicle are illustrated in Figure B-1. Thus

$$F_x = F_{x1} + F_{x2} + F_{x3} + F_{x4} - F_D, \qquad (B-6)$$

$$F_y = F_{y1} + F_{y2} + F_{y3} + F_{y4}, \qquad (B-7)$$

$$T_{xh} = -h\,(F_{y1} + F_{y2} + F_{y3} + F_{y4}), \qquad (B-8)$$

$$T_{yh} = h \ (F_{x1} + F_{x2} + F_{x3} + F_{x4}), \tag{B-9}$$

$$T_z = t_f(F_{x1} - F_{x2}) + t_r \ (F_{x4} - F_{x3})$$

$$+ \ a(F_{y1} + F_{y2}) - b \ (F_{y3} + F_{y4}) \tag{B-10}$$

The aerodynamic drag force, F_D , is computed from

$$F_D = (1/2) \ C_D \ \rho \ A_D \ u^2 \tag{B-11}$$

where C_D is the vehicle's aerodynamic drag coefficient, ρ is the mass density of the ambient air (taken as .00238 sl/ft^3) and A_D is the cross-sectional (frontal) area of the vehicle.

The components of tire forces in the horizontal plane are computed on the basis of a comprehensive tire shear force model developed in a previous HSRI study [8]. Components in the tire axis system (see Fig. B-2) are given by

$$F_{xwi} = - \frac{C_{si} \ s_i}{1 - s_i} \ f(\lambda_i), \tag{B-12}$$

$$F_{ywi} = - \frac{C_{\alpha i} \ \tan \alpha_i'}{1 - s_i} \ f(\lambda_i), \tag{B-13}$$

where

$$f(\lambda_i) = \begin{cases} (2 - \lambda_i) \ \lambda_i, & \text{for } \lambda_i < 1, \\ \\ 1 & \text{, for } \lambda_i \geq 1, \end{cases} \tag{B-14}$$

$$\lambda_i = (1/2)\mu_i |F_{zi}| (1-s_i) [(C_{si} s_i)^2 + (C_{\alpha i} \ \tan \alpha_i')^2]^{-1/2}$$

SPIN
VELOCITY
(Ω_i)

ALIGNING
TORQUE
(M_{zi})

γ_i

WHEEL PLANE

DIRECTION OF
WHEEL HEADING

LONGITUDINAL
FORCE
(F_{xw})

$x_i^!$

α_i

DIRECTION OF
WHEEL TRAVEL

GROUND
PLANE

SPIN AXIS

$y_i^!$

LATERAL FORCE
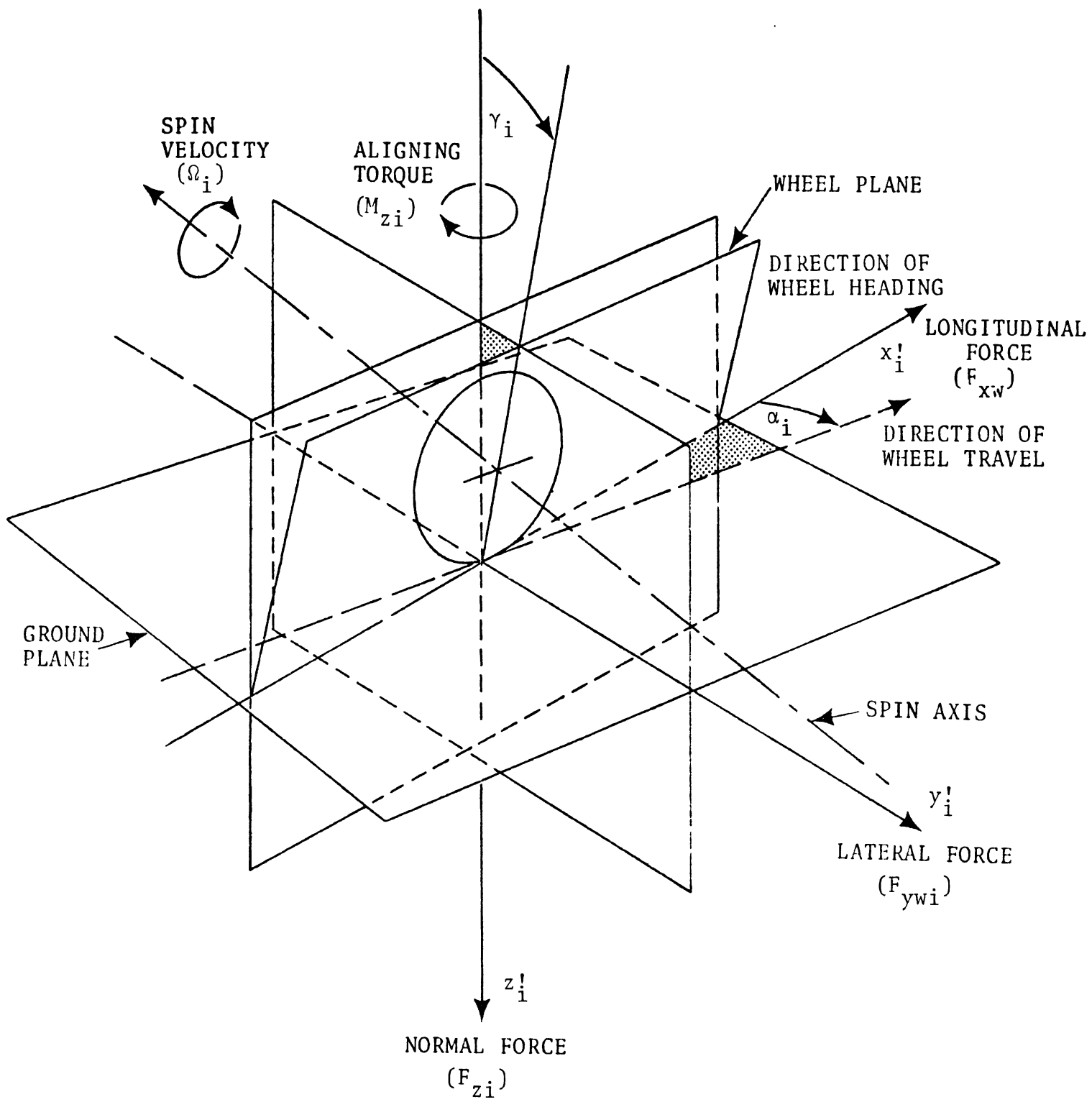(F_{ywi})

$z_i^!$

NORMAL FORCE
(F_{zi})

FIGURE B-2   TIRE AXIS SYSTEM AND KINEMATIC VARIABLES

The representation involves three empirical compliance parameters; the longitudinal stiffness, C_{si} , defined as the absolute value of the slope of the curve of longitudinal force versus longitudinal slip, s , evaluated at s=0 , with the slip angle, α , and inclination angle, γ , equal to zero; the lateral stiffness $C_{\alpha i}$, defined as the absolute value of the rate of change of lateral force with respect to slip angle, evaluated at α=0 , with γ=s=0 ; and the camber stiffness, $C_{\gamma i}$, defined as the absolute value of the rate of change of lateral force with respect to inclination angle, evaluated at γ=o, with α=s=0. It can be shown (see Reference 8) that the non-dimensional variable λ_i represents the longitudinal coordinate (in the tire axis system) of the point on the tire carcass associated with the inception of sliding in the contact patch.

The sideslip angle, α_i , and the inclination angle, γ_i , are kinematic variables defined as indicated in Figure B-2. The effective sideslip angle, α_i' , which appears in tne tire model equations, B-12 through B-14, is given by

$$\alpha_i' = \alpha_i - \frac{C_{\gamma i}}{C_{\alpha i}} \gamma_i \qquad (B-15)$$

The longitudinal slip ratio, s_i , is defined by

$$s_i = 1 - \frac{\Omega_i R_{ei}}{u_{wi}} . \qquad (B-16)$$

where Ω_i is the wheel spin velocity (see Figure B-2), u_{wi} is the component of the tire velocity along the longitudinal (x_i') axis (see equation B-30), and R_{ei} is the effective rolling radius of the tire (see equation B-31).

The coefficient of tire-road friction, μ_i , is computed from

$$\mu_i = \mu_{oi}(1 - A_{si}V_{si}), \qquad \text{(B-17)}$$

where V_{si} , the effective sliding velocity, is given by

$$V_{si} = u_{wi} [s_i^2 + (\tan \alpha_i')^2]^{1/2} \qquad \text{(B-18)}$$

and μ_{oi} and A_{si} are characterizing parameters that must be evaluated empirically for any specific tire/pavement combination.

The tire shear force components along the vehicle axes are computed by application of the following coordinate transformation equations:

$$F_{xi} = F_{xwi} \cos \delta_i - F_{ywi} \sin \delta_i \qquad \text{(B-19)}$$

$$F_{yi} = F_{xwi} \sin \delta_i + F_{ywi} \cos \delta_i \ . \qquad \text{(B-20)}$$

The angle δ_i is the steering angle of the ith wheel. For the front wheels, δ_i is determined by the effective steering angle δ_f (see equation B-28). For the rear wheels, δ_i is given by the rear axle roll steer angle δ_r (see equation B-33).

The tire normal loads are given by

$$F_{z1} = - \frac{mgb}{2(a+b)} + \frac{K_{f\phi}}{2t_f} \phi + \frac{K_\theta}{2(a+b)} \theta \ , \qquad \text{(B-21)}$$

$$F_{z2} = - \frac{mgb}{2(a+b)} - \frac{K_{f\phi}}{2t_f} \phi + \frac{K_\theta}{2(a+b)} \theta \ , \qquad \text{(B-22)}$$
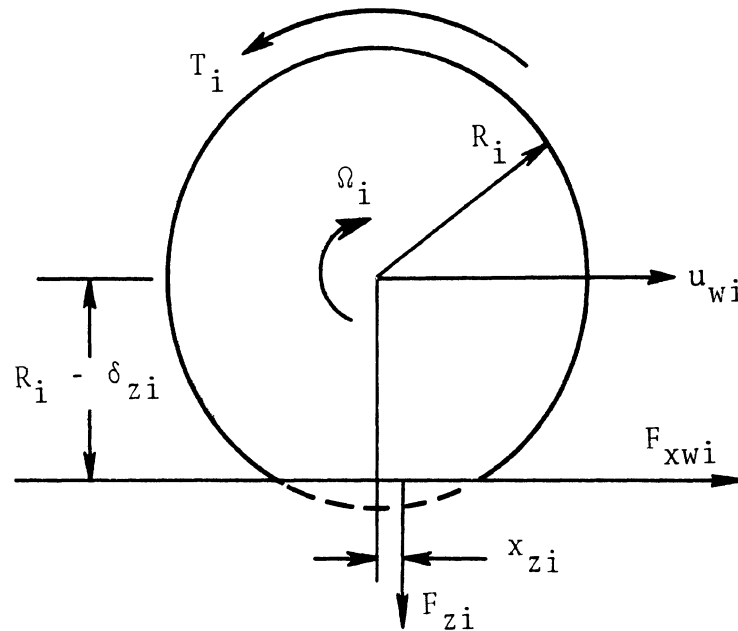
$$F_{z3} = - \frac{mga}{2(a+b)} - \frac{K_{r\phi}}{2t_r} \phi - \frac{K_\theta}{2(a+b)} \theta \ , \qquad \text{(B-23)}$$

$$F_{z4} = - \frac{mga}{2(a+b)} + \frac{K_{r\phi}}{2t_r} \phi - \frac{K_\theta}{2(a+b)} \theta \ , \qquad \text{(B-24)}$$

where $K_{f\phi}$ is the front roll stiffness, $K_{r\phi}$ is the rear roll stiffness, and K_θ is the pitch stiffness, all of which are determined empirically.

WHEEL ROTATION DYNAMICS

The coordinate system employed to describe the dynamics of the ith wheel is shown in the sketch below.

Application of Newton's second law for moments about the wheel spin axis yields

$$I_{wyi}\dot{\Omega}_i = x_{zi} F_{zi} - T_i - F_{xwi}(R_i - \delta_{zi}) - C_{wi}\Omega_i \quad (B\text{-}25)$$

I_{wyi} is the moment of inertia of the rotating part of the wheel about the spin axis of the wheel, Ω_i is the spin velocity of the wheel, T_i is the brake torque applied to the wheel, F_{xwi} is the longitudinal tire force in the wheel plane, R_i is the undeflected radius of the tire, δ_{zi} is the vertical tire deflection, F_{zi} is the normal load on the tire, x_{zi} is the longitudinal offset of the center of vertical pressure from the wheel center. and C_{wi}

is the wheel damping coefficient.

The vertical tire deflection is computed from an empirical equation,

$$\delta_{zi} = C_{zi} (-F_{zi}) + .033 R_i, \qquad (B-26)$$

where C_{zi} , the vertical deflection rate of the tire. is an empirically determined property. The longitudinal offset of the center of vertical pressure is computed from

$$x_{zi} = C_{xi}F_{xwi} + x_{ri} \qquad (B-27)$$

where C_{xi} , the "vertical force offset rate," and x_{ri} , the "rolling resistance factor," are also determined empirically.

STEERING SYSTEM DYNAMICS

The dynamics of the steering system are treated in approximate fashion. The degrees of freedom associated with wheel inertias are neglected, and both front wheels are considered to assume the same effective steering angle, δ_f. The following steering system torque balance is assumed:

$$K_{ss}(\delta^*_{sw} - \delta_f) + k(F_{xw1} - F_{xw2}) - x_p(F_{yw1} + F_{yw2}) = 0$$

K_{ss} is the torsional compliance of the system; k is the kingpin offset; x_p is the pneumatic trail of the tires, assumed to be a constant, and δ^*_{sw}, the "effective steer input", is computed from the first order differential equation

$$\tau_{ss}\dot{\delta}^*_{sw} = \delta'_{sw} - \delta^*_{sw} , \qquad (B-28)$$

where δ'_{sw} is the steering wheel angle divided by the steering gear ratio and τ_{ss} is an "effective lag" for the system.

TIRE KINEMATICS

The longitudinal and lateral components of the velocities of each wheel are given by (see Figure B-1)

$$u_1 = u + t_f r, \qquad\qquad v_1 = v + ar,$$

$$u_2 = u - t_f r, \qquad\qquad v_2 = v + ar,$$

$$u_3 = u - t_r r, \qquad\qquad v_3 = v - br,$$

$$u_4 = u + t_r r, \qquad\qquad v_4 = v - br. \qquad \text{(B-29)}$$

The velocity components in the wheel plane u_{wi} , are computed from the above using the following equation:

$$u_{wi} = u_i \cos \delta_i + v_i \sin \delta_i , \qquad\qquad \text{(B-30)}$$

where δ_i is the steering angle of the ith wheel (see note after equation B-20).

The longitudinal slip ratios, s_i , are computed from equation B-16, using u_{wi} from equation B-30, Ω_i from equation B-25, and values for R_{ei} , the effective rolling radius, estimated from

$$R_{ei} = R_i - \frac{\delta_{zi}}{3} \qquad\qquad \text{(B-31)}$$

where δ_{zi} , the vertical tire deflection, is given by equation B-26.

111

The tire sideslip angles, α_i are given by (see sketch):

$$\alpha_i = \tan^{-1}\left(\frac{v_i}{u_i}\right) - \delta_i \qquad (B-32)$$

wheel heading
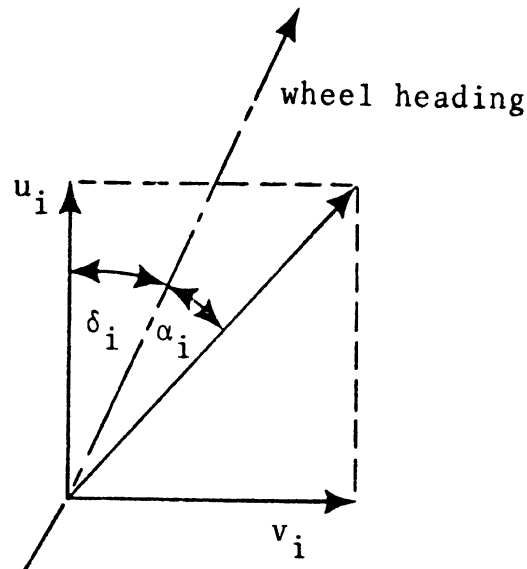
The rear axle roll steer is given by

$$\delta_r = -C_r \phi , \qquad (B-33)$$

where C_r , the roll steer coefficient, is an empirically derived parameter.

The camber angles of the front wheels, γ_i , are functions of the vertical wheel deflections, $\bar{z}_i$, which are given by

$$\bar{z}_1 = \frac{mgb}{2(a+b) K_f} + \theta a - \phi t_f , \qquad (B-34)$$

$$\bar{z}_2 = \frac{mgb}{2(a+b) K_f} + \theta a + \phi t_f , \qquad (B-35)$$

where K_f is the front spring rate. Expirical functions expressing the camber angles as functions of $\bar{z}_i$ are implemented in the simulation with diode function generators using input data from [17].

TRAJECTORY KINEMATICS

The angular orientation of the vehicle body axes with respect to x, y- axes fixed in the earth is illustrated in the sketch below:
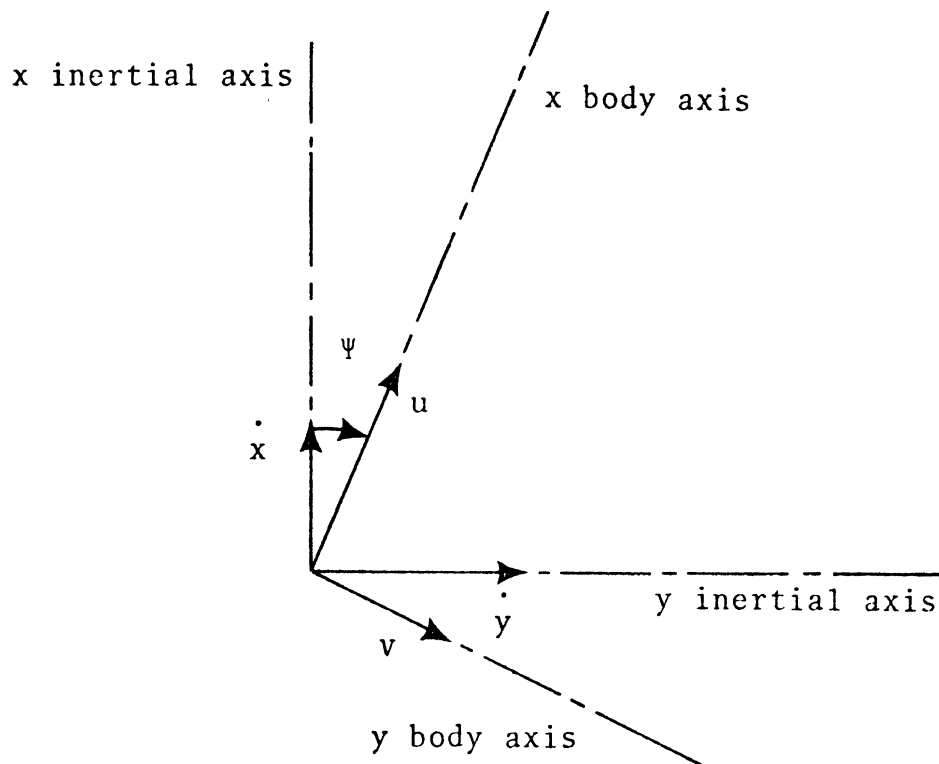
The orientation angle Ψ is the result of the vehicle rotating away from its original orientation angle. Since this rotation takes place with angular velocity r ,

$$\Psi(t) = \int_{t_o}^{t} r(t)dt + \Psi(t_o) \tag{B-36}$$

The components of the vehicle velocity in the body axis system u and v , are resolved into the earth axis system by using the following coordinate conversions:

$$\dot{x} = u \cos \Psi - v \sin \Psi , \qquad \text{(B-37)}$$

$$\dot{y} = u \sin \Psi + v \cos \Psi . \qquad \text{(B-38)}$$

The position of the vehicle is obtained by integrating the velocities. Thus

$$x(t) = \int_{t_0}^{t} \dot{x} \, dt + x(t_0) \qquad \text{(B-39)}$$

$$y(t) = \int_{t_0}^{t} \dot{y} \, dt + y(t_0) \qquad \text{(B-40)}$$

SIMULATION MECHANIZATION

The vehicle simulation, summarized in block diagram form in Figure B-3, was mechanized on a hybrid system comprised of an expanded AD4 analog computer and an IBM 1130 digital computer. To minimize operating time (hence costs), all integration and function generation was performed on the analog component. The analog circuits for calculating tire forces were time-shared, under the digital computer's control, using digital core for inter-update data storage. Each computed tire force was updated every 5 milliseconds, i.e., 200 times per second. This update frequency appears to be adequate for representing continuous phenomena occurring at frequencies up to approximately 40 Hertz.

In addition to controlling the time sharing of analog circuitry, and generally managing the computational process per se, the digital component was employed to set up and

Aerodynamic Drag

x,y,ψ

F_D

Trajectory Kinematics

u,v,r

Horizontal Plane Dynamics

u,v,r

ϕ,θ

$F_{xi},\, F_{yi}$

Roll & Pitch Dynamics

$F_{xi},\, F_{yi}$

Coordinate Transformations

δ_i

Tire Kinematics

δ_f

$F_{xwi},\, F_{ywi}$

Ω_i

$a_i,\, s_i,\, u_{wi}$

$\phi,\theta \ (F_{zi})$

Tire Mechanics

F_{xwi}

Wheel Rotation Dynamics

$F_{xwi},\, F_{ywi}$
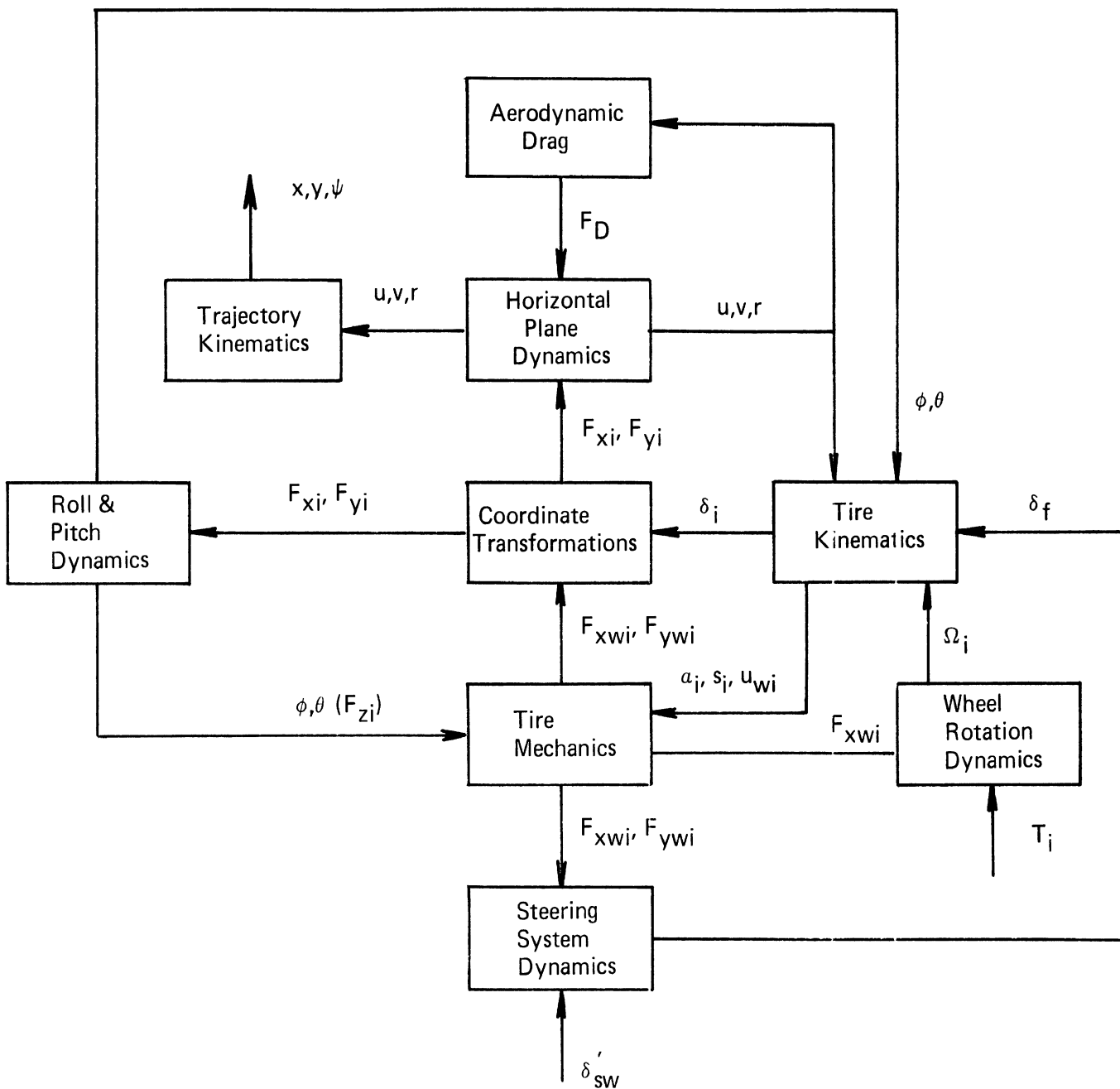
T_i

Steering System Dynamics

δ'_{sw}

FIGURE B-3. BLOCK DIAGRAM OF VEHICLE SIMULATION

check out the analog component automatically (e.g., to set and verify potentiometer settings and perform static checks). Parametric studies were run in either of two operating modes; (1) pre-programmed, wherein parameters were automatically changed between runs according to a program and data listings stored in the digital computer, or (2) conversational, wherein the computer would hold between runs until the operator supplied a new parameter value by typing it in at the digital computer console.

The highly automated hybrid mechanization permitted the economical conduct of a large number of application runs. Approximately 1400 runs were made in all at an average operating cost of less than twenty cents per run.

MODEL VALIDATION

The simulation was applied to investigate vehicle performance in each of three maneuvers; straight line braking, response to quasi-step steering, and braking in a turn. Comparisons between simulation results and corresponding experimental data, for each case, are illustrated in Figures B-4 through B-6. The vehicle configuration employed for the validation effort was the Ford station wagon with nominal service factors. (This configuration also represented the "central case" in the parametric studies which were performed.) The parametric data utilized in the calculations are tabulated in Table B-1.

The agreement between simulation and test exhibited in Figures B-4 through B-6 is by no means perfect. Additional research directed towards achieving improved correlation is certainly recommended. For the purposes to which it was employed in this study, however, the existing simulation is considered to be entirely adequate.
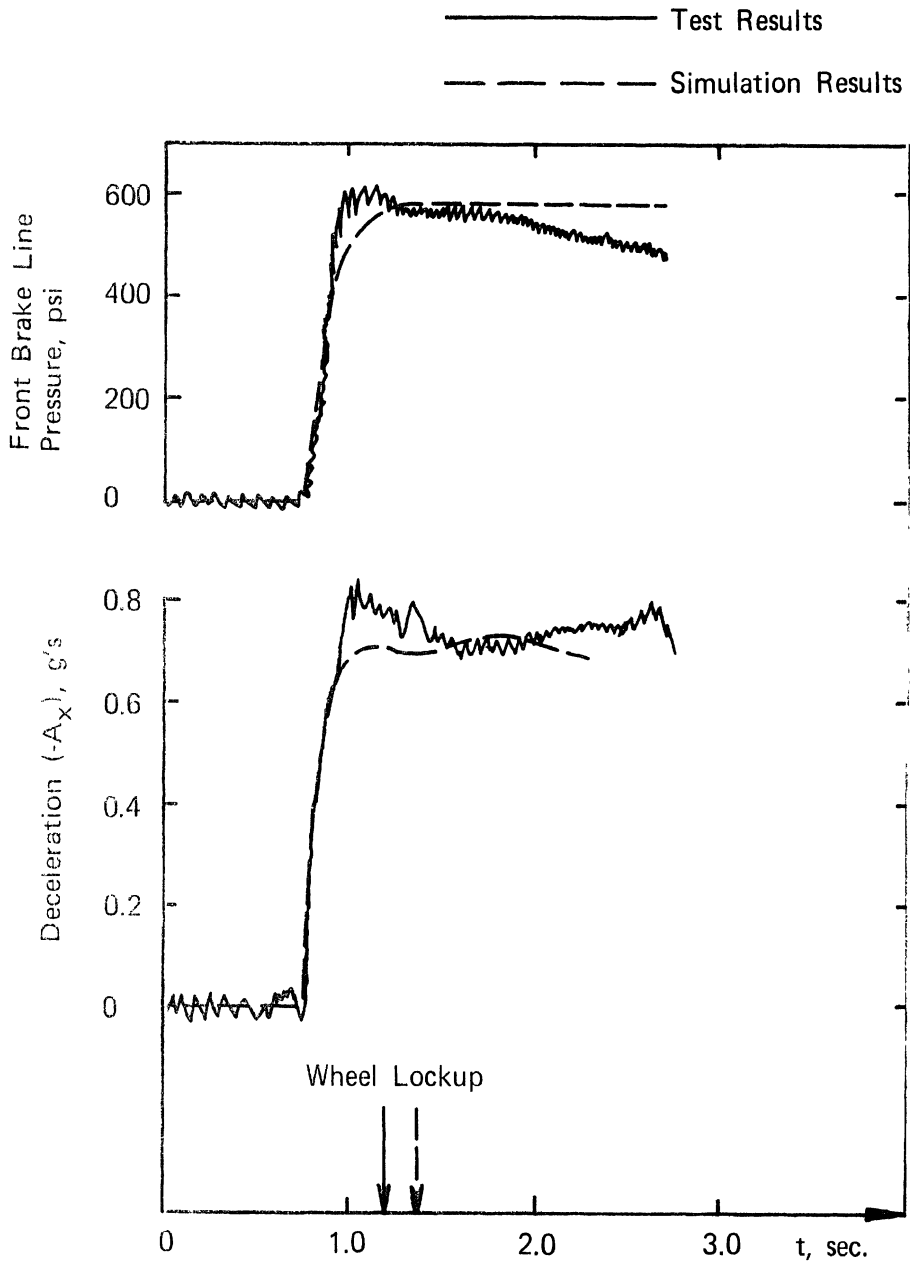
1967 Ford Station Wagon
Nominal Service Factors

———————— Test Results

— — — — Simulation Results

FIGURE B-4.   COMPARISON OF SIMULATION AND TEST RESULTS:
STRAIGHT LINE BRAKING
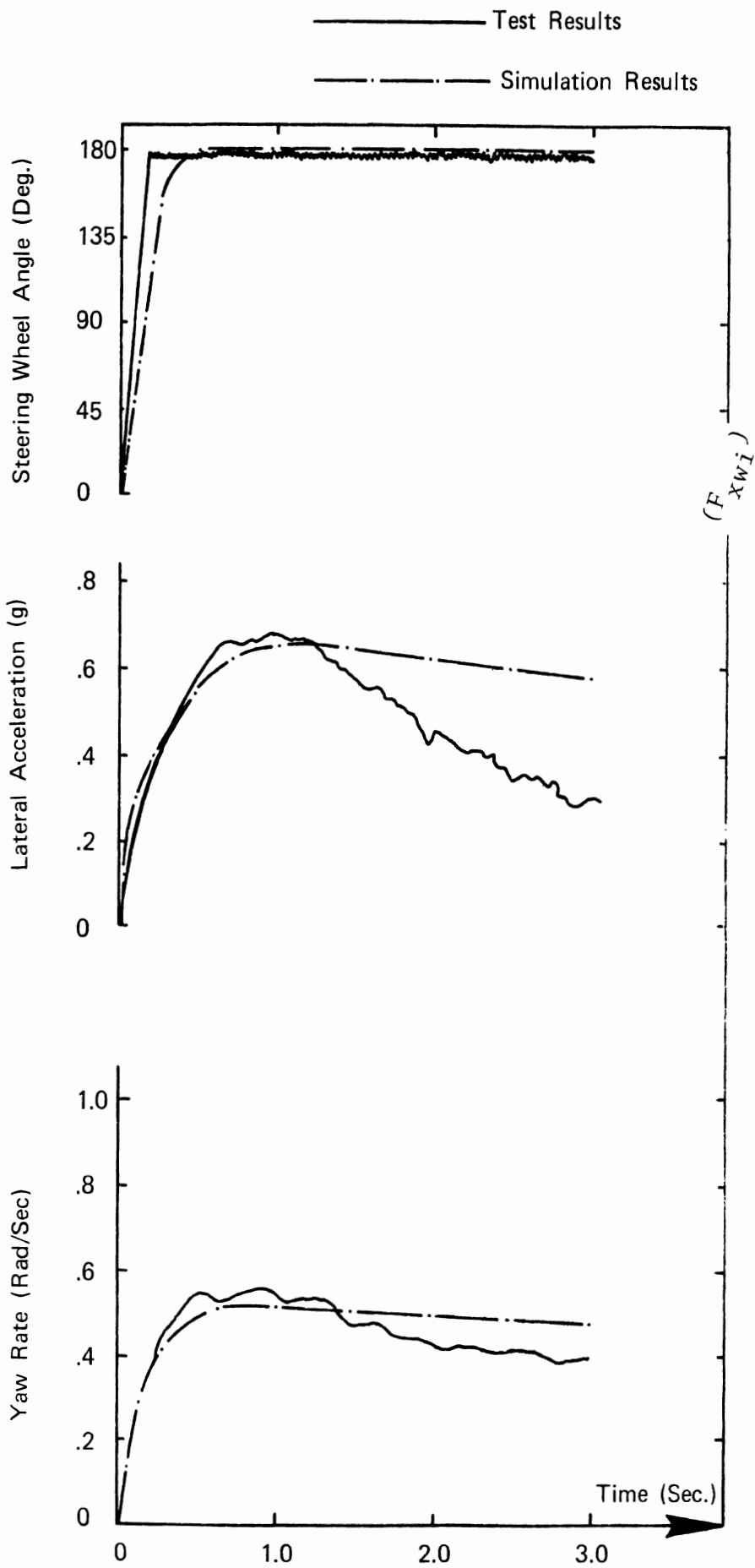
FIGURE B-5. COMPARISON OF SIMULATION AND TEST RESULTS:
RESPONSE TO QUASI-STEP STEERING

118

────────── Test Results
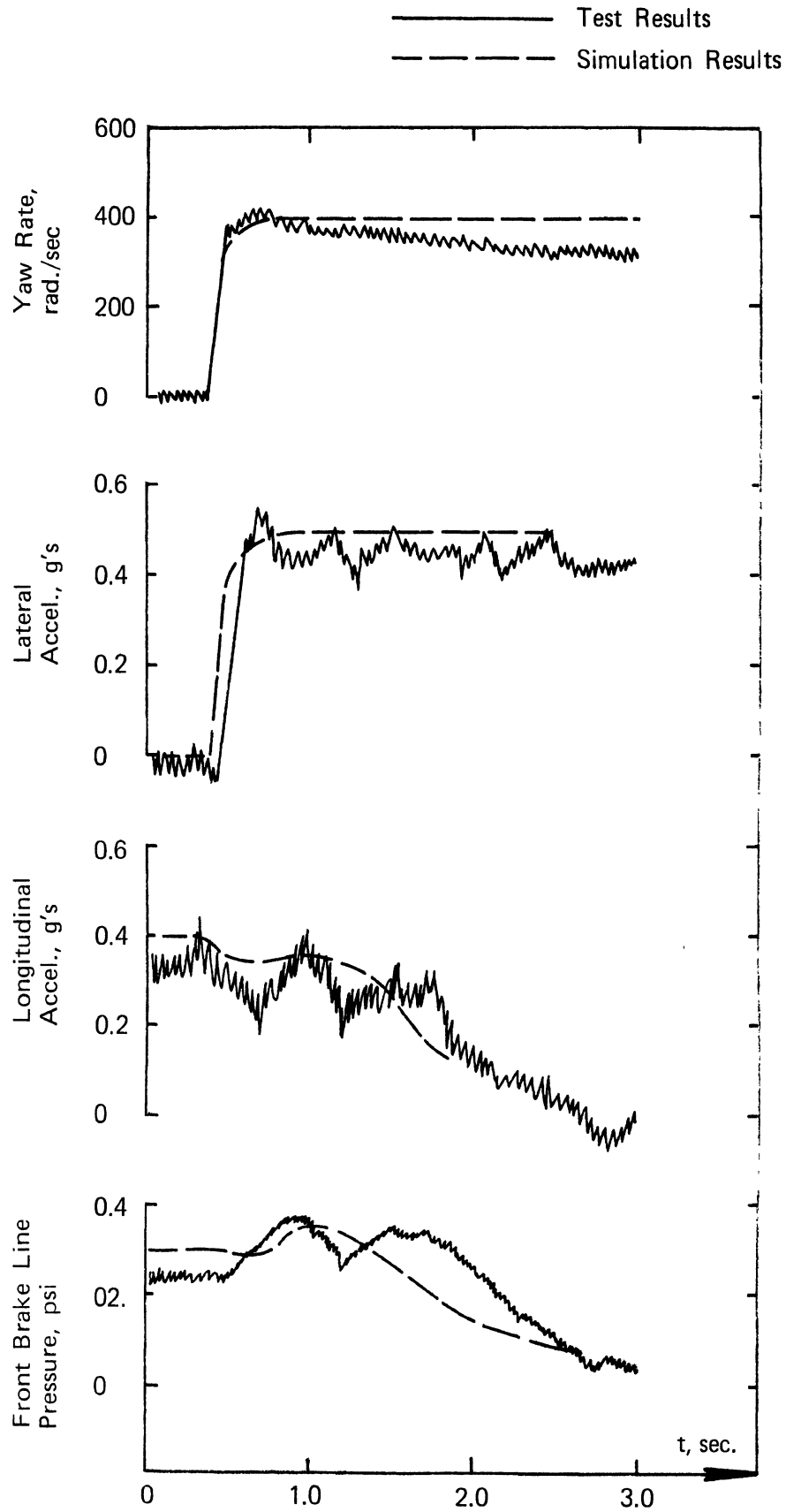
── ── ── ── ── Simulation Results

FIGURE B-6.   COMPARISON OF SIMULATION AND TEST RESULTS:
BRAKING IN A TURN

119

TABLE B-1

PARAMETRIC DATA FOR SIMULATION VALIDATION RUNS

(1967 Ford Station Wagon; Nominal Service Factors)

SYMBOL	NAME	VALUE
m	Mass	154.1 slugs
t_f	Front wheel half tread	2.61 ft
t_r	Rear wheel half tread	2.61 ft
a	Distance, C.G. to front axle	5.13 ft
b	Distance, C.G. to rear axle	4.73 ft
h	C.G. height	1.83 ft
A_D	Cross-sectional (frontal) area	25 ft^2
I_z	Yaw moment of inertia	4070 slug ft^2
I_{xs}	Sprung mass roll moment of inertia	540 slug ft^2
I_{ys}	Sprung mass pitch moment of inertia	3500 slug ft^2
$\omega_{n\phi}$	Roll natural frequency	10.26 rad/sec
ζ_ϕ	Roll damping	0.32
$\omega_{n\theta}$	Pitch natural frequency	8.05 rad/sec
ζ_θ	Pitch damping	0.3
C_D	Aerodynamic drag coefficient	0.45
$K_{f\phi}$	Front roll stiffness	37,600 ft lb/rad
$K_{r\phi}$	Rear roll stiffness	19,260 ft lb/rad
K_θ	Pitch stiffness	227,000 ft lb/rad
K_{ss}	Steering system stiffness	9560 ft lb/rad
τ_{ss}	Steering system lag	0.06 sec
k	Kingpin offset	0.2 ft

TABLE B-1

Continued

SYMBOL	NAME	VALUE
I_{wy}	Wheel inertia about axle	1.417 slug ft^2
C_w	Wheel damping coefficient	0.0
C_r	Rear roll steer coefficient	0.04 rad/rad
K_f	Front spring rate	1335 lb/ft
C_α	Tire lateral stiffness	$13,100$ lb/rad
C_s	Tire longitudinal stiffness	$22,500$ lb/unit slip
C_γ	Tire camber stiffness	$2,180$ lb/rad
μ_o	Nominal (zero speed) friction coefficient	1.05
A_s	Friction reduction factor	$.0037$ ft^{-1}
x_p	Pneumatic trail	0.1 ft
R	Nominal tire radius	1.15 ft
C_z	Tire vertical deflection rate	$12,000$ lbs/ft
C_x	Tire vertical force offset rate	$24,000$ lbs/ft
x_r	Tire rolling resistance factor	0.02 ft

REFERENCES

1. "Basic Vehicle Handling Properties - Phase I," Final Report, Federal Highway Administration Contract FH-6528, Highway Safety Research Institute of the University of Michigan, Nov. 1967.

2. L. Segel, "Display Versus Vehicle Augmentation as a Means for Improving Man-Vehicle Performance," ASME Publication 65-WA/HUF-10, paper presented at Winter Annual Meeting, Nov. 7-11, 1965.

3. J. A. Rouse, "The Distribution of Braking on Road Vehicles," Proceedings of the Symposium on Control of Vehicles during Braking and Cornering, Institute of Mechanical Engineers, London, 1963.

4. I. D. Neilson, "An Introductory Discussion of the Factors Affecting Car Handling," Road Research Laboratory, Report LR 133, 1968.

5. D. L. Nordeen, Discussion at TACT (Technical Advisory Committee on Tires) Meeting, North Carolina State University, Raleigh, N.D., Nov. 15, 1968.

6. W. Bergman, "Considerations in Determining Vehicle Handling Requirements," SAE Paper 690234, January 1969.

7. T. Nakatsuka and K. Takanami, "Cornering Ability Analysis Based on Vehicle Dynamics System," 1970 International Automobile Safety Conference Compendium, SAE, 1970.

8. H. Dugoff, P. S. Fancher, and L. Segel, "An Analysis of Tire Traction Properties and Their Influence on Vehicle Dynamic Performance," 1970 International Automobile Safety Conference Compendium, SAE, 1970.

9. D. K. Fisher, "Brake System Component Dynamic Performance Measurement and Analysis," 1970 International Automobile Safety Conference Compendium, SAE, 1970.

10. L. Segel, "Theoretical Prediction and Experimental Substantiation of the Response of the Automobile to Steering Control," Research in Automotive Stability and Control and in Tyre Performance, The Institute of Mechanical Engineers, Automobile Division, August 1956.

11. R. G. Mortimer, et al, "Brake Force Requirement Study: Driver-Vehicle Braking Performance as a Function of Brake System Design Variables," HSRI Report No. HUF-6, Final Report NHSB Contract FH-11-6952, April 1970.

12. P. S. Fancher, Jr., et al, "Experimental Studies of Tire Shear Force Mechanics -- a Summary Report," Final Report NBS Contract CST-928-5, HSRI, in press.

13. H. Dugoff and B. J. Brown, "Measurement of Tire Shear Forces," SAE Paper No. 700092, January 1970.

14. J. L. Harvey and F. C. Brenner, "Tire Use Survey, The Physical Condition, Use, and Performance of Passenger Car Tires in the United States of America," NBS Technical Note 528, May 1970.

15. I. R. Ehrlich and M. P. Jurkat, "Characteristics of Tire Usage in the Eastern United States, A Survey," Davidson Laboratory Technical Note 784, February 1968.

16. I. O. Kamm and F. Parsons, "A Procedure for Determining Ambient Tire Pressures frp, Field Measurements," Davidson Laboratory Technical Note 784, February 1968.

17. R. R. McHenry, D. J. Segal, N. J. Deleys, "Determination of Physical Criteria for Roadside Energy Conversion Systems," Cornell Aeronautical Laboratory, Inc., CAL No. VJ-2251-V-1, Final Report Contract No. CPR-11-3988, July 1967.